

Global analysis of GPDs with GUMP program

— near forward and beyond

Yuxun Guo

Lawrence Berkeley National Laboratory

Precision QCD Predictions for ep Physics at the EIC (II)

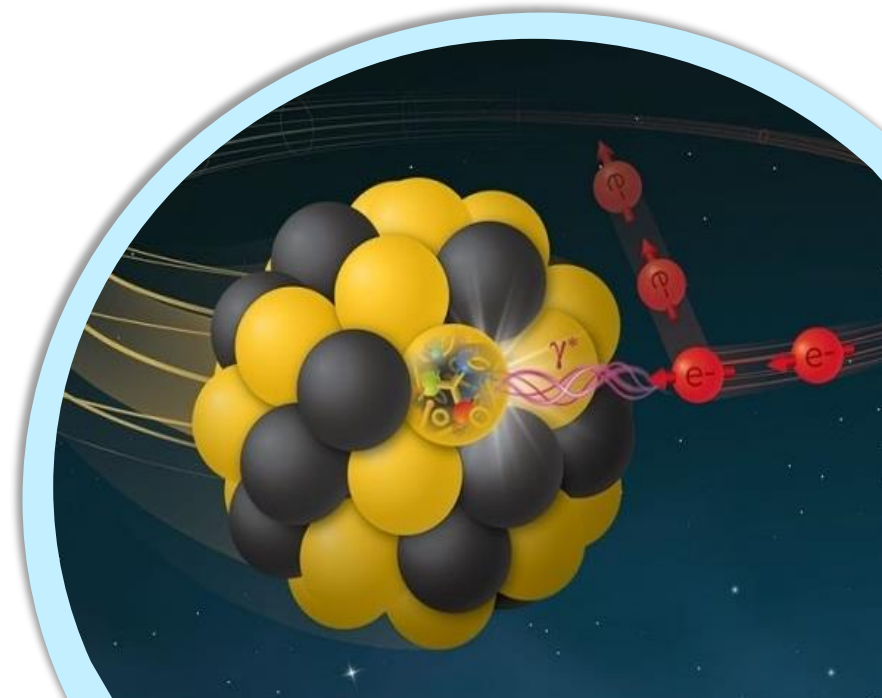
CFNS, Stony Brook University, New York

Sep. 18 – 22nd, 2023



Outline

- » Intro - why 3D structure?
- » Nucleon 3D structure from experiments
- » Lattice inputs of GPDs
- » 3D global analysis program
- » Summary and outlook



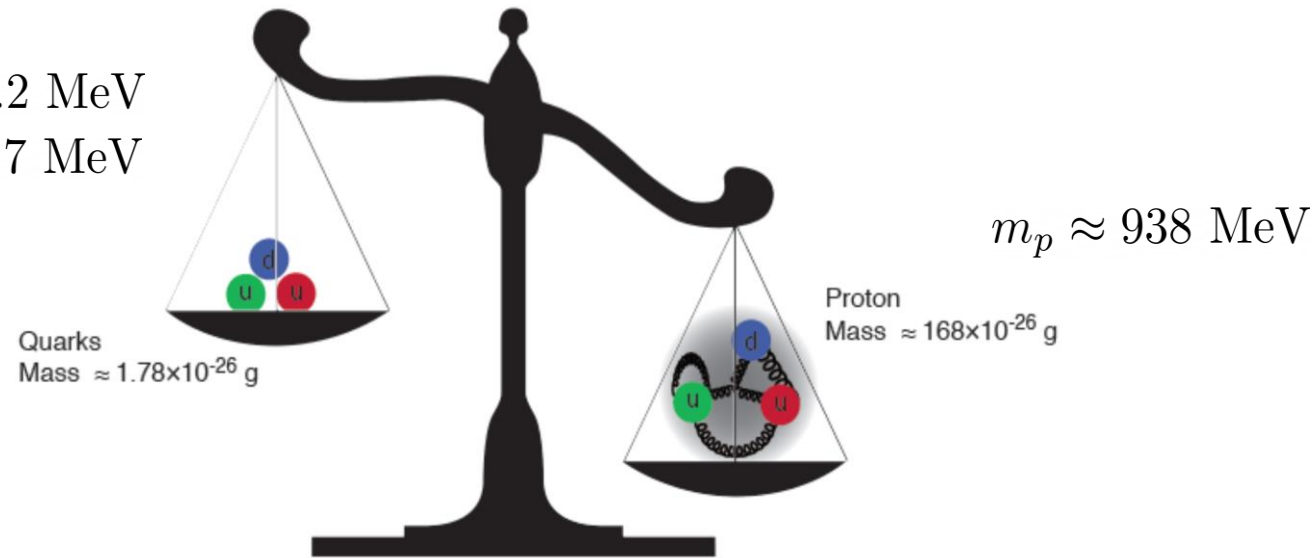
Why 3D structure? – nucleon mass

Nucleon mass is largely from strong interaction:

$$m_u \approx 2.2 \text{ MeV}$$

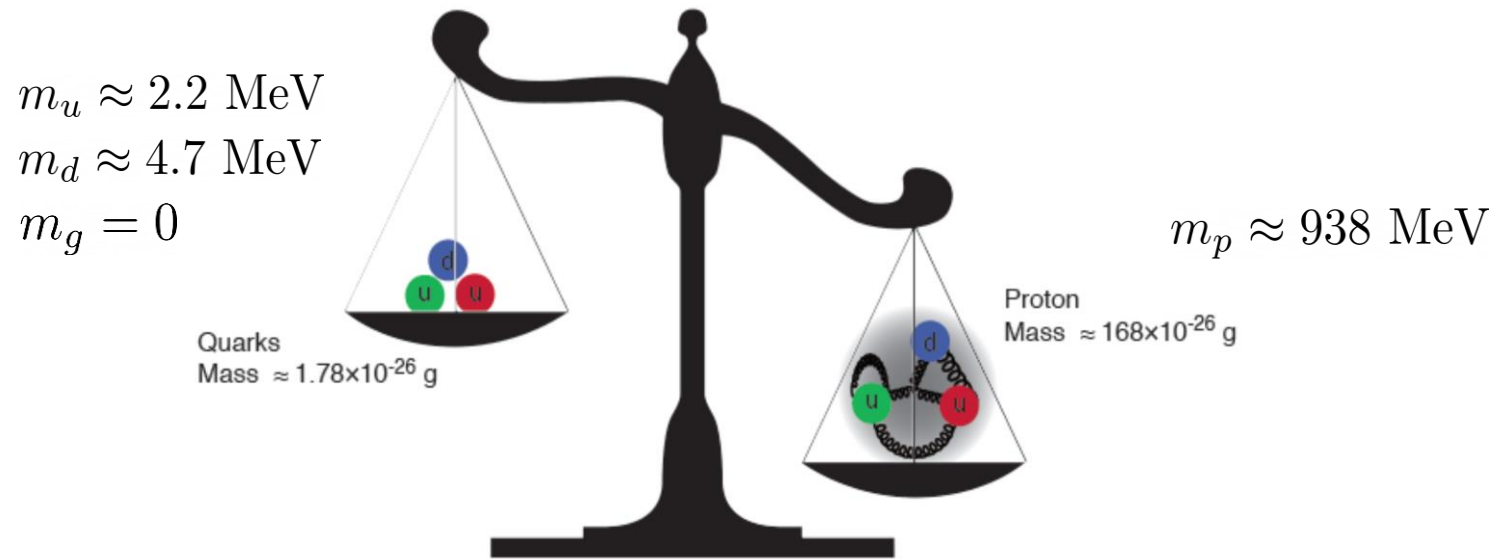
$$m_d \approx 4.7 \text{ MeV}$$

$$m_g = 0$$



Why 3D structure? – nucleon mass

Nucleon mass is largely from strong interaction:



which can be studied with QCD Hamiltonian,

X. Ji Phys. Rev. Lett. 74 1071 (1995)

$$H_{\text{QCD}} = \int d^3 \mathbf{x} T_{\text{QCD}}^{00}(0, \mathbf{x}) = H_q + H_m + H_g + H_a$$

Quark energy
Quark mass
Gluon energy
Quantum anomalous energy

Energy-momentum tensor form factors

Matrix element of EMT can be expressed as gravitational form factors:

$$\langle P' | T_{q,g}^{\mu\nu} | P \rangle = \bar{u}(P') \left[A_{q,g}(t) \gamma^{(\mu} \bar{P}^{\nu)} + B_{q,g}(t) \frac{\bar{P}^{(\mu} i \sigma^{\nu)\alpha} \Delta_\alpha}{2M_N} \right. \\ \left. + C_{q,g}(t) \frac{\Delta^\mu \Delta^\nu - g^{\mu\nu} \Delta^2}{M_N} + \bar{C}_{q,g}(t) M_N g^{\mu\nu} \right] u(P)$$

X. Ji Phys. Rev. Lett. 78, 610 (1997)

Energy-momentum tensor form factors

Matrix element of EMT can be expressed as gravitational form factors:

$$\langle P' | T_{q,g}^{\mu\nu} | P \rangle = \bar{u}(P') \left[A_{q,g}(t) \gamma^{(\mu} \bar{P}^{\nu)} + B_{q,g}(t) \frac{\bar{P}^{(\mu} i \sigma^{\nu)\alpha} \Delta_\alpha}{2M_N} \right. \\ \left. + C_{q,g}(t) \frac{\Delta^\mu \Delta^\nu - g^{\mu\nu} \Delta^2}{M_N} + \bar{C}_{q,g}(t) M_N g^{\mu\nu} \right] u(P)$$

X. Ji Phys. Rev. Lett. 78, 610 (1997)

Quantum anomalous energy and mass form factors:

Energy-momentum tensor form factors

Matrix element of EMT can be expressed as gravitational form factors:

$$\langle P' | T_{q,g}^{\mu\nu} | P \rangle = \bar{u}(P') \left[A_{q,g}(t) \gamma^{(\mu} \bar{P}^{\nu)} + B_{q,g}(t) \frac{\bar{P}^{(\mu} i \sigma^{\nu)\alpha} \Delta_\alpha}{2M_N} \right. \\ \left. + C_{q,g}(t) \frac{\Delta^\mu \Delta^\nu - g^{\mu\nu} \Delta^2}{M_N} + \bar{C}_{q,g}(t) M_N g^{\mu\nu} \right] u(P)$$

X. Ji Phys. Rev. Lett. 78, 610 (1997)

Quantum anomalous energy and mass form factors:

$$\langle P' | T_{\mu}^{\mu} | P \rangle = \bar{u}(P') G_s(t) u(P) \quad G_s(t) = M \left[A(t) + \frac{t}{4M_N^2} B(t) - \frac{t}{4M^2} 3C(t) \right]$$

Energy-momentum tensor form factors

Matrix element of EMT can be expressed as gravitational form factors:

$$\langle P' | T_{q,g}^{\mu\nu} | P \rangle = \bar{u}(P') \left[A_{q,g}(t) \gamma^{(\mu} \bar{P}^{\nu)} + B_{q,g}(t) \frac{\bar{P}^{(\mu} i \sigma^{\nu)\alpha} \Delta_\alpha}{2M_N} + C_{q,g}(t) \frac{\Delta^\mu \Delta^\nu - g^{\mu\nu} \Delta^2}{M_N} + \bar{C}_{q,g}(t) M_N g^{\mu\nu} \right] u(P)$$

X. Ji Phys. Rev. Lett. 78, 610 (1997)

Quantum anomalous energy and mass form factors:

$$\langle P' | T^\mu_\mu | P \rangle = \bar{u}(P') G_s(t) u(P) \quad G_s(t) = M \left[A(t) + \frac{t}{4M_N^2} B(t) - \frac{t}{4M^2} 3C(t) \right]$$

$$\langle P' | T^{00} | P \rangle = \bar{u}(P') G_m(t) u(P) \quad G_M(t) = M \left[A(t) + \frac{t}{4M_N^2} B(t) - \frac{t}{4M^2} C(t) \right]$$

Energy-momentum tensor form factors

Matrix element of EMT can be expressed as gravitational form factors:

$$\langle P' | T_{q,g}^{\mu\nu} | P \rangle = \bar{u}(P') \left[A_{q,g}(t) \gamma^{(\mu} \bar{P}^{\nu)} + B_{q,g}(t) \frac{\bar{P}^{(\mu} i \sigma^{\nu)\alpha} \Delta_\alpha}{2M_N} + C_{q,g}(t) \frac{\Delta^\mu \Delta^\nu - g^{\mu\nu} \Delta^2}{M_N} + \bar{C}_{q,g}(t) M_N g^{\mu\nu} \right] u(P)$$

X. Ji Phys. Rev. Lett. 78, 610 (1997)

Quantum anomalous energy and mass form factors:

$$\langle P' | T_{\mu}^{\mu} | P \rangle = \bar{u}(P') G_s(t) u(P) \quad G_s(t) = M \left[A(t) + \frac{t}{4M_N^2} B(t) - \frac{t}{4M^2} 3C(t) \right]$$
$$\langle P' | T^{00} | P \rangle = \bar{u}(P') G_m(t) u(P) \quad G_M(t) = M \left[A(t) + \frac{t}{4M_N^2} B(t) - \frac{t}{4M^2} C(t) \right]$$

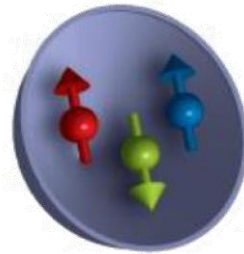
Gravitational form factors are fundamental for nucleon structures!

Why 3D structure? – nucleon spin

Naïve quark model

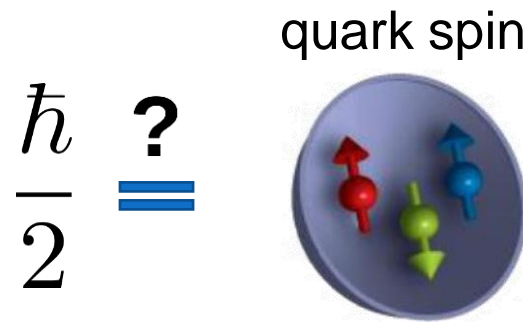
$$\frac{\hbar}{2} = ?$$

quark spin



Why 3D structure? – nucleon spin

Naïve quark model



Proton spin crisis

Why 3D structure? – nucleon spin

Naïve quark model

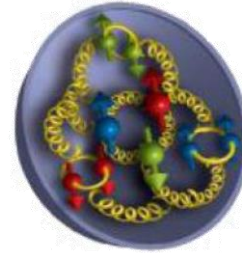
gluon contribution

$$\frac{\hbar}{2} = ?$$

quark spin



gluon spin



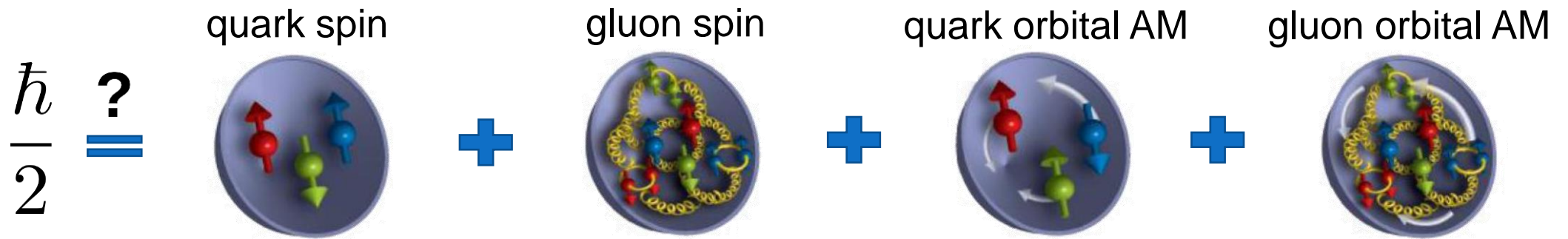
Proton spin crisis

Why 3D structure? – nucleon spin

Naïve quark model

gluon contribution

transverse motion



Why 3D structure? – nucleon spin

Naïve quark model

gluon contribution

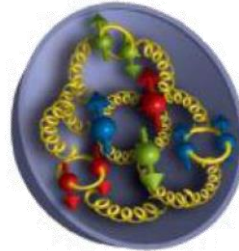
transverse motion

$$\frac{\hbar}{2} = ?$$

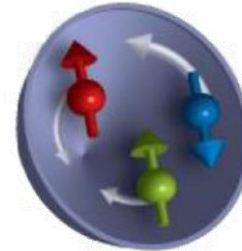
quark spin



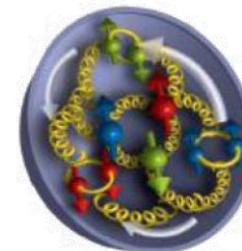
gluon spin



quark orbital AM



gluon orbital AM



Jaffe-Manohar sum rule

R. Jaffe and A. Manohar
Nucl. Phys. B 337, 509 (1990)

Why 3D structure? – nucleon spin

Naïve quark model

gluon contribution

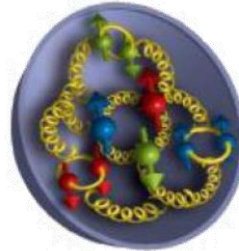
transverse motion

$$\frac{\hbar}{2} = ?$$

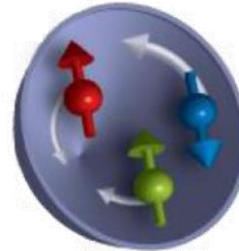
quark spin



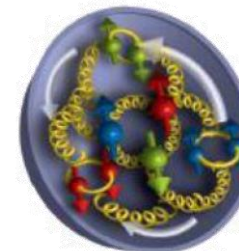
gluon spin



quark orbital AM



gluon orbital AM



Jaffe-Manohar sum rule

R. Jaffe and A. Manohar
Nucl. Phys. B 337, 509 (1990)

Why 3D structure? – nucleon spin

Naïve quark model

gluon contribution

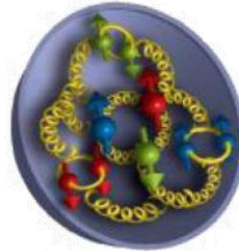
transverse motion

$$\frac{\hbar}{2} = ?$$

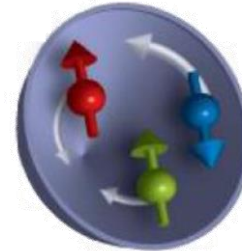
quark spin



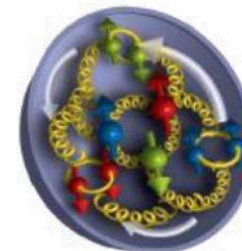
gluon spin



quark orbital AM

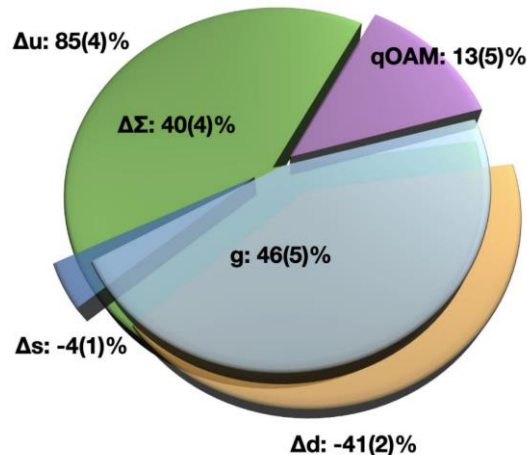


gluon orbital AM



Jaffe-Manohar sum rule

R. Jaffe and A. Manohar
Nucl. Phys. B 337, 509 (1990)



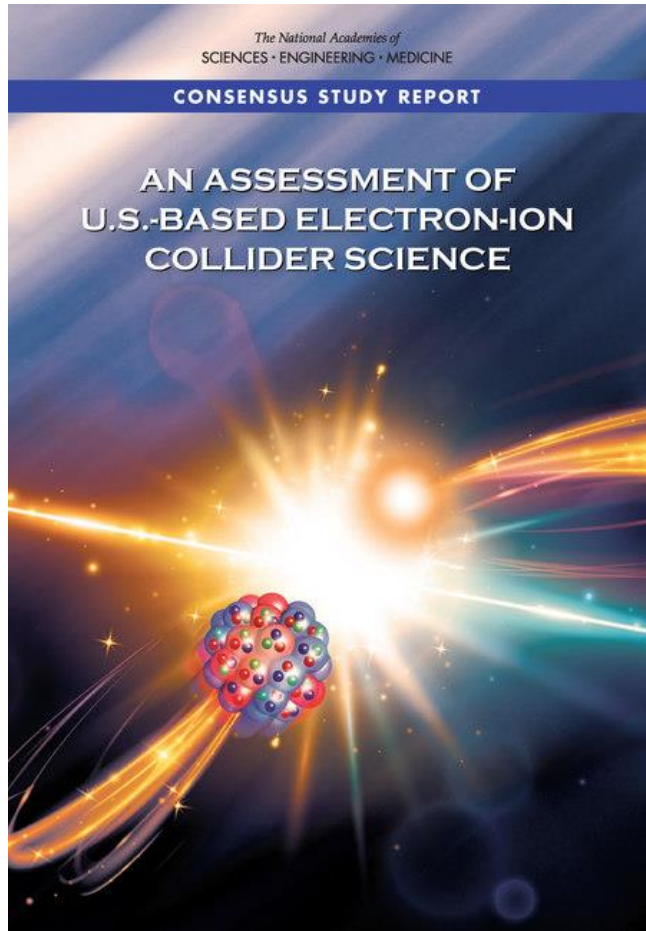
Proton spin decomposition from lattice

by χ QCD collaboration

G. Wang et. al. Phys. Rev. D 106, 014512 (2022)

See also ETMC Collaboration Phys. Rev. D 101 9, 094513 (2020)

Nucleon 3D structure with EIC



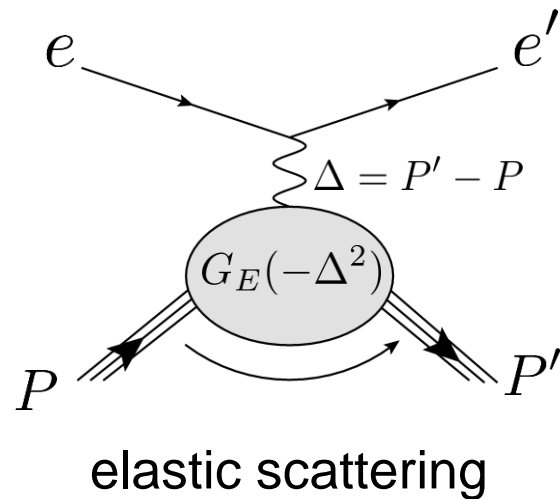
Finding 1:

An EIC can uniquely address three profound questions about nucleons — neutrons and protons — and how they are assembled to form the nuclei of atoms:

- How does the mass of the nucleon arise?
- How does the spin of the nucleon arise?
- What are the emergent properties of dense systems of gluons?

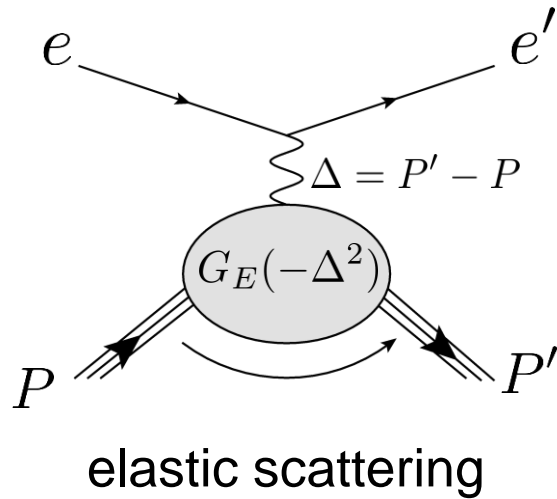
3D distributions of quarks and gluons

Diffractive process is a classic approach to accessing the 3D structures.



3D distributions of quarks and gluons

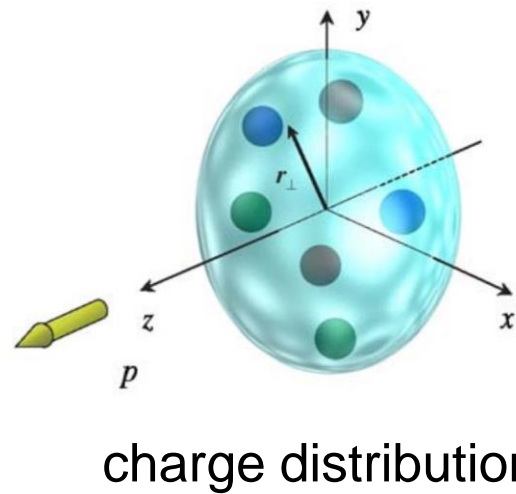
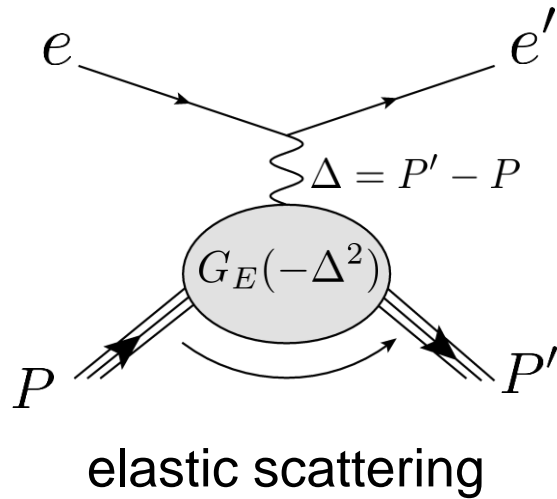
Diffractive process is a classic approach to accessing the 3D structures.



$$\rho_{\text{NR}}(\mathbf{r}) = \int \frac{d^3 \Delta}{(2\pi)^3} e^{-i\Delta \cdot \mathbf{r}} G_E(-\Delta^2)$$

3D distributions of quarks and gluons

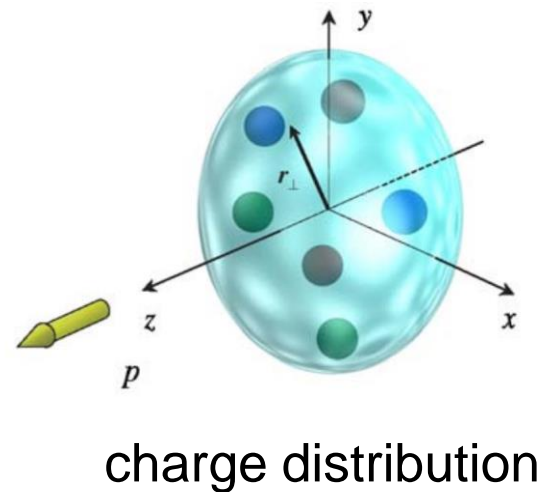
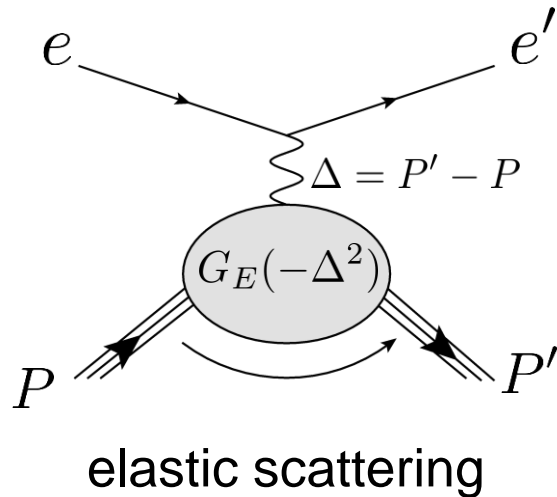
Diffractive process is a classic approach to accessing the 3D structures.



$$\rho_{\text{NR}}(\mathbf{r}) = \int \frac{d^3 \Delta}{(2\pi)^3} e^{-i\Delta \cdot \mathbf{r}} G_E(-\Delta^2)$$

3D distributions of quarks and gluons

Diffractive process is a classic approach to accessing the 3D structures.

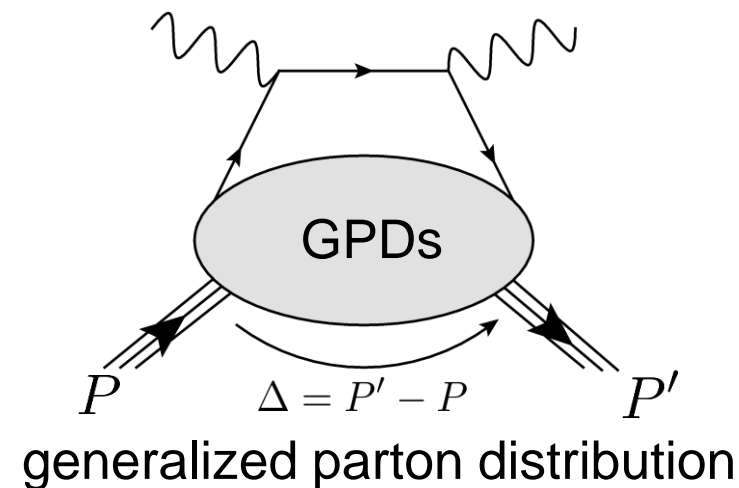
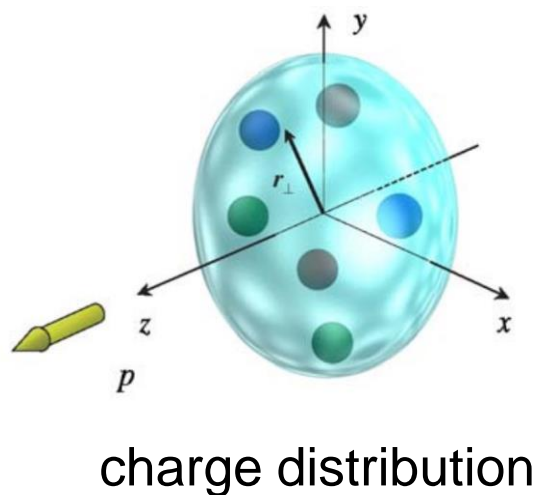
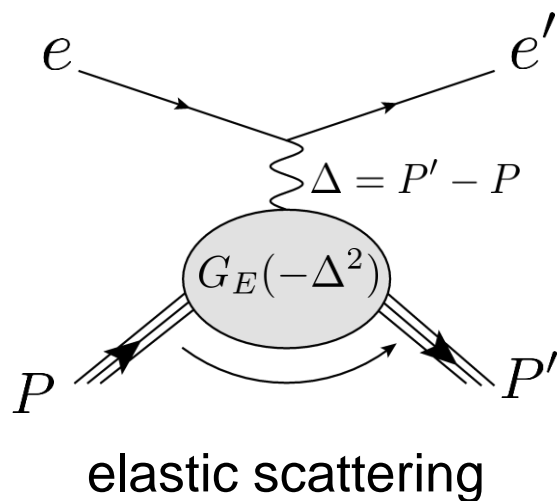


$$\rho_{\text{NR}}(\mathbf{r}) = \int \frac{d^3 \Delta}{(2\pi)^3} e^{-i\Delta \cdot \mathbf{r}} G_E(-\Delta^2)$$

Quarks/gluons 3D structure can be accessed by diffractive scattering.

3D distributions of quarks and gluons

Diffractive process is a classic approach to accessing the 3D structures.



D. Muller et. al. Fortsch.Phys. 42 101 (1994)

X. Ji Phys. Rev. Lett. 78, 610 (1997)

$$\rho_{\text{NR}}(\mathbf{r}) = \int \frac{d^3 \Delta}{(2\pi)^3} e^{-i\Delta \cdot \mathbf{r}} G_E(-\Delta^2)$$

Quarks/gluons 3D structure can be accessed by diffractive scattering.

3D mass & spin structures with GPDs

GPDs are 3D distributions unifying parton distributions and form factors

$$F(x, \Delta^\mu) = F(x, \xi, t)$$

3D mass & spin structures with GPDs

GPDs are 3D distributions unifying parton distributions and form factors

$$F(x, \Delta^\mu) = F(x, \xi, t)$$

x : parton momentum fraction

ξ : skewness parameter – longitudinal momentum transfer $\xi \equiv -n \cdot \Delta/2$

t : total momentum transfer squared $t \equiv \Delta^2$

3D mass & spin structures with GPDs

GPDs are 3D distributions unifying parton distributions and form factors

$$F(x, \Delta^\mu) = F(x, \xi, t)$$

x : parton momentum fraction

ξ : skewness parameter – longitudinal momentum transfer $\xi \equiv -n \cdot \Delta/2$

t : total momentum transfer squared $t \equiv \Delta^2$

GPDs reduce to form factors when integrated over x X. Ji, J. Phys. G 24 1181-1205 (1998)

3D mass & spin structures with GPDs

GPDs are 3D distributions unifying parton distributions and form factors

$$F(x, \Delta^\mu) = F(x, \xi, t)$$

x : parton momentum fraction

ξ : skewness parameter – longitudinal momentum transfer $\xi \equiv -n \cdot \Delta/2$

t : total momentum transfer squared $t \equiv \Delta^2$

GPDs reduce to form factors when integrated over x X. Ji, J. Phys. G 24 1181-1205 (1998)

$$\begin{aligned} \text{Charge FFs } \int dx H(x, \xi, t) &= F_1(t) \\ \int dx E(x, \xi, t) &= F_2(t) \end{aligned}$$

3D mass & spin structures with GPDs

GPDs are 3D distributions unifying parton distributions and form factors

$$F(x, \Delta^\mu) = F(x, \xi, t)$$

x : parton momentum fraction

ξ : skewness parameter – longitudinal momentum transfer $\xi \equiv -n \cdot \Delta/2$

t : total momentum transfer squared $t \equiv \Delta^2$

GPDs reduce to form factors when integrated over x X. Ji, J. Phys. G 24 1181-1205 (1998)

$$\begin{array}{ll} \text{Charge FFs} & \int dx H(x, \xi, t) = F_1(t) \\ & \int dx E(x, \xi, t) = F_2(t) \\ \text{Gravitational FFs} & \int dx xH(x, \xi, t) = A(t) + (2\xi)^2 C(t) \\ & \int dx xE(x, \xi, t) = B(t) - (2\xi)^2 C(t) \end{array}$$

3D mass & spin structures with GPDs

GPDs are 3D distributions unifying parton distributions and form factors

$$F(x, \Delta^\mu) = F(x, \xi, t)$$

x : parton momentum fraction

ξ : skewness parameter – longitudinal momentum transfer $\xi \equiv -n \cdot \Delta/2$

t : total momentum transfer squared $t \equiv \Delta^2$

GPDs reduce to form factors when integrated over x X. Ji, J. Phys. G 24 1181-1205 (1998)

$$\begin{array}{ll} \text{Charge FFs} & \int dx H(x, \xi, t) = F_1(t) \\ & \int dx E(x, \xi, t) = F_2(t) \\ \text{Gravitational FFs} & \int dx xH(x, \xi, t) = A(t) + (2\xi)^2 C(t) \\ & \int dx xE(x, \xi, t) = B(t) - (2\xi)^2 C(t) \end{array}$$

We cannot easily access GFFs in experiment, but we can access GPDs!

3D mass & spin structures with GPDs

GPDs are 3D distributions unifying parton distributions and form factors

$$F(x, \Delta^\mu) = F(x, \xi, t)$$

x : parton momentum fraction

ξ : skewness parameter – longitudinal momentum transfer $\xi \equiv -n \cdot \Delta/2$

t : total momentum transfer squared $t \equiv \Delta^2$

GPDs also provide an intuitive 3D image of nucleon:

3D mass & spin structures with GPDs

GPDs are 3D distributions unifying parton distributions and form factors

$$F(x, \Delta^\mu) = F(x, \xi, t)$$

x : parton momentum fraction

ξ : skewness parameter – longitudinal momentum transfer $\xi \equiv -n \cdot \Delta/2$

t : total momentum transfer squared $t \equiv \Delta^2$

GPDs also provide an intuitive 3D image of nucleon:

$$\rho_q^{\text{Unp}}(x, \mathbf{b}) = \int \frac{d^2 \Delta}{(2\pi)^2} e^{-i\Delta \cdot \mathbf{b}} H_q(x, -\Delta^2) = \mathcal{H}_q(x, \mathbf{b})$$

M. Burkardt, Int. J. Mod. Phys. A 18 173-208 (2003)

3D mass & spin structures with GPDs

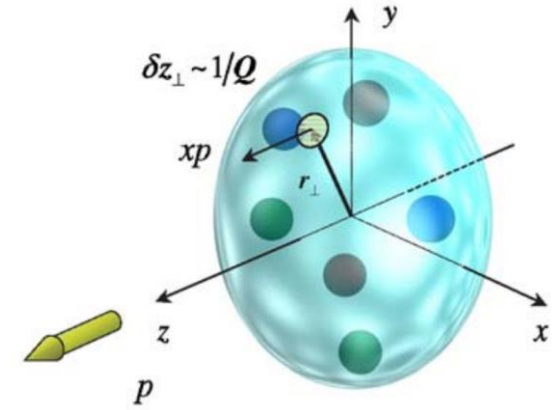
GPDs are 3D distributions unifying parton distributions

$$F(x, \Delta^\mu) = F(x, \xi, t)$$

x : parton momentum fraction

ξ : skewness parameter – longitudinal momentum

t : total momentum transfer squared $t \equiv \Delta^2$



3D quark/gluon dist.

GPDs also provide an intuitive 3D image of nucleon:

$$\rho_q^{\text{Unp}}(x, \mathbf{b}) = \int \frac{d^2 \Delta}{(2\pi)^2} e^{-i\Delta \cdot \mathbf{b}} H_q(x, -\Delta^2) = \mathcal{H}_q(x, \mathbf{b})$$

M. Burkardt, Int. J. Mod. Phys. A 18 173-208 (2003)

3D mass & spin structures with GPDs

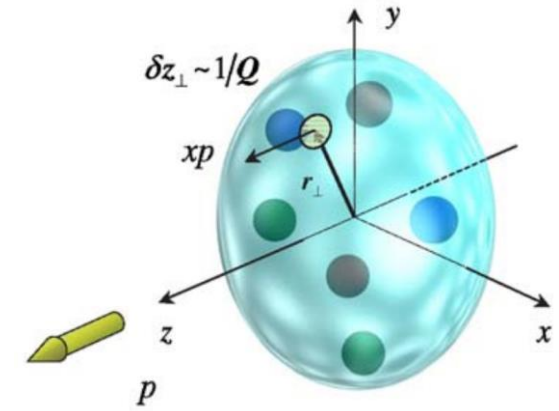
GPDs are 3D distributions unifying parton distribution functions

$$F(x, \Delta^\mu) = F(x, \xi, t)$$

x : parton momentum fraction

ξ : skewness parameter – longitudinal momentum fraction

t : total momentum transfer squared $t \equiv \Delta^2$



3D quark/gluon dist.

GPDs also provide an intuitive 3D image of nucleon:

$$\rho_q^{\text{Unp}}(x, \mathbf{b}) = \int \frac{d^2 \Delta}{(2\pi)^2} e^{-i\Delta \cdot \mathbf{b}} H_q(x, -\Delta^2) = \mathcal{H}_q(x, \mathbf{b})$$

M. Burkardt, Int. J. Mod. Phys. A 18 173-208 (2003)

which contains information of nucleon spin structure, e. g. transverse spin

3D mass & spin structures with GPDs

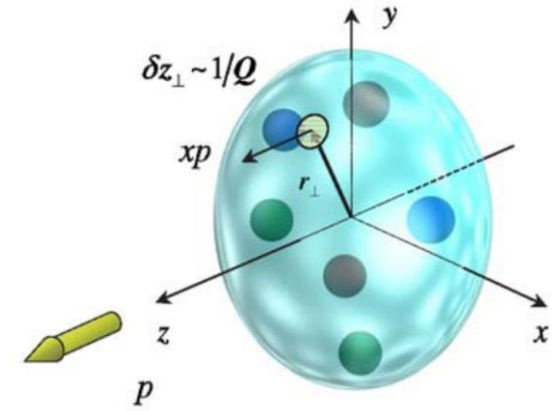
GPDs are 3D distributions unifying parton distribution functions

$$F(x, \Delta^\mu) = F(x, \xi, t)$$

x : parton momentum fraction

ξ : skewness parameter – longitudinal momentum fraction

t : total momentum transfer squared $t \equiv \Delta^2$



3D quark/gluon dist.

GPDs also provide an intuitive 3D image of nucleon:

$$\rho_q^{\text{Unp}}(x, \mathbf{b}) = \int \frac{d^2 \Delta}{(2\pi)^2} e^{-i\Delta \cdot \mathbf{b}} H_q(x, -\Delta^2) = \mathcal{H}_q(x, \mathbf{b})$$

M. Burkardt, Int. J. Mod. Phys. A 18 173-208 (2003)

which contains information of nucleon spin structure, e. g. transverse spin

$$J_q^T(x) = \int d^2 \mathbf{b} (b^y \times x P^+) \rho_q^T(x, \mathbf{b})$$

Y. Guo et. al. Nucl. Phys. B 969 115440 (2021)

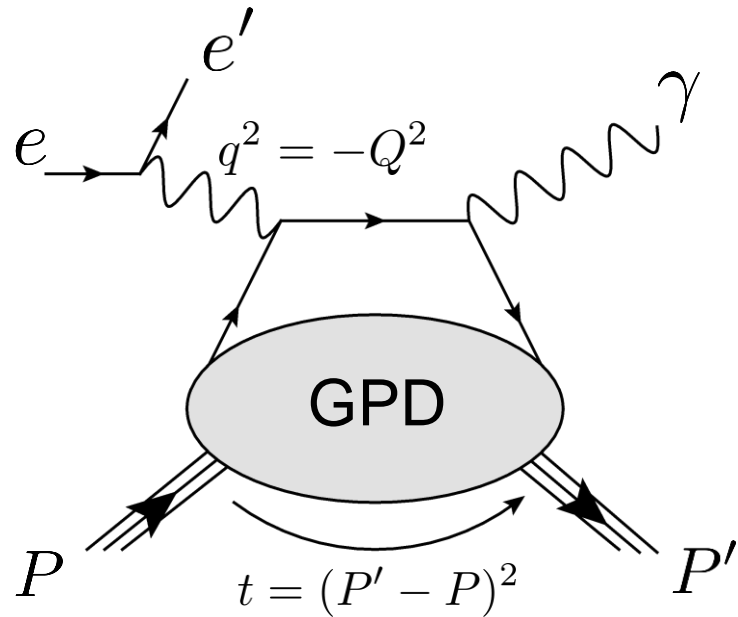
3D Structures from Experiment

Deeply virtual processes

Recall that diffractive processes can provide us access to the 3D structures.

Deeply virtual processes

Recall that diffractive processes can provide us access to the 3D structures.

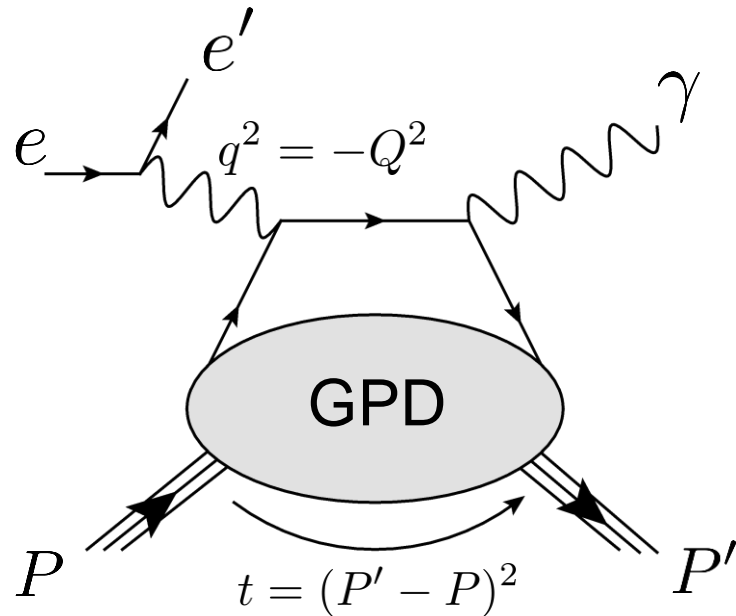


Deeply virtual Compton scattering

X. Ji, Phys. Rev. D 55, 7114 (1997)

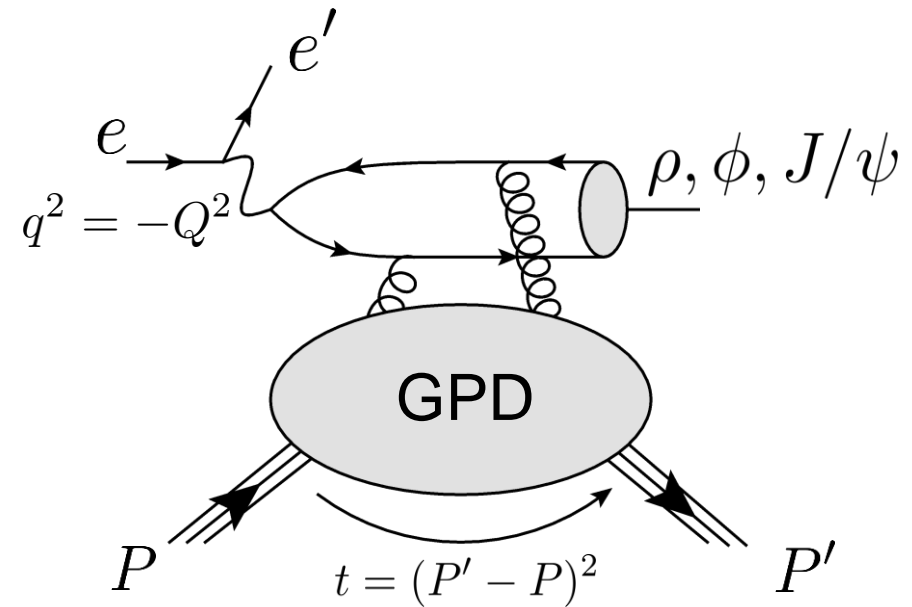
Deeply virtual processes

Recall that diffractive processes can provide us access to the 3D structures.



Deeply virtual Compton scattering

X. Ji, Phys. Rev. D 55, 7114 (1997)

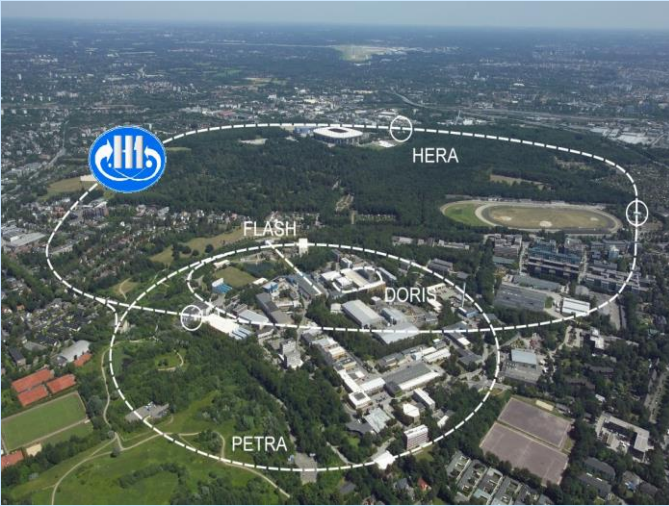


Deeply virtual meson production

A.V. Radyushkin Phys. Lett. B 385 333-342 (1996)
J. C. Collins et. al. Phys. Rev. D 56 2982-3006 (1997)

Deep exclusive measurements

HERA (*Hadron-Elektron-Ringanlage*)

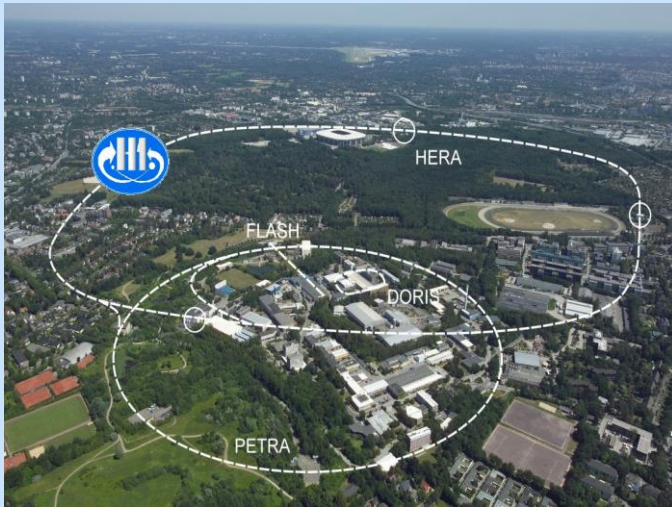


H1, ZEUS (Col), HERMES (FT)

- Col. w. electron/positron beam
- DVCS and DVMP measurements
- Running ended in 2007

Deep exclusive measurements

HERA (*Hadron-Elektron-Ringanlage*)



H1, ZEUS (Col), HERMES (FT)

- Col. w. electron/positron beam
- DVCS and DVMP measurements
- Running ended in 2007

CERN (European Organization for Nuclear Research)

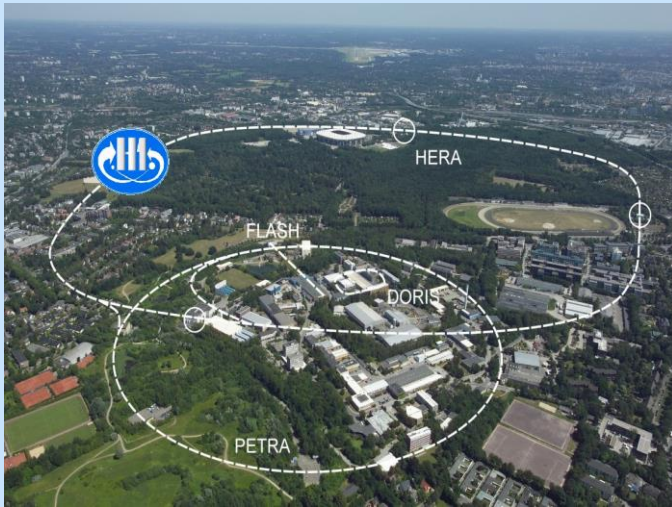


COMPASS

- FT w. Muon/antimuon beam
- DVCS measurements (2016)
- Running ended in 2022

Deep exclusive measurements

HERA (*Hadron-Elektron-Ringanlage*)



H1, ZEUS (Col), HERMES (FT)

- Col. w. electron/positron beam
- DVCS and DVMP measurements
- Running ended in 2007

CERN (European Organization for Nuclear Research)



COMPASS

- FT w. Muon/antimuon beam
- DVCS measurements (2016)
- Running ended in 2022

CEBAF (Continuous Electron Beam Accelerator Facility)

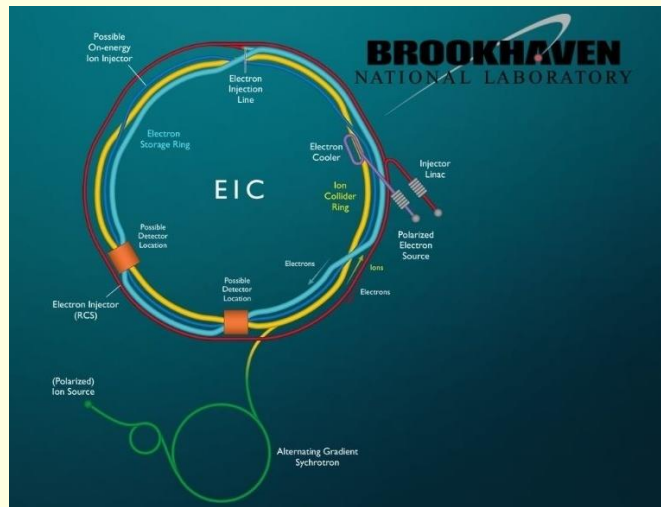


Hall A, B, C and D

- FT with electron/photon beam
- Large exclusive measurements
- Still are and will be running

Deep exclusive measurements

EIC (Electron-Ion Collider)



- High Lum. (100~1000 times HERA)
- Polarization configurations
- Plan to operate in the next decade

CEBAF (Continuous Electron Beam Accelerator Facility)

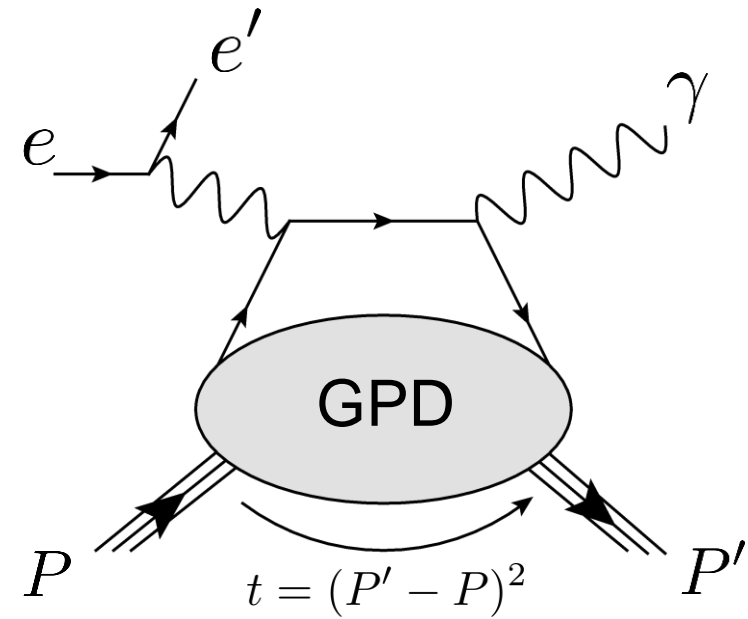


Hall A, B, C and D

- FT with electron/photon beam
- Large exclusive measurements
- Still are and will be running

Quarks structures from DVCS

DVCS is considered the golden channel to probe GPDs.



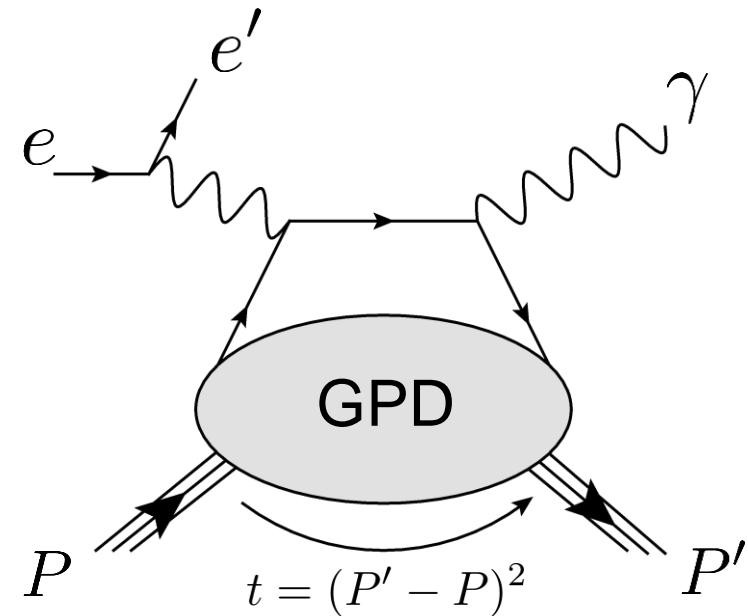
Quarks structures from DVCS

DVCS is considered the golden channel to probe GPDs.

Pros:

Clean final-state -- photon

Sensitive to quark GPDs



Quarks structures from DVCS

DVCS is considered the golden channel to probe GPDs.

Pros:

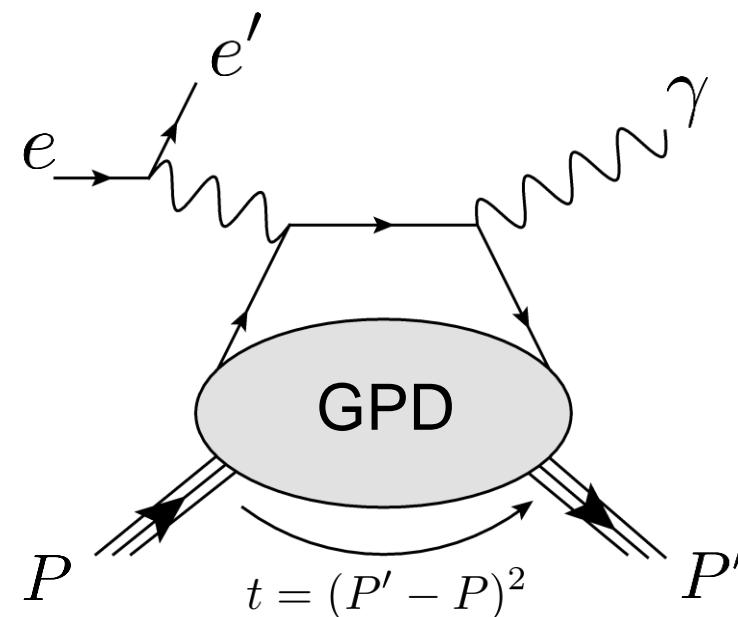
Clean final-state -- photon

Sensitive to quark GPDs

Cons:

No gluon sensitivity at LO

Flavor separation is hard



Quarks structures from DVCS

DVCS is considered the golden channel to probe GPDs.

Pros:

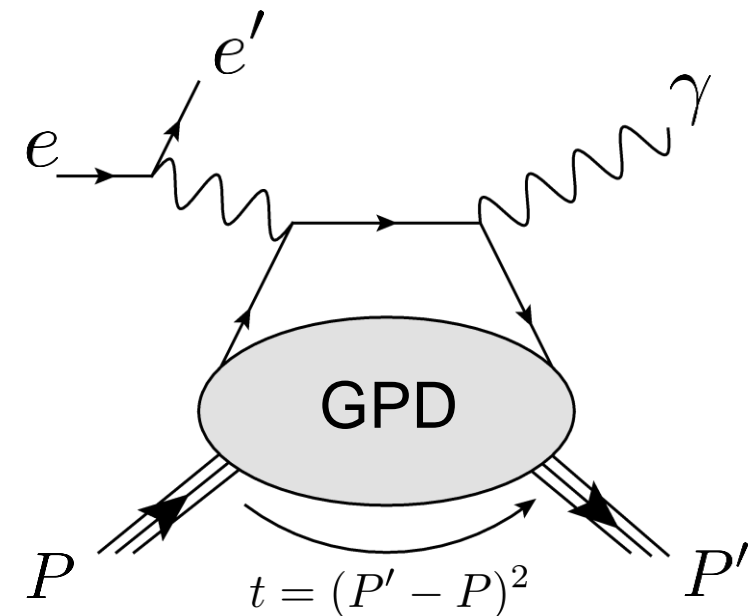
Clean final-state -- photon

Sensitive to quark GPDs

Cons:

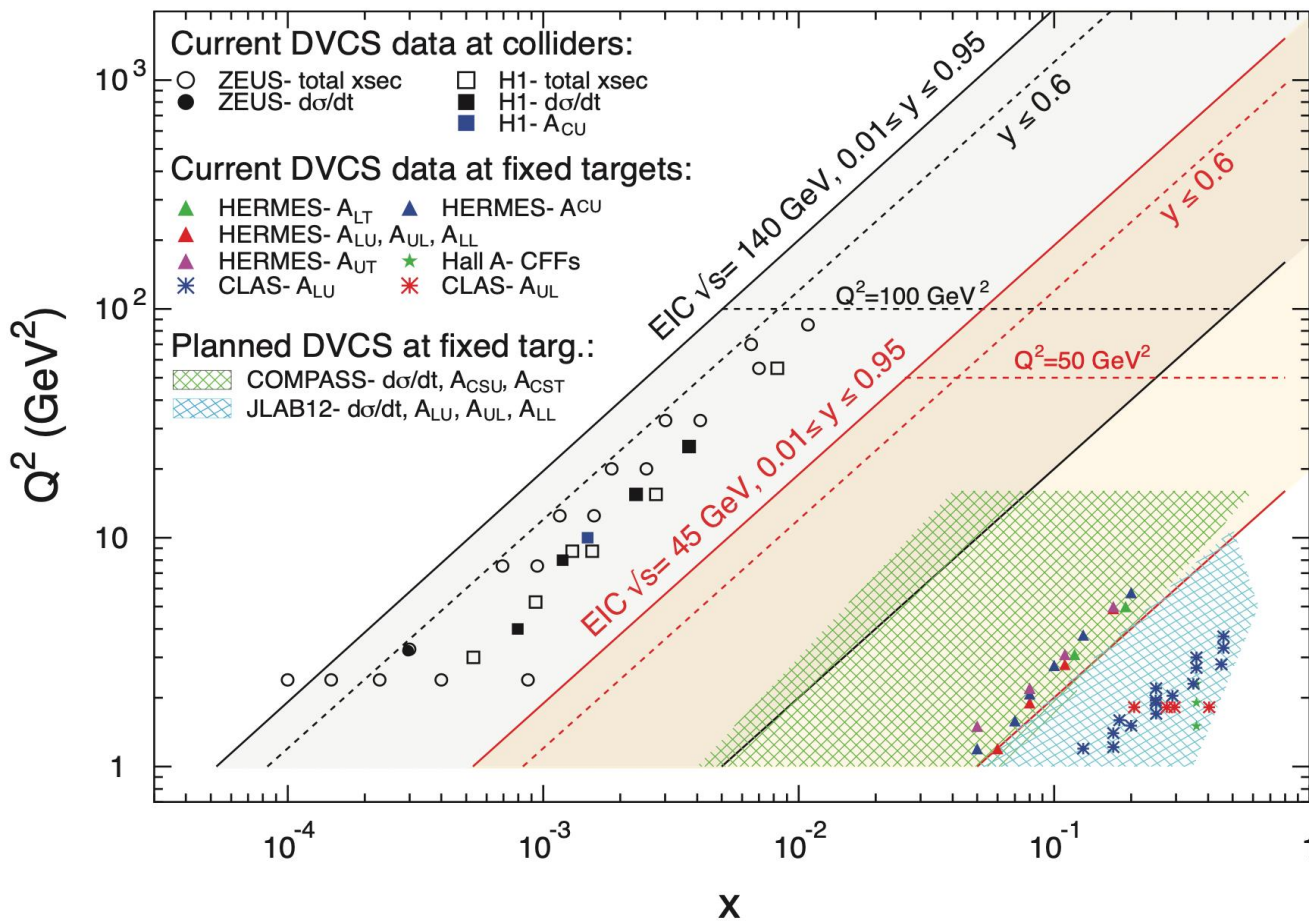
No gluon sensitivity at LO

Flavor separation is hard



Shohini's talk

DVCS measurements



EIC white paper arXiv:1212.1701

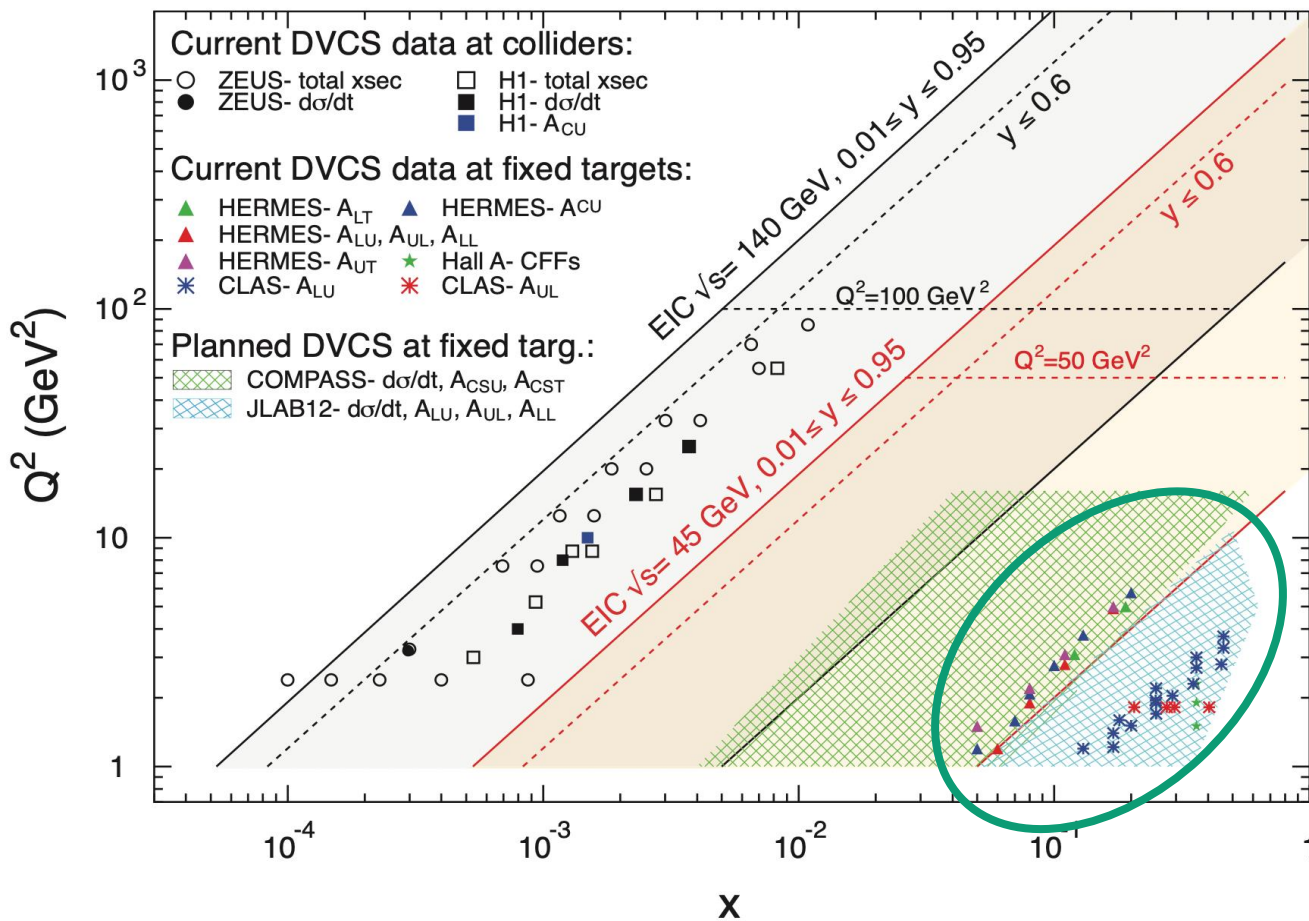
Plots in 2012 -> some recent update:

JLab has upgraded to 12 GeV (2014)

Also considering upgrading to 20+ GeV

COMPASS with asymmetry (2016)

DVCS measurements



EIC white paper arXiv:1212.1701

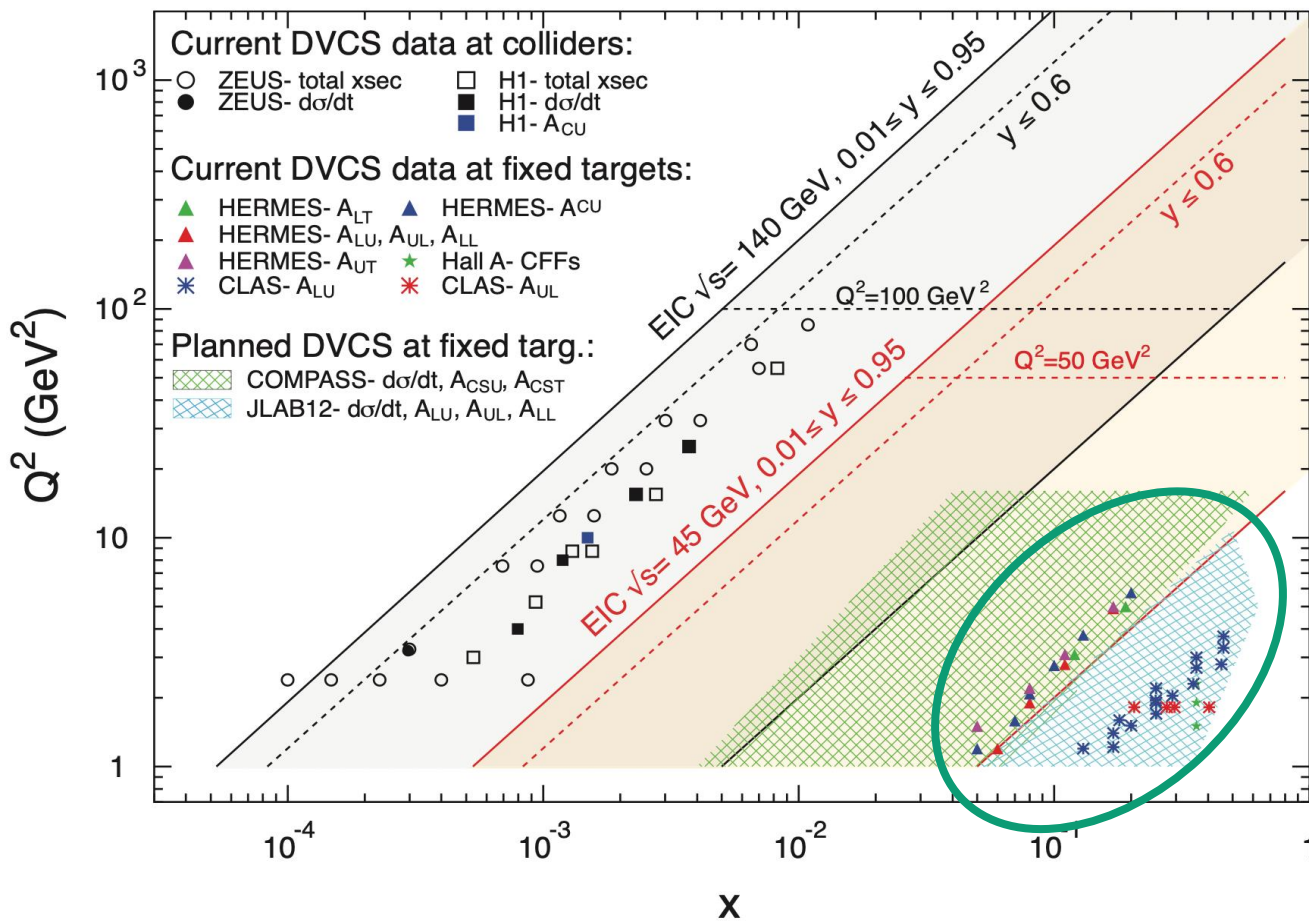
Plots in 2012 -> some recent update:

JLab has upgraded to 12 GeV (2014)

Also considering upgrading to 20+ GeV

COMPASS with asymmetry (2016)

DVCS measurements



EIC white paper arXiv:1212.1701

Plots in 2012 -> some recent update:

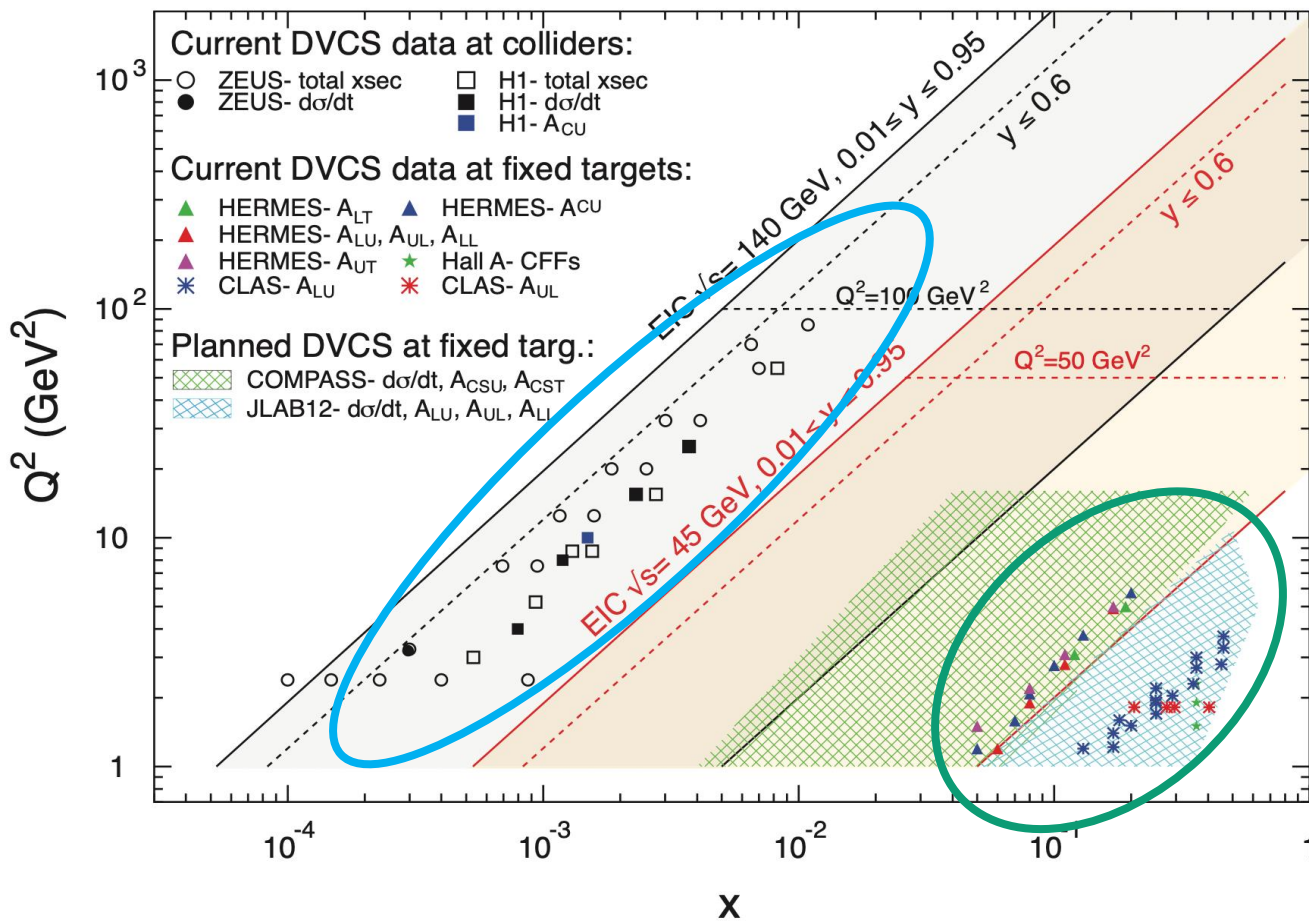
JLab has upgraded to 12 GeV (2014)

Also considering upgrading to 20+ GeV

COMPASS with asymmetry (2016)

JLab can access the valence structures well.

DVCS measurements



EIC white paper arXiv:1212.1701

Plots in 2012 -> some recent update:

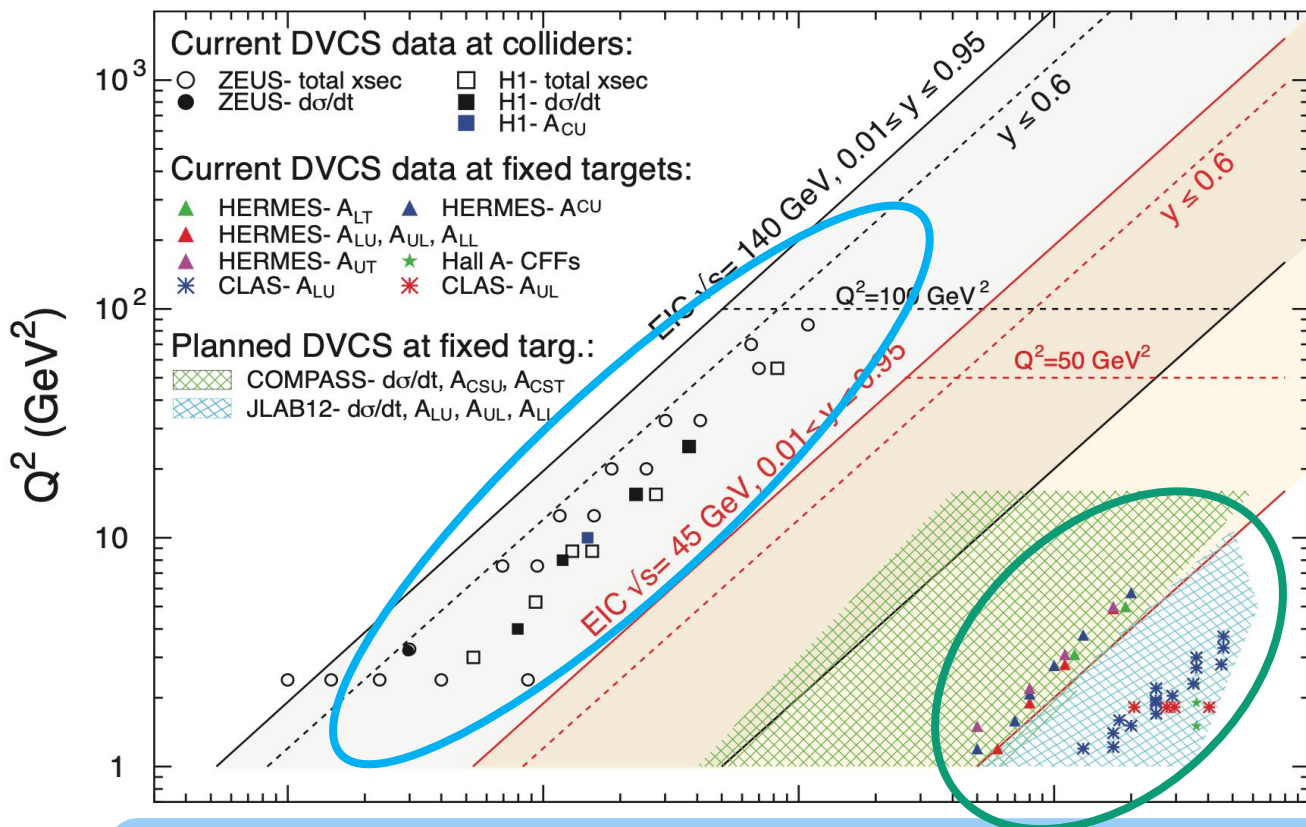
JLab has upgraded to 12 GeV (2014)

Also considering upgrading to 20+ GeV

COMPASS with asymmetry (2016)

JLab can access the valence structures well.

DVCS measurements



Plots in 2012 -> some recent update:

JLab has upgraded to 12 GeV (2014)

Also considering upgrading to 20+ GeV

COMPASS with asymmetry (2016)

JLab can access the valence structures well.

EIC is essential for exploring the sea quarks and gluons!

EIC white paper arXiv:1212.1701

Compton form factors and deconvolution

DVCS probes the GPDs via the Compton form factors

$$\mathcal{H}_{CFF}(\xi, t) = - \sum_q Q_q^2 \int_{-1}^1 dx \left(\frac{1}{x - \xi + i0} + \frac{1}{x + \xi - i0} \right) H_q(x, \xi, t) ,$$

Compton form factors and deconvolution

DVCS probes the GPDs via the Compton form factors

$$\mathcal{H}_{CFF}(\xi, t) = - \sum_q Q_q^2 \int_{-1}^1 dx \left(\frac{1}{x - \xi + i0} + \frac{1}{x + \xi - i0} \right) H_q(x, \xi, t) ,$$

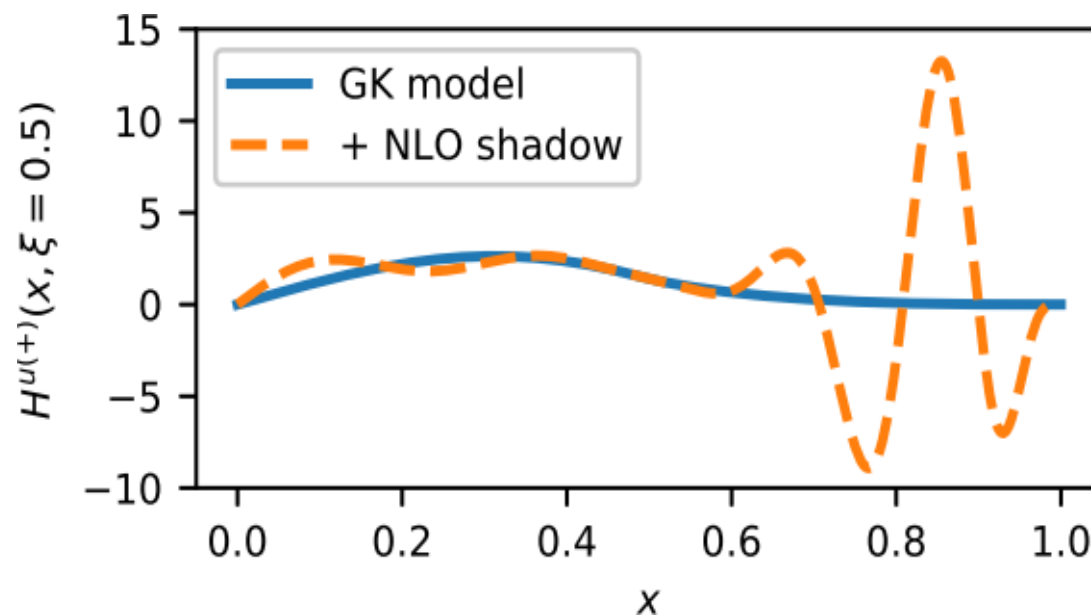
Deconvolution does not give a
unique solution – inverse problem

Compton form factors and deconvolution

DVCS probes the GPDs via the Compton form factors

$$\mathcal{H}_{CFF}(\xi, t) = - \sum_q Q_q^2 \int_{-1}^1 dx \left(\frac{1}{x - \xi + i0} + \frac{1}{x + \xi - i0} \right) H_q(x, \xi, t) ,$$

Deconvolution does not give a unique solution – inverse problem



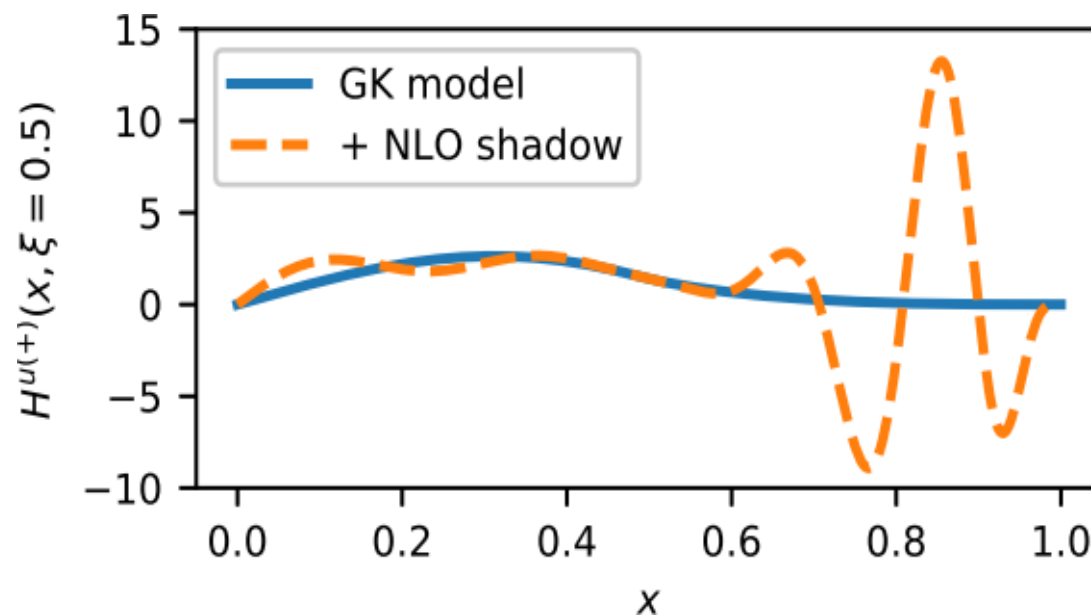
V. Bertone et. al. SciPost Phys.Proc. 8 (2022) 107

Compton form factors and deconvolution

DVCS probes the GPDs via the Compton form factors

$$\mathcal{H}_{CFF}(\xi, t) = - \sum_q Q_q^2 \int_{-1}^1 dx \left(\frac{1}{x - \xi + i0} + \frac{1}{x + \xi - i0} \right) H_q(x, \xi, t) ,$$

Deconvolution does not give a unique solution – inverse problem



Dr. Qiu's talk

V. Bertone et. al. SciPost Phys.Proc. 8 (2022) 107

Compton form factors and deconvolution

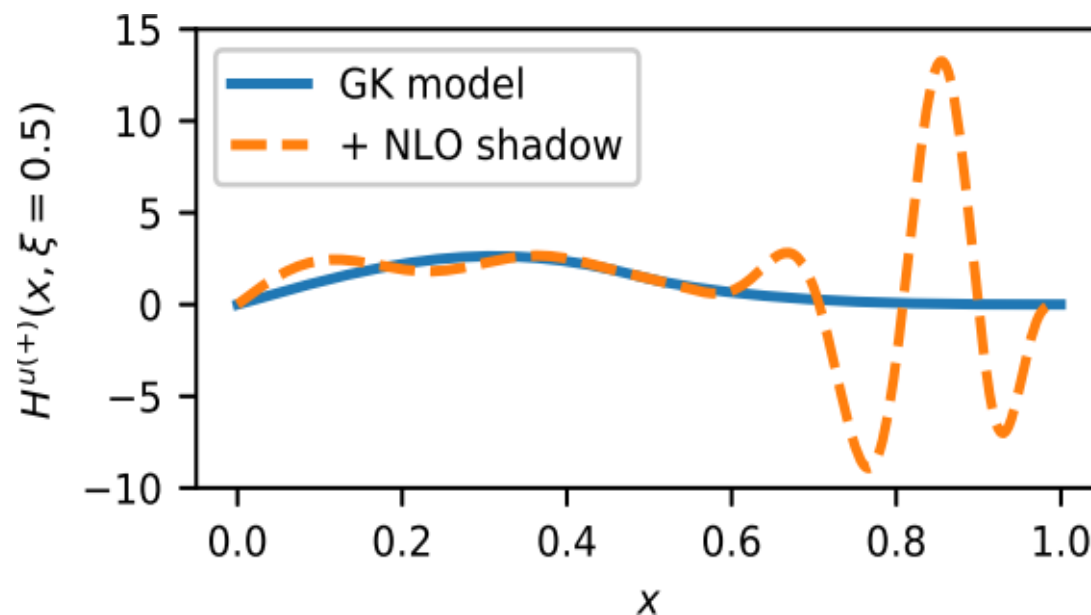
DVCS probes the GPDs via the Compton form factors

$$\mathcal{H}_{CFF}(\xi, t) = - \sum_q Q_q^2 \int_{-1}^1 dx \left(\frac{1}{x - \xi + i0} + \frac{1}{x + \xi - i0} \right) H_q(x, \xi, t) ,$$

Deconvolution does not give a unique solution – inverse problem



Global analysis needed



Dr. Qiu's talk

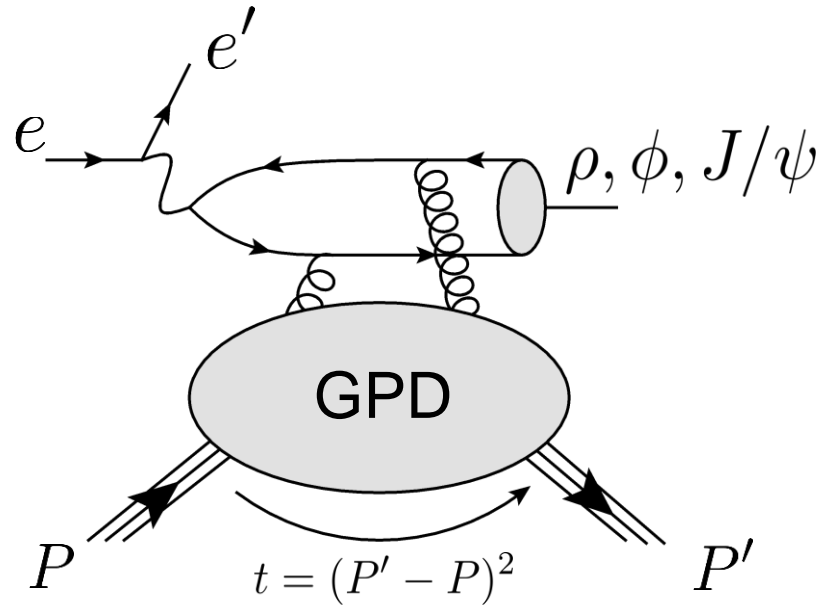
V. Bertone et. al. SciPost Phys.Proc. 8 (2022) 107

Gluon 3D structures from experiment

Gluon can only be directly probed by strongly interacting particles – meson ...

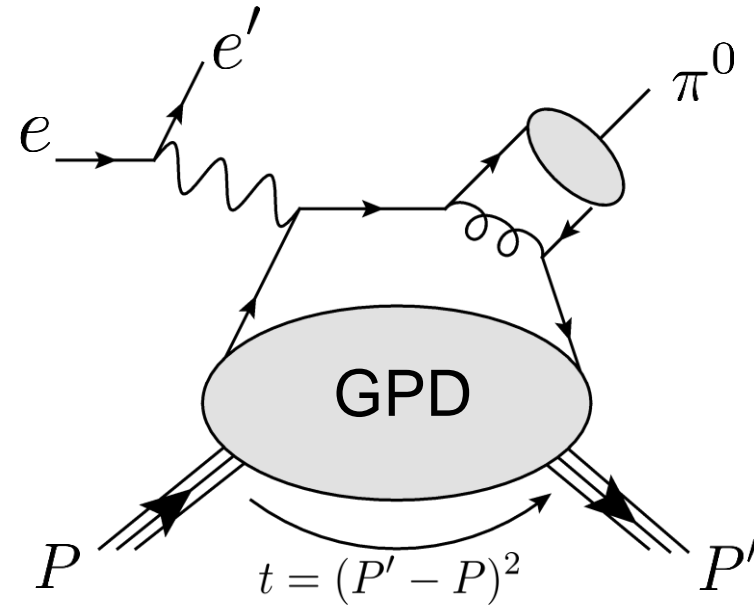
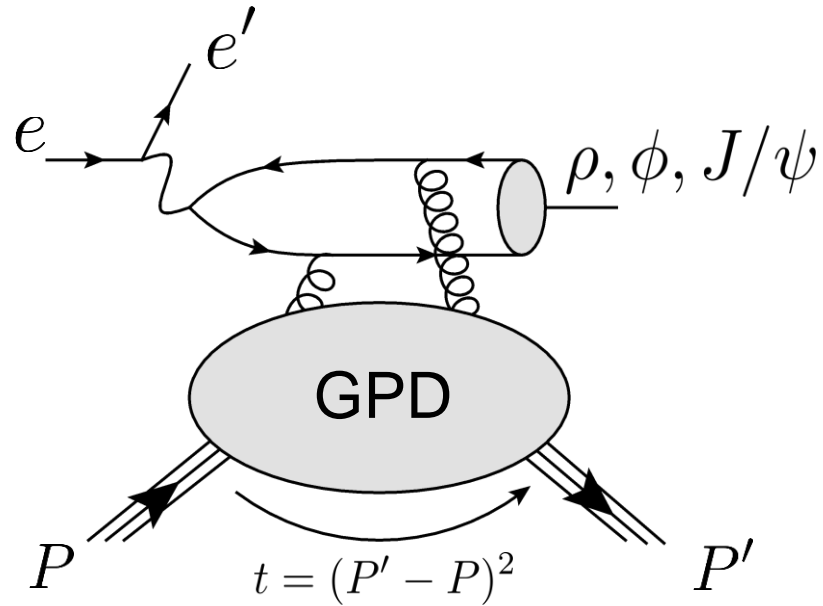
Gluon 3D structures from experiment

Gluon can only be directly probed by strongly interacting particles – meson ...



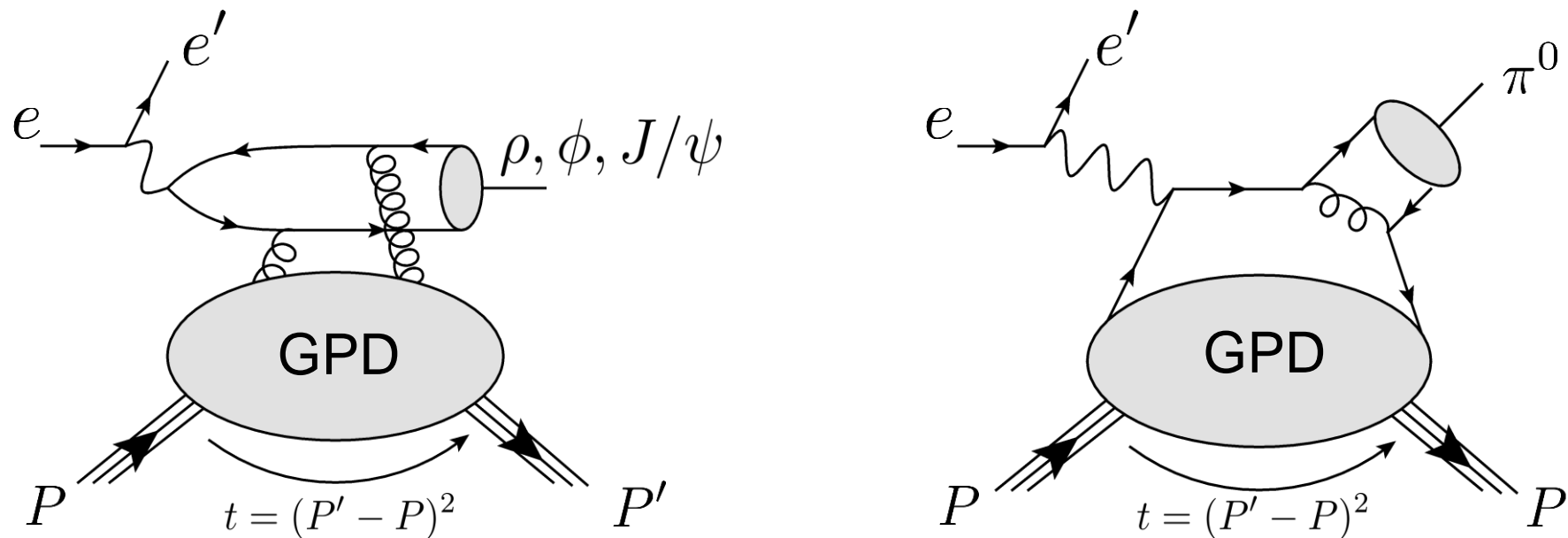
Gluon 3D structures from experiment

Gluon can only be directly probed by strongly interacting particles – meson ...



Gluon 3D structures from experiment

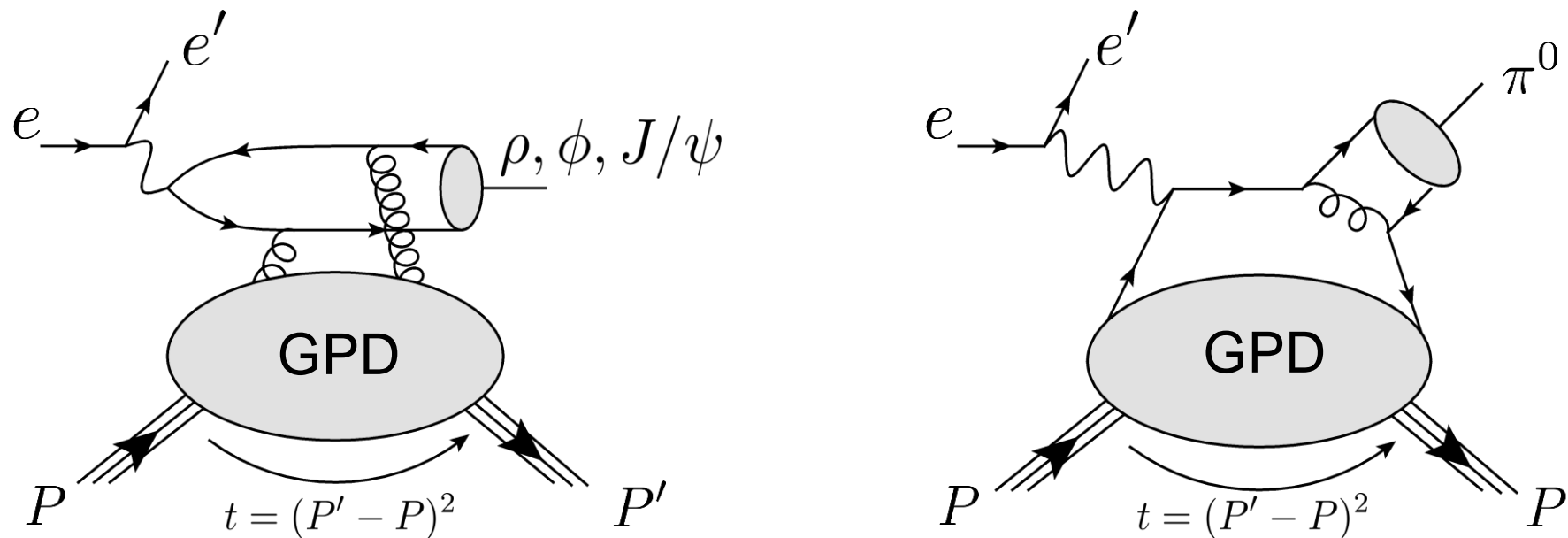
Gluon can only be directly probed by strongly interacting particles – meson ...



Heavy meson preferred to suppress the intrinsic quark contributions.

Gluon 3D structures from experiment

Gluon can only be directly probed by strongly interacting particles – meson ...

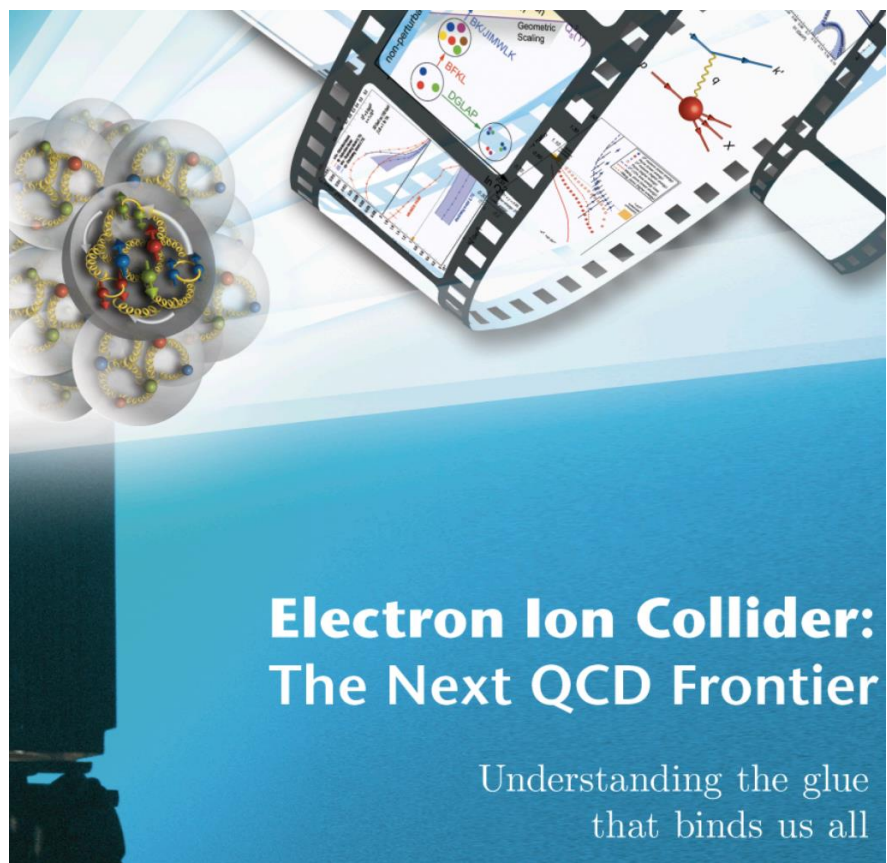


Heavy meson preferred to suppress the intrinsic quark contributions.

Higher energy required. (Hard to reach with fixed target)

Gluon 3D structures from experiment

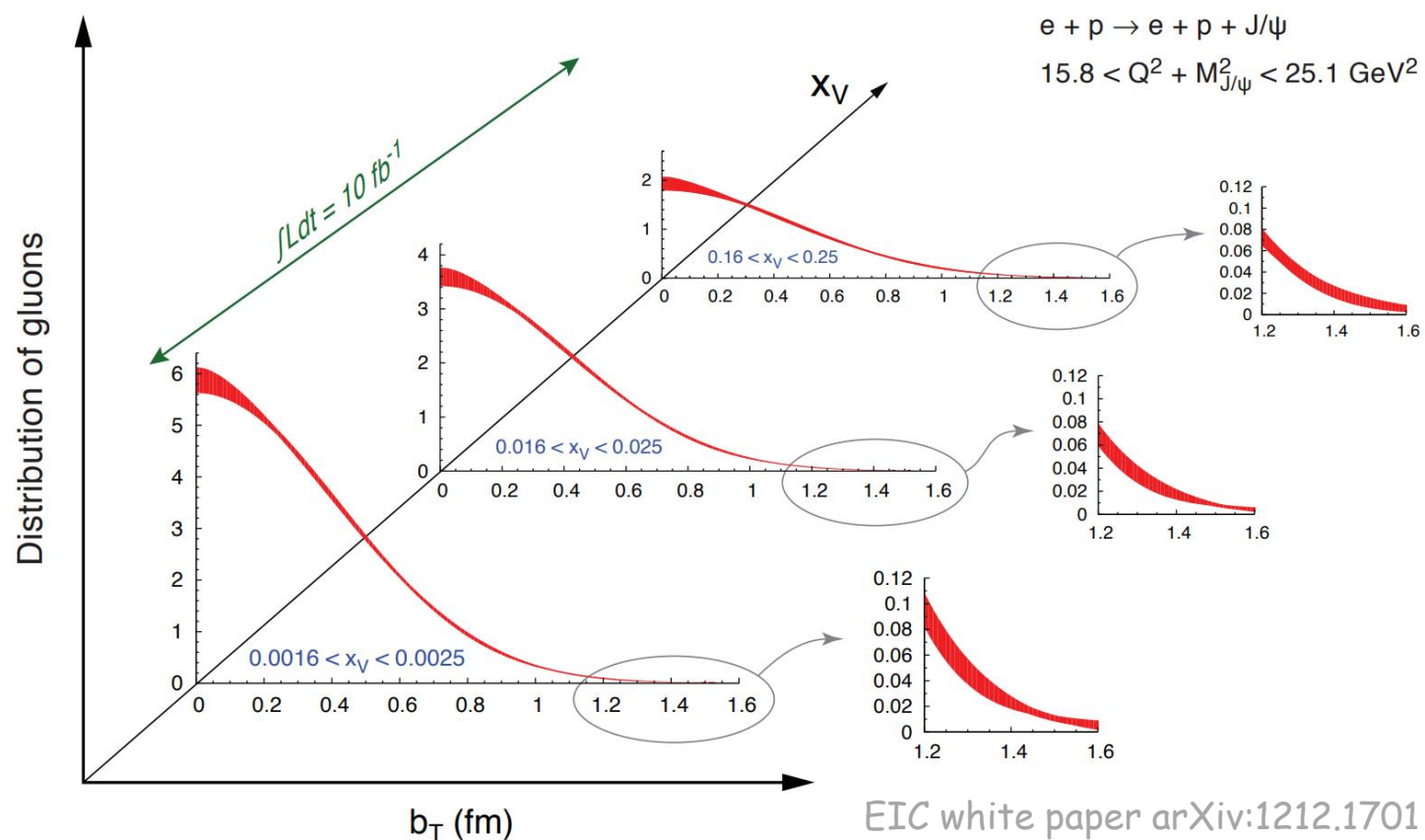
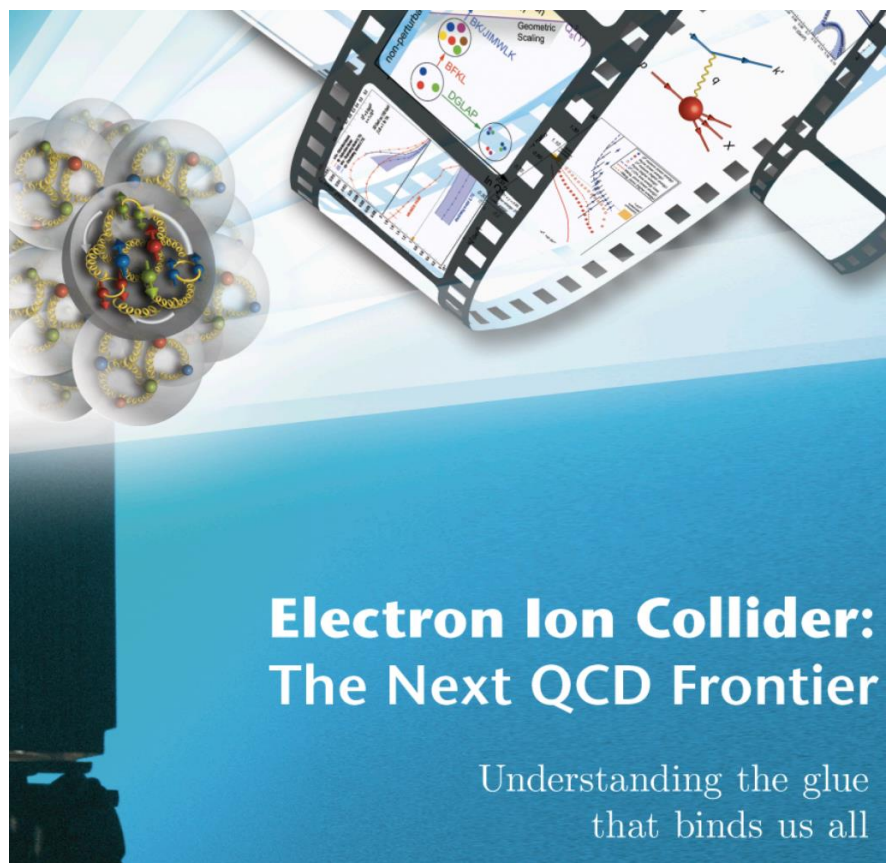
Main task of EIC – exploring the gluons (with meson production, jet production ...)



EIC white paper arXiv:1212.1701

Gluon 3D structures from experiment

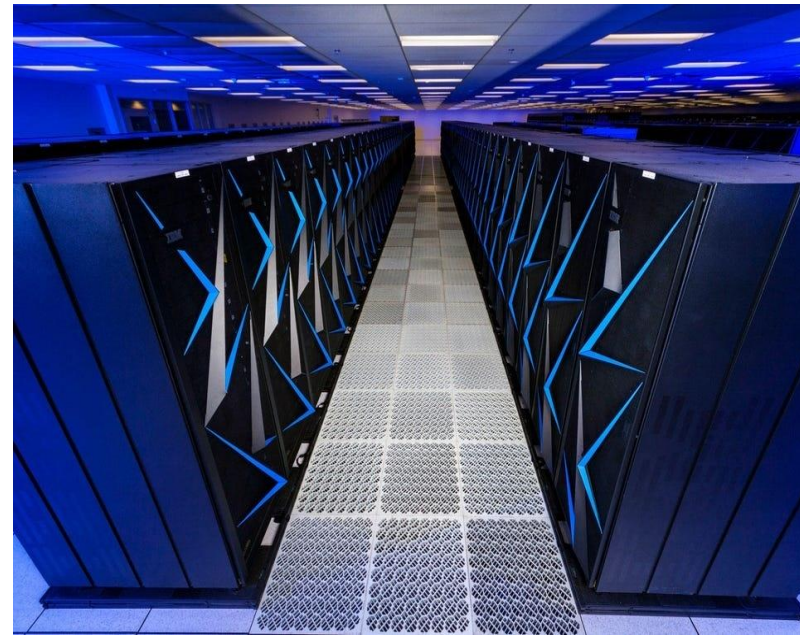
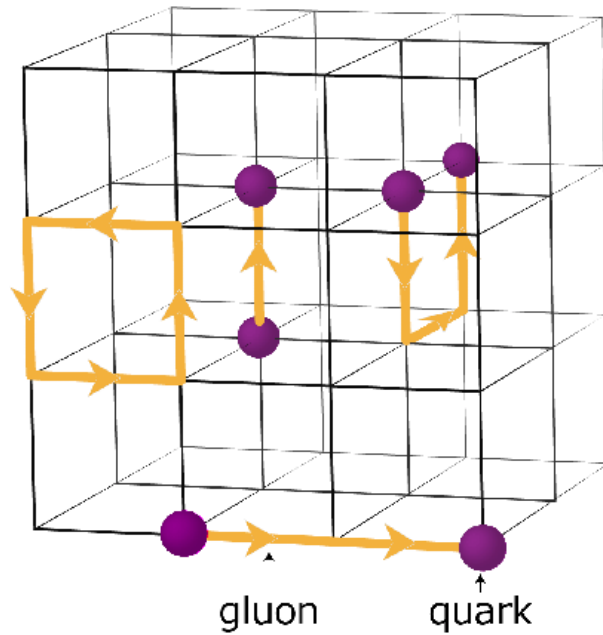
Main task of EIC – exploring the gluons (with meson production, jet production ...)



3D Structures with Lattice QCD

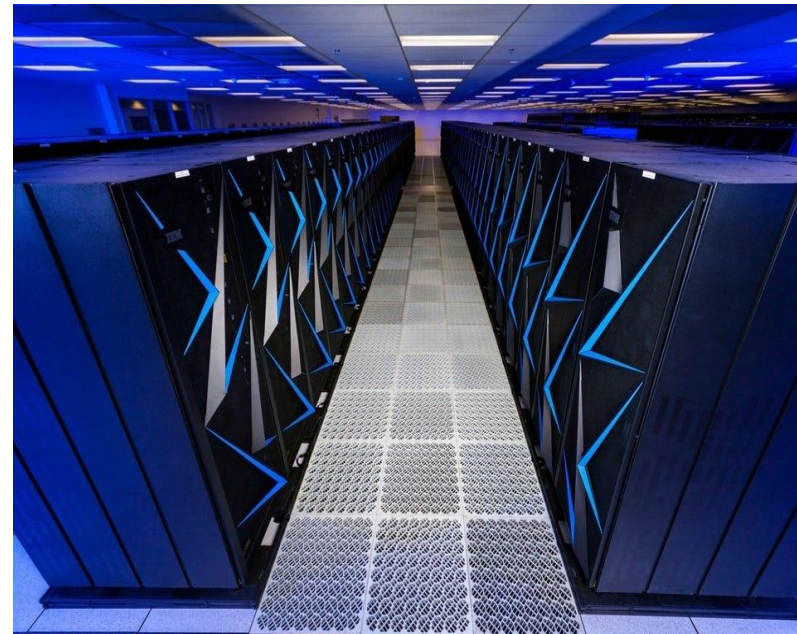
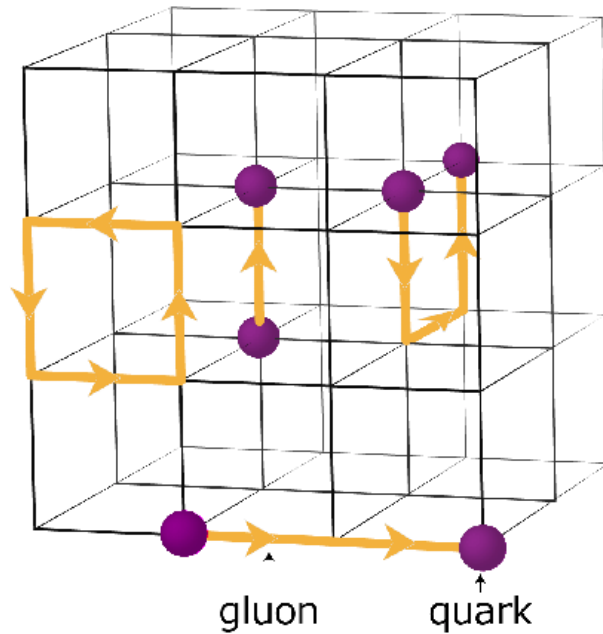
Lattice QCD

Simulation of discretized, finite-volume system with super computers.



Lattice QCD

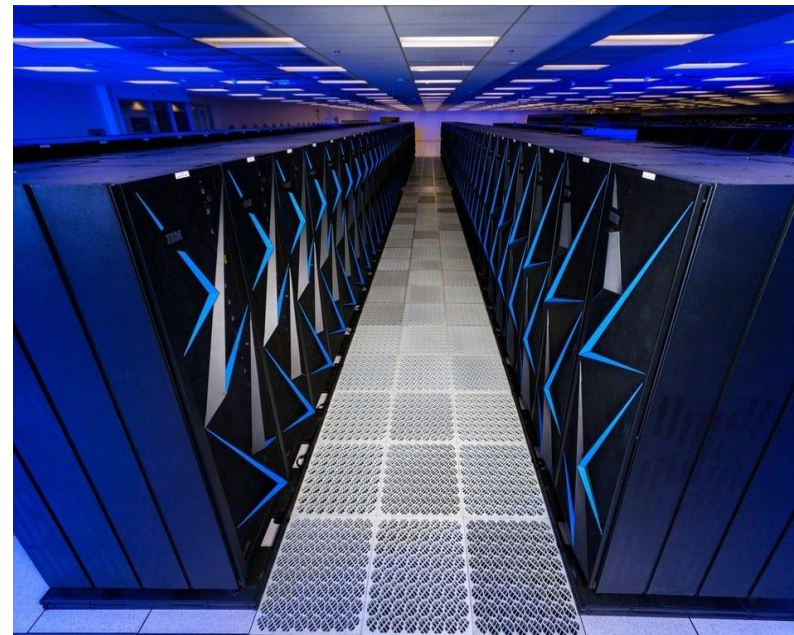
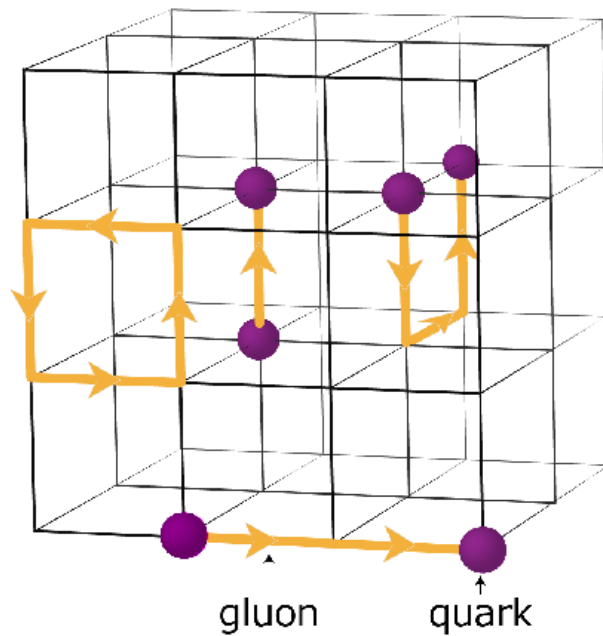
Simulation of discretized, finite-volume system with super computers.



From first-principle and systematically improvable.

Lattice QCD

Simulation of discretized, finite-volume system with super computers.



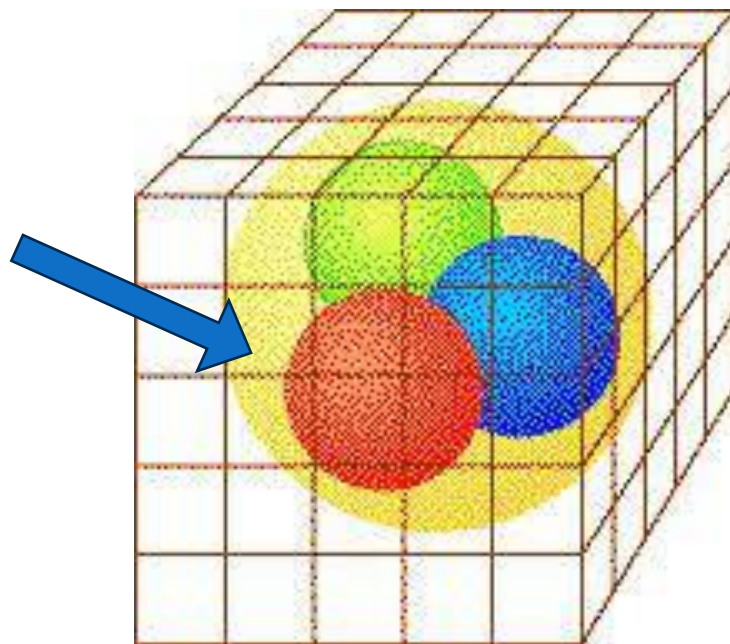
From first-principle and systematically improvable.

Nucleon form factors on lattice

Lattice QCD is most efficient in capturing the feature of the whole nucleon.

$$\hat{O}_q^\mu = \sum_q e_q \bar{\psi}_q \gamma^\mu \psi_q$$
$$\hat{O}_q^{\mu\nu} = \sum_q \bar{\psi}_q \gamma^{(\mu} i \overleftrightarrow{D}^{\nu)} \psi_q$$

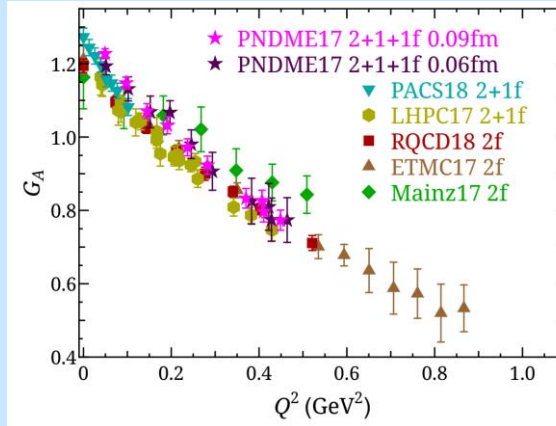
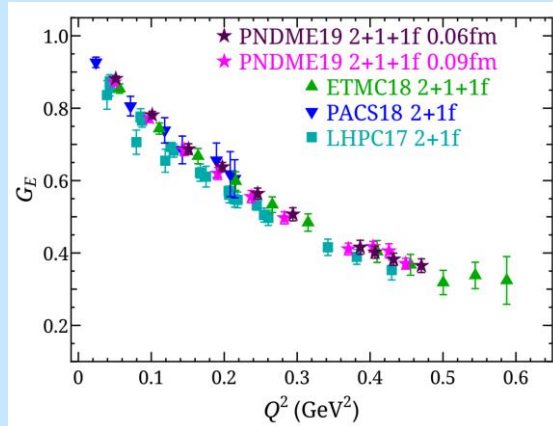
...



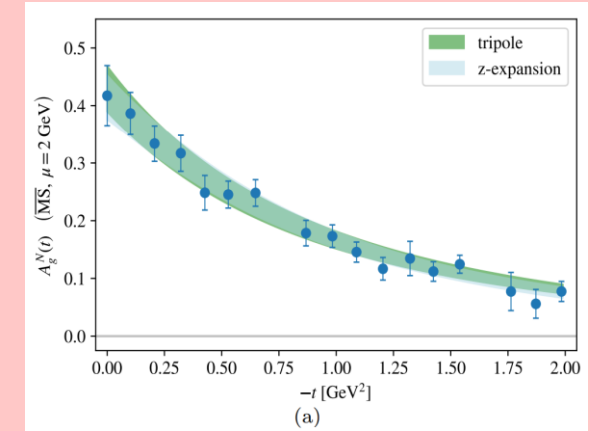
Relatively easy so long as you can prepare a static nucleon on the lattice

Nucleon form factors on lattice

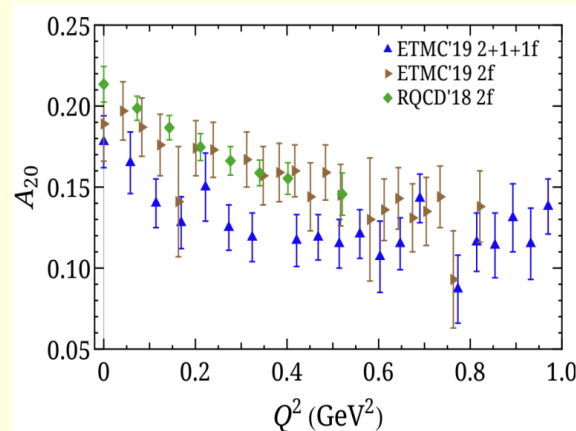
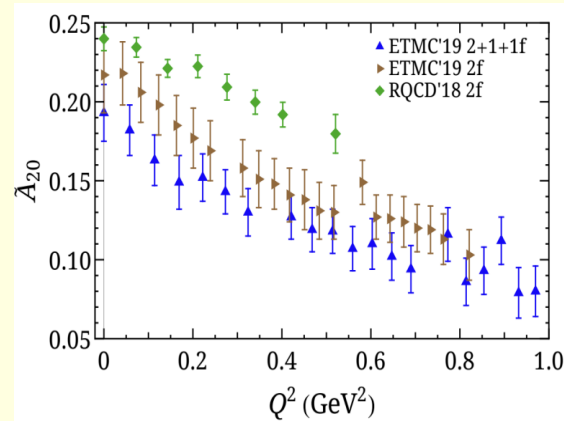
Isovector (axial) charge form factors with lattice QCD



Gluon gravitational form factors



Isovector (axial) gravitational form factors with lattice QCD



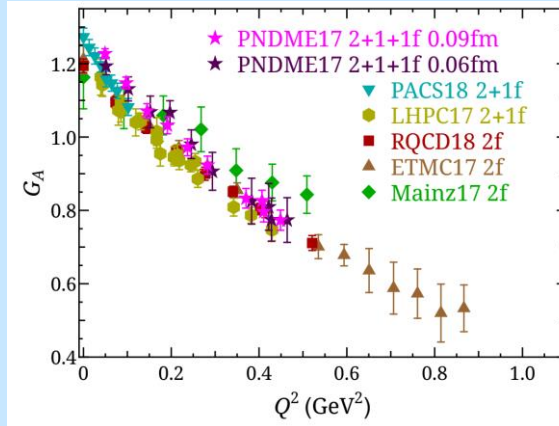
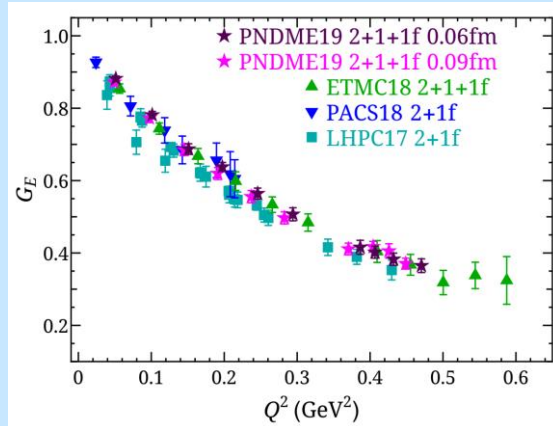
D. A. Pefkou et al.
Phys. Rev. D 105, 054509 (2022)

Reviewed in M. Constantinou et al. Prog. Part. Nucl. Phys. 121 103908 (2021)

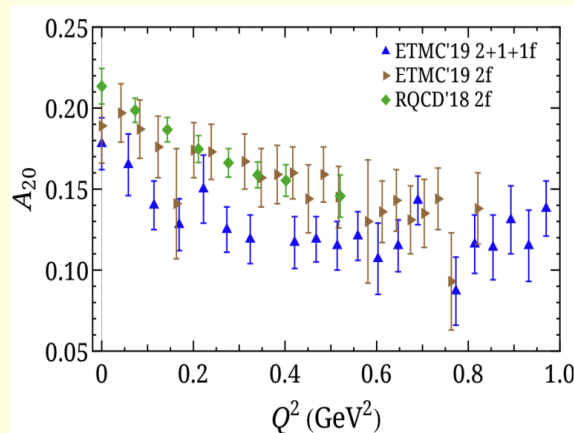
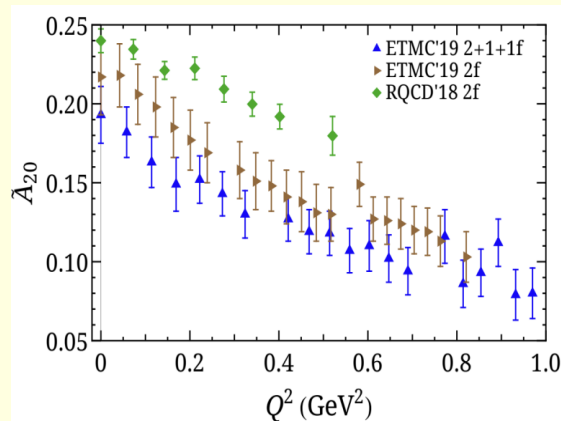
Collected results from lattice community including ETMC, LHPC, Mainz, PACS, PNDME, RQCD

Nucleon form factors on lattice

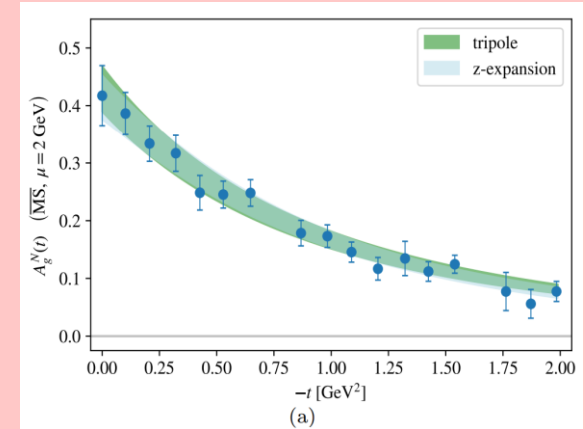
Isovector (axial) charge form factors with lattice QCD



Isovector (axial) gravitational form factors with lattice QCD



Gluon gravitational form factors



D. A. Pefkou et al .
Phys. Rev. D 105, 054509 (2022)

Many are almost impossible
to get from experiments!

Reviewed in M. Constantinou et. al. Prog. Part. Nucl. Phys. 121 103908 (2021)

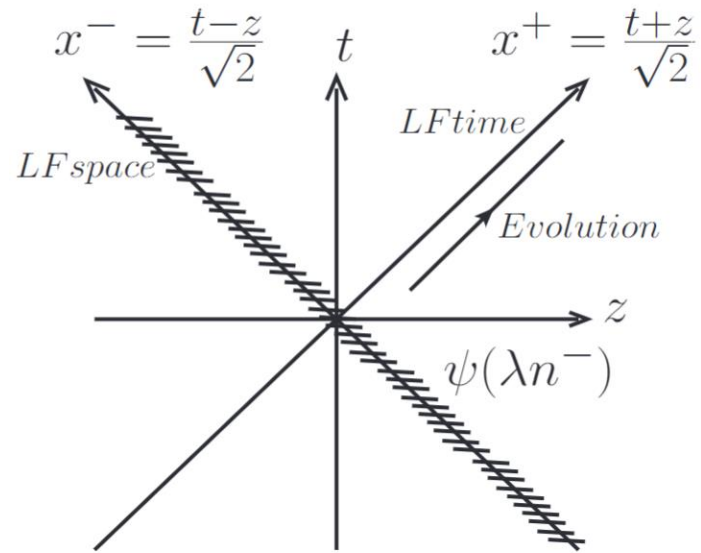
Collected results from lattice community including ETMC, LHPC, Mainz, PACS, PNDME, RQCD

Parton distributions on lattice

Measuring the real-time dynamics, on the other hand, is much harder on lattice.

Parton distributions on lattice

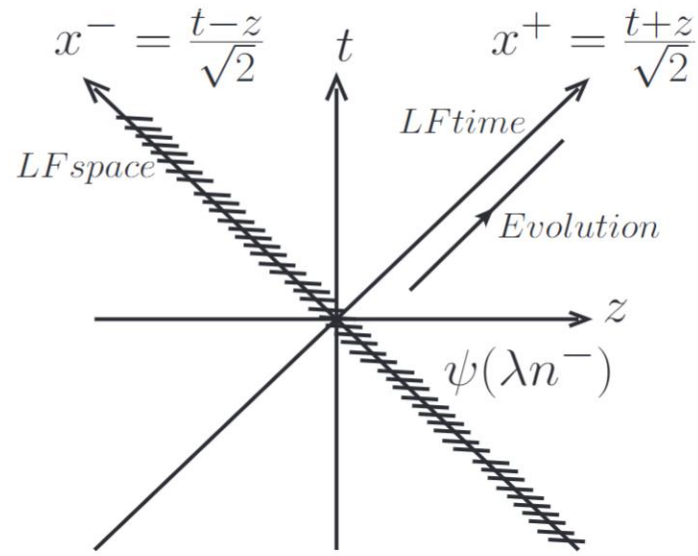
Measuring the real-time dynamics, on the other hand, is much harder on lattice.



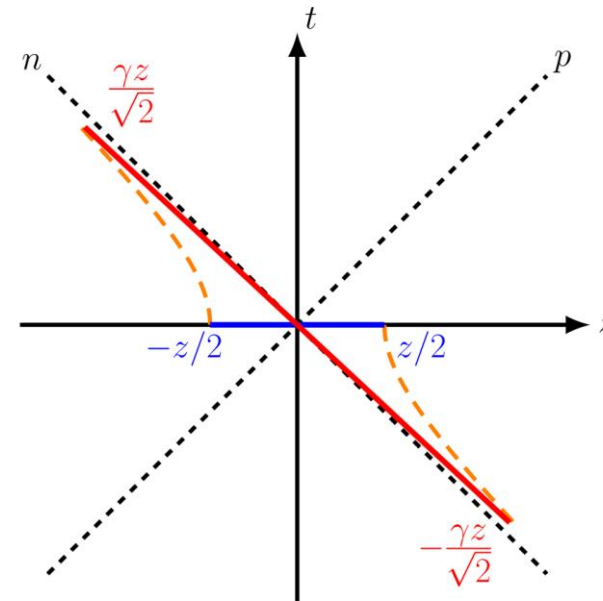
Partons live on light front.

Parton distributions on lattice

Measuring the real-time dynamics, on the other hand, is much harder on lattice.



Partons live on light front.

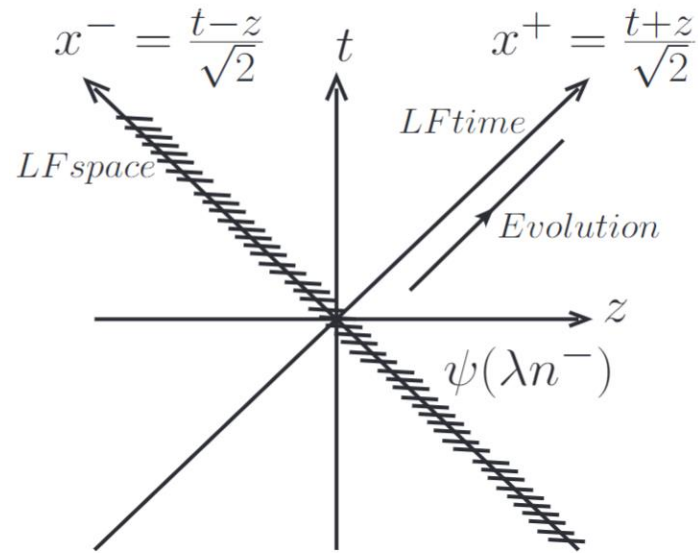


Large Momentum Effective Theory (LaMET)

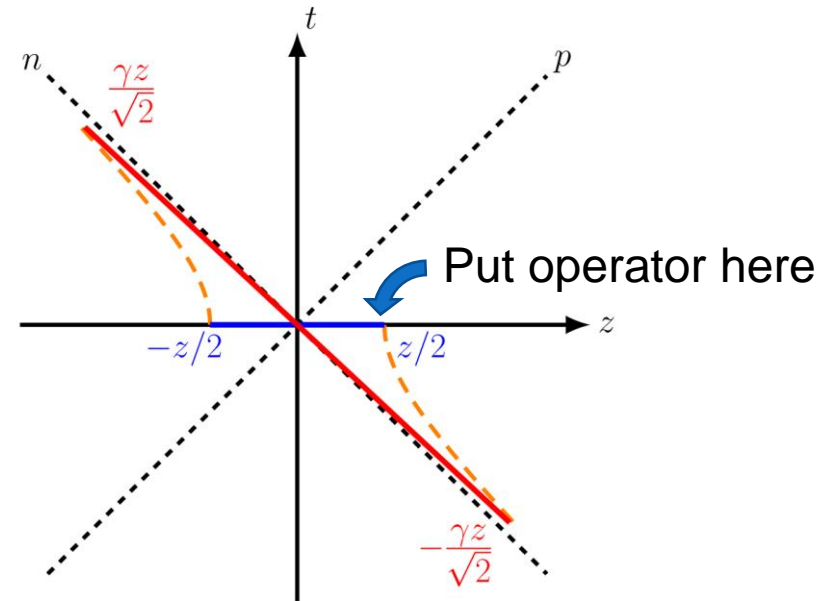
X. Ji et. al. Rev. Mod. Phys. 93 3, 035005 (2021)

Parton distributions on lattice

Measuring the real-time dynamics, on the other hand, is much harder on lattice.



Partons live on light front.

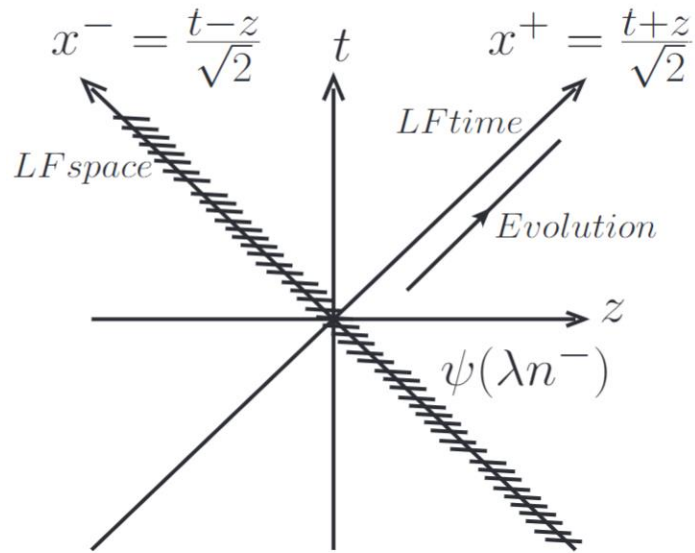


Large Momentum Effective Theory (LaMET)

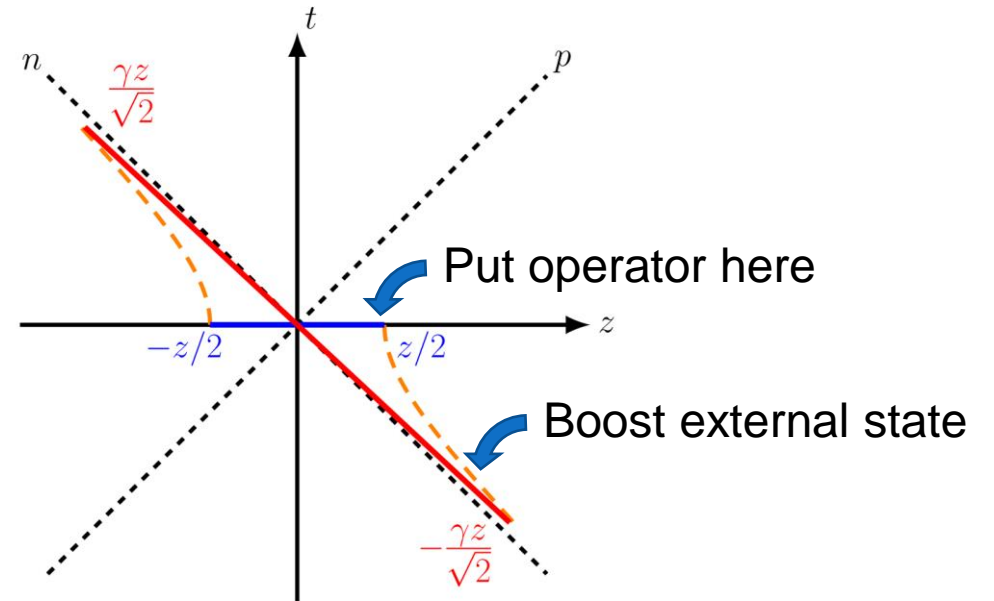
X. Ji et. al. Rev. Mod. Phys. 93 3, 035005 (2021)

Parton distributions on lattice

Measuring the real-time dynamics, on the other hand, is much harder on lattice.



Partons live on light front.

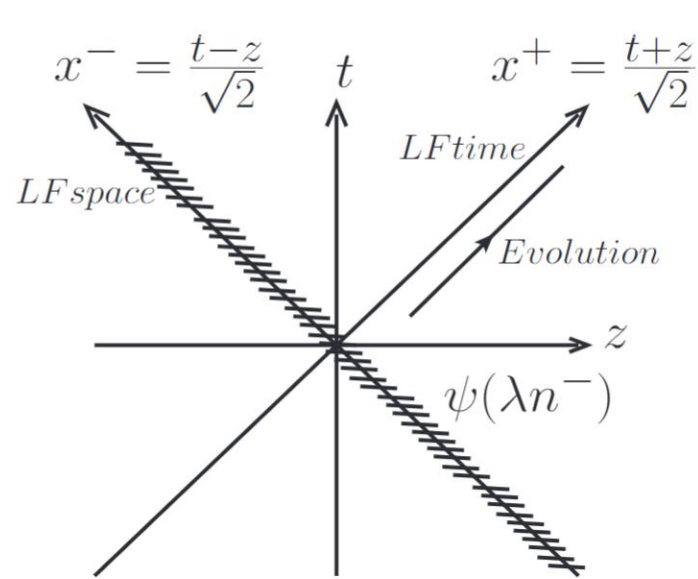


Large Momentum Effective Theory (LaMET)

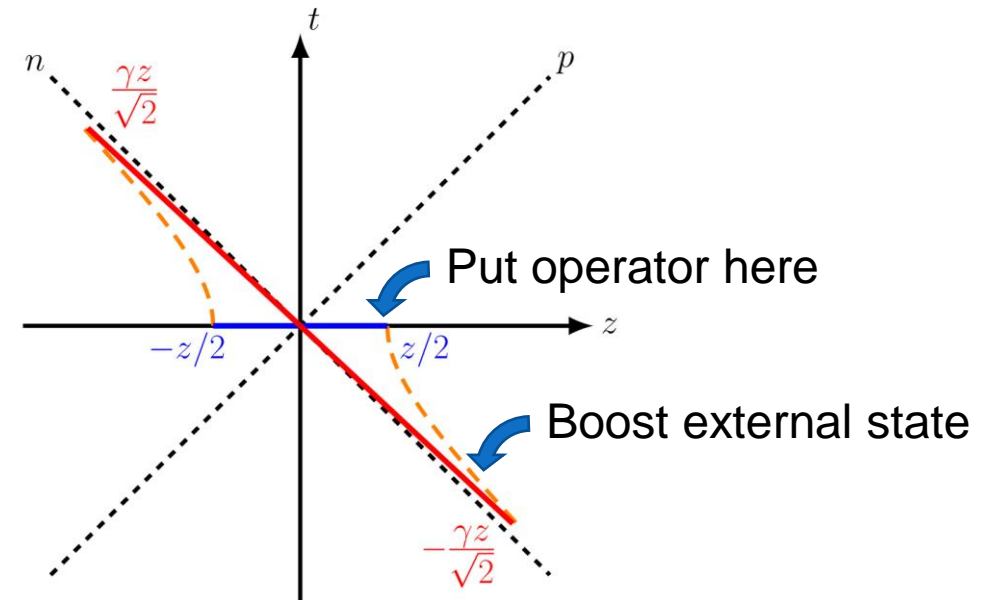
X. Ji et. al. Rev. Mod. Phys. 93 3, 035005 (2021)

Parton distributions on lattice

Measuring the real-time dynamics, on the other hand, is much harder on lattice.



Partons live on light front.



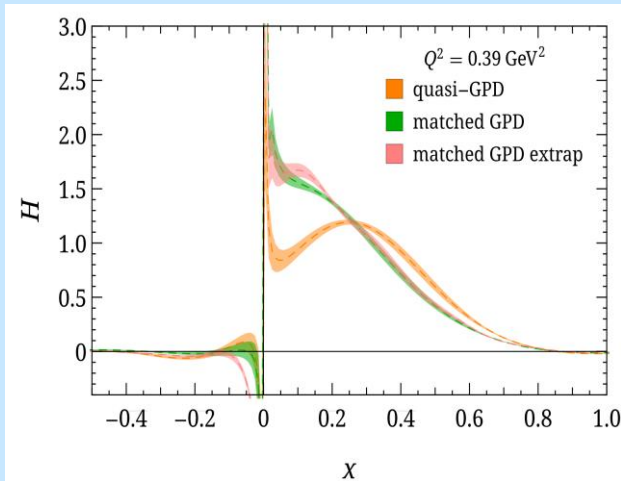
Large Momentum Effective Theory (LaMET)

X. Ji et. al. Rev. Mod. Phys. 93 3, 035005 (2021)

Massive progresses have been made for PDFs/DAs. Here we focus on GPDs.

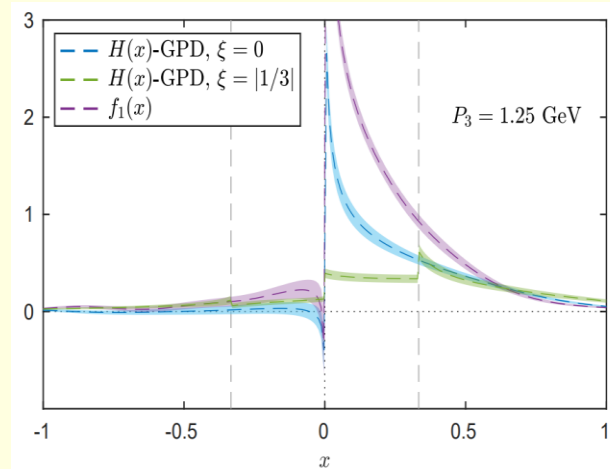
Parton distributions on lattice

Isovector H GPDs



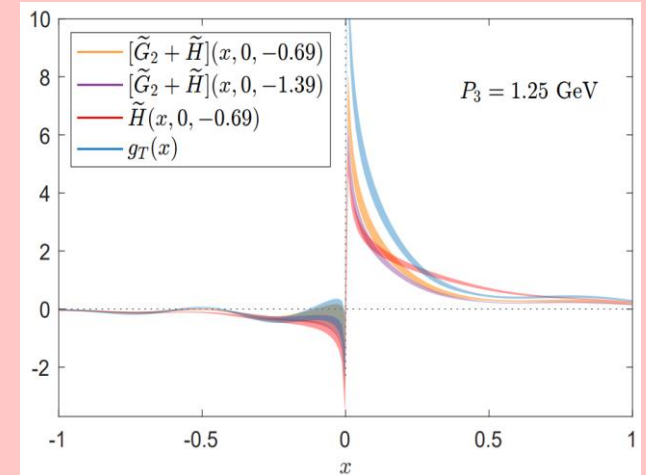
Huey-Wen Lin
Phys.Rev.Lett. 127 18, 182001 (2021)

Isovector H GPDs (skewness)



C. Alexandrou et. al. (ETMC)
Phys.Rev.Lett. 125 26, 262001 (2020)

Isovector Twist-3 GPDs

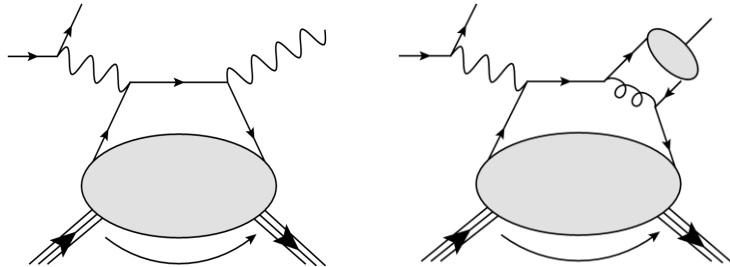


S. Bhattacharya et. al.
PoS LATTICE2021 054 (2022)

3D GPD global analysis

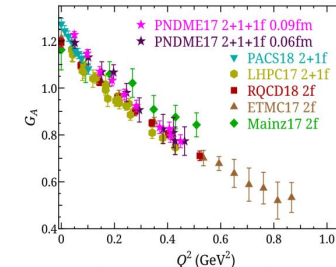
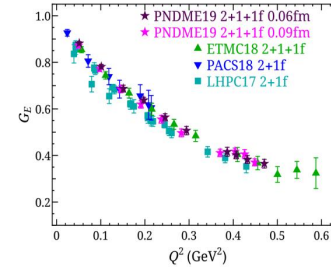
Composite tasks for GPD study

The high-dimensional nature of GPD requires composite inputs.



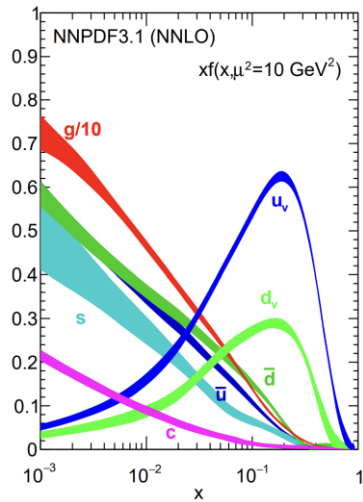
X. Ji, Phys. Rev. D 55, 7114 (1997) A.V. Radyushkin, Phys. Lett. B 385 333 (1996)
J. C. Collins et. al. Phys. Rev. D 56 2982 (1997)

Deeply virtual exclusive processes



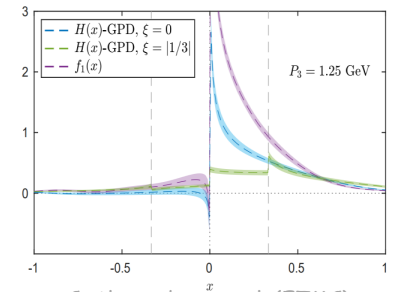
Review in M. Constantinou et. al. Prog. Part. Nucl. Phys. 121 103908 (2021). And references therein

Nucleon form factors from lattice

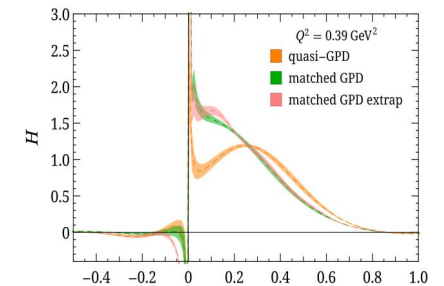


NNPDF et al., Eur. Phys. J. C 77, 663 (2017)

Parton Distribution Function



C. Alexandrou et. al. (ETMC) Phys. Rev. Lett. 125, 262001 (2020)

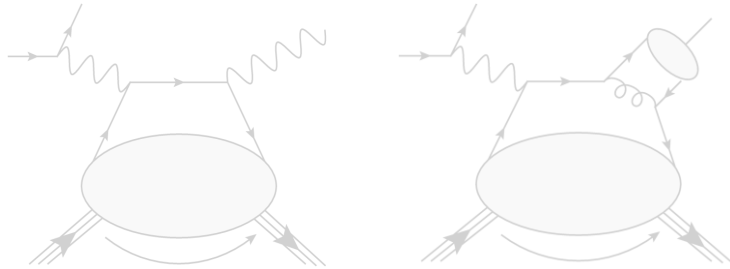


Huey^xWen Lin Phys. Rev. Lett. 127, 182001 (2021)

x-dependence from lattice

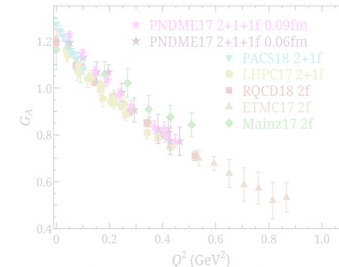
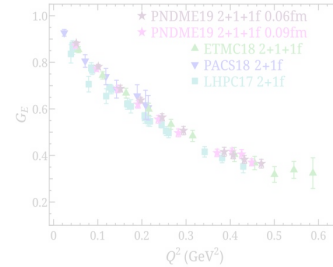
Composite tasks for GPD study

The high-dimensional nature of GPD requires composite inputs.



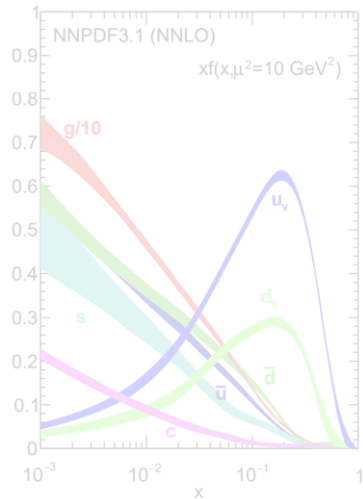
X. Ji, Phys. Rev. D 55, 7114 (1997) A.V. Radyushkin, Phys. Lett. B 385 333 (1996)
J. C. Collins et. al. Phys. Rev. D 56 2982 (1997)

Deeply virtual exclusive processes



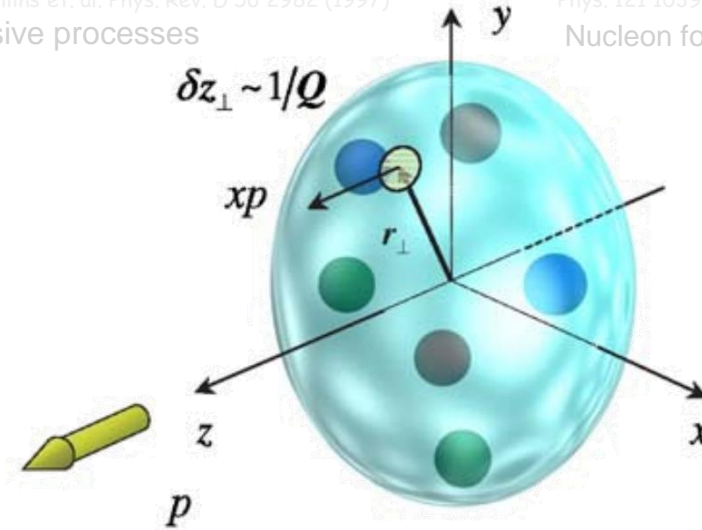
Review in M. Constantinou et. al. Prog. Part. Nucl. Phys. 121 103908 (2021). And references therein

Nucleon form factors from lattice



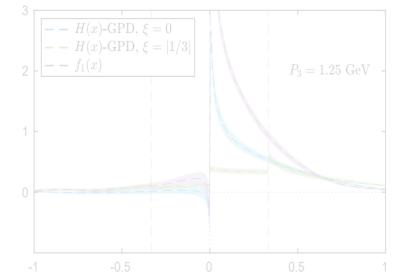
NNPDF et al., Eur. Phys. J. C 77, 663 (2017)

Parton Distribution Function

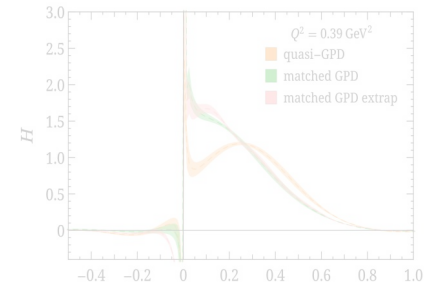


3D Quark-Gluon Tomography

Yuxun Guo @ CFNS Stony Brook



C. Alexandrou et. al. (ETMC) Phys. Rev. Lett. 125, 262001 (2020)



Huey-xWen Lin Phys. Rev. Lett. 127, 182001 (2021)
x-dependence from lattice

Global GPD Global analysis efforts

The logo for Gepard features the word "Gepard" in a stylized font. The "G" is blue, and the "epard" is green.

K. Kumericki et al.
Nucl. Phys. B 794 244-323 (2008)

The logo for PARTONS features the word "PARTONS" in a stylized font. The "P" is blue, and the "ARTONS" is black. A stylized orange and blue particle symbol is integrated into the "O".The logo for STRONG 2020 features the word "STRONG" in blue, with a stylized particle symbol in the "O". Below it is a blue box with white stars and the number "2020".

B. Berthou et al.
Eur. Phys. J. C 78 6, 478 (2018)

The logo for the Quark-Gluon Tomography Collaboration features a circular design with three overlapping segments in blue, red, and green. The text "PHENOMENOLOGY" is at the top, "LATTICE QCD" is on the left, and "THEORY" is on the right. To the right of the circle, the text "QUARK-GLUON TOMOGRAPHY COLLABORATION" is written in blue.

Machine Learning Approach

Eric Moffat et al.
Phys. Rev. D 108 3, 036027 (2023)

GUMP

Y. Guo et al. JHEP 09 215 (2022)
Y. Guo et al. JHEP 05 150 (2023)

The logo for FemtoNET features a stylized particle symbol on the left and the text "FemtoNET" in white on a black background.

M. Almaeen et al.
arxiv: 2207.10766

GPD global analysis

While each task faces its own challenge, the global analysis is the gatekeeper.

GPD global analysis

While each task faces its own challenge, the global analysis is the gatekeeper.



Parameterization of GPDs

Compute GPD observables

Constraints on GPDs

Compare and iterate

GPD global analysis

While each task faces its own challenge, the global analysis is the gatekeeper.



Parameterization of GPDs

Compute GPD observables

Constraints on GPDs

Compare and iterate

- Massive degrees of freedom

GPD global analysis

While each task faces its own challenge, the global analysis is the gatekeeper.



Parameterization of GPDs

Compute GPD observables

Constraints on GPDs

Compare and iterate

- Massive degrees of freedom

- Both x & moment space with evolution

GPD global analysis

While each task faces its own challenge, the global analysis is the gatekeeper.

Parameterization of GPDs

- Massive degrees of freedom

Compute GPD observables

- Both x & moment space with evolution

Constraints on GPDs

- Various inputs from very different system

Compare and iterate

GPD global analysis

While each task faces its own challenge, the global analysis is the gatekeeper.

Parameterization of GPDs

- Massive degrees of freedom

Compute GPD observables

- Both x & moment space with evolution

Constraints on GPDs

- Various inputs from very different system

Compare and iterate

- Computation efficiency!

Parameterization of GPD

We employ the established conformal partial wave expansion of GPD

$$F(x, \xi, t) = \sum_{j=0}^{\infty} (-1)^j p_j(x, \xi) \mathcal{F}_j(\xi, t)$$

D. Mueller and A. Schafer Nucl. Phys. B 739 1-59 (2006)

Advantages:

- Polynomiality condition: $\int_{-1}^1 dx x^{n-1} F(x, \xi, t) = \sum_{k=0, \text{even}}^n \xi^k F_{n,k}(t)$ X. Ji, J. Phys. G 24 1181-1205 (1998)
- Conformal moments are (LO) multiplicatively renormalizable

I. Balitsky and V. Braun Nucl. Phys. B 311 541-584 (1989)

GPDs through Universal Moment Parameterization (GUMP)

Collaborators: Xiangdong Ji, Kyle Shiells, Gabriel Santiago, Jinghong Yang

Y. Guo et. al. JHEP 09 215 (2022)

Y. Guo et. al. JHEP 05 150 (2023)

Inputs for the global analysis

Experiments

- PDFs from global analysis
 - Polarized and unpolarized PDFs from JAM

JAM, Phys. Rev. D 106 3, L031502 (2022)

- Charge form factors from global analysis

- YAHL global analysis of EM form factors
- Flavor separation combining proton and neutron data

CLAS, Phys. Rev. Lett. 123 3, 032502 (2019)

JLab Hall A, PoS Hadron2017 170 (2018)

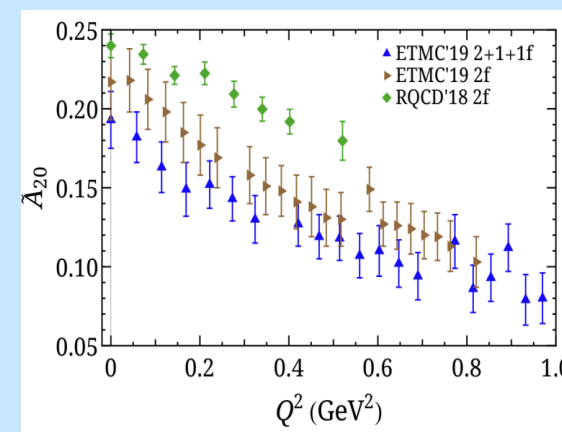
- DVCS cross-section measurements

- Combined data from CLAS and Hall A (UU and LU)
- H1 experiments at HERA

H1, Phys. Lett. B 681 391-399 (2009)

Lattice

- Different setups used in lattice simulations induce systematical uncertainties and deviations.



M. Constantinou et. al. Prog. Part. Nucl. Phys. 121 103908 (2021)

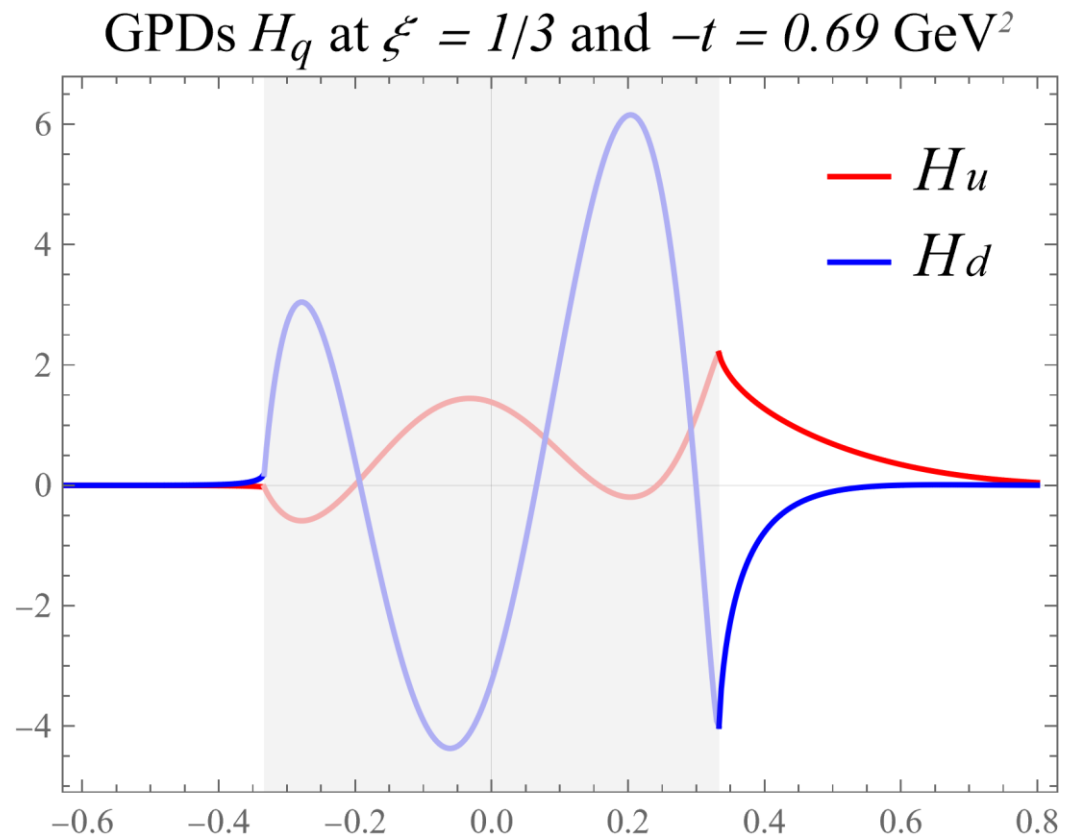
- Lattice form factors and GPDs from a single group.

C. Alexandrou et. al. Phys. Rev. Lett. 125 26, 262001 (2020)

C. Alexandrou et. al. PoS LATTICE2021 250 (2022)

Extracted GPDs

The extracted GPDs encounter degeneracy - the inverse problem.



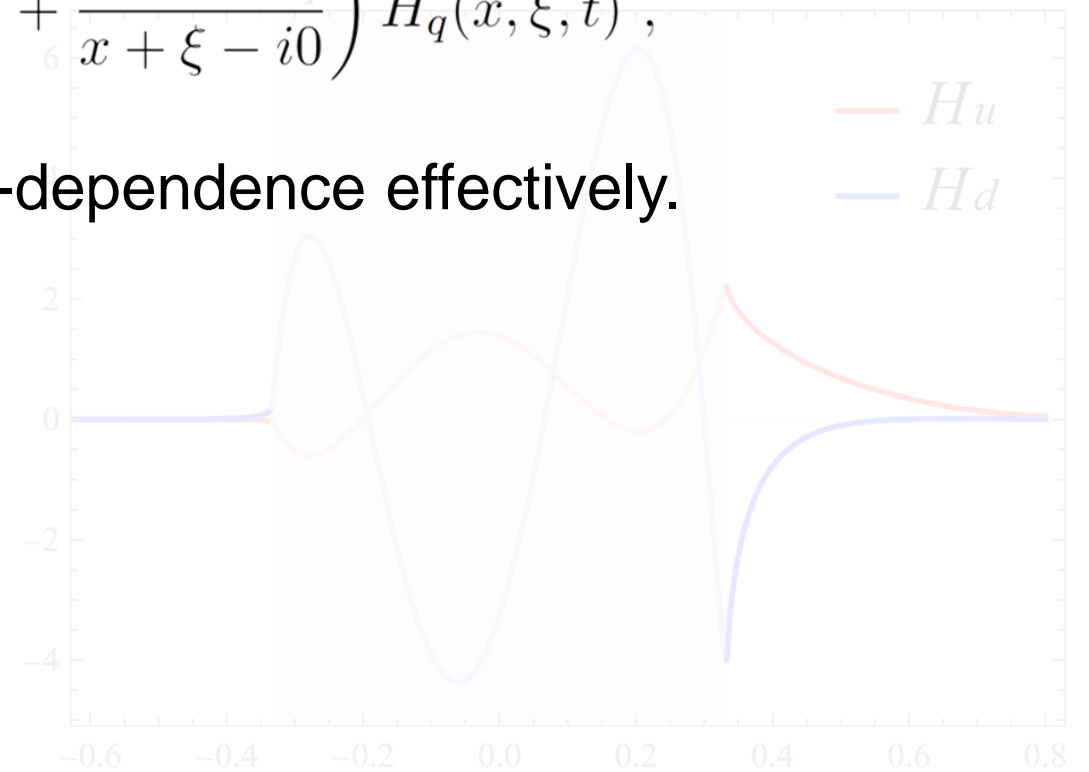
\mathcal{X} Y. Guo et. al. JHEP 05 150 (2023)

Extracted GPDs

The extracted GPDs encounter degeneracy - the inverse problem.

$$\mathcal{H}_{\text{CFR}}(\xi, t) = - \sum_q Q_q^2 \int_{-1}^1 dx \left(\frac{1}{x - \xi + i0} + \frac{1}{x + \xi - i0} \right) H_q(x, \xi, t),$$

The left-hand side does not constrain the x-dependence effectively.



X. Y. Guo et. al. JHEP 05 150 (2023)

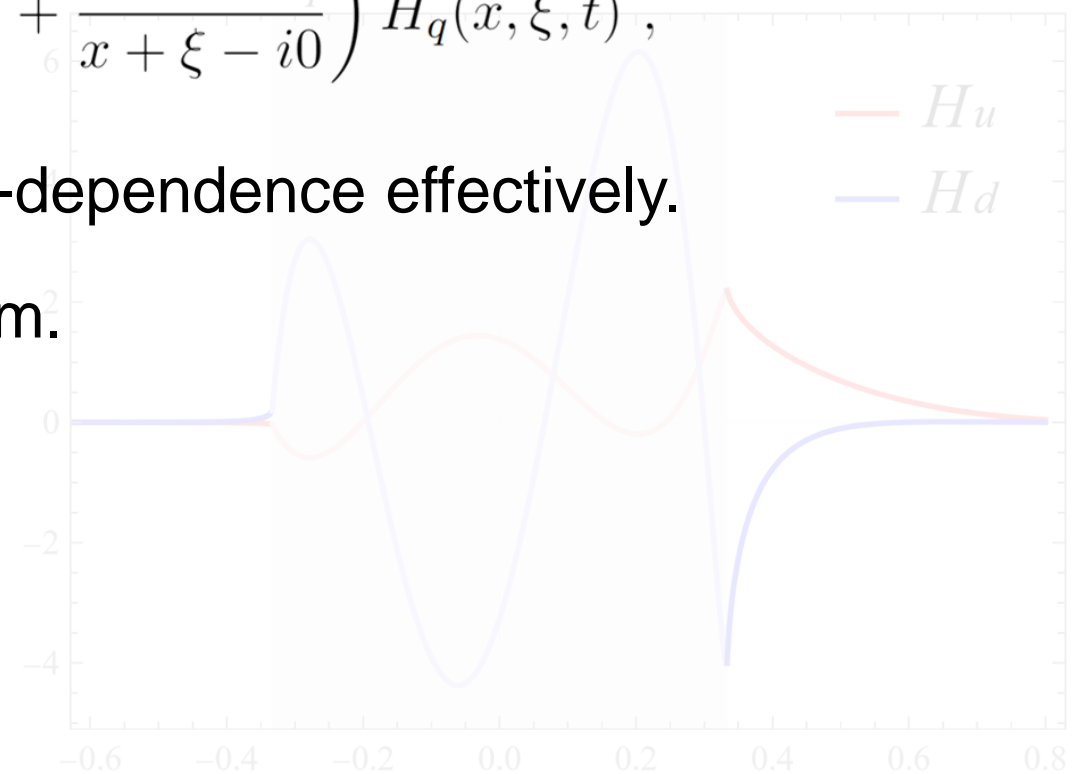
Extracted GPDs

The extracted GPDs encounter degeneracy - the inverse problem.

$$\mathcal{H}_{\text{CFR}}(\xi, t) = - \sum_q Q_q^2 \int_{-1}^1 dx \left(\frac{1}{x - \xi + i0} + \frac{1}{x + \xi - i0} \right) H_q(x, \xi, t),$$

The left-hand side does not constrain the x-dependence effectively.

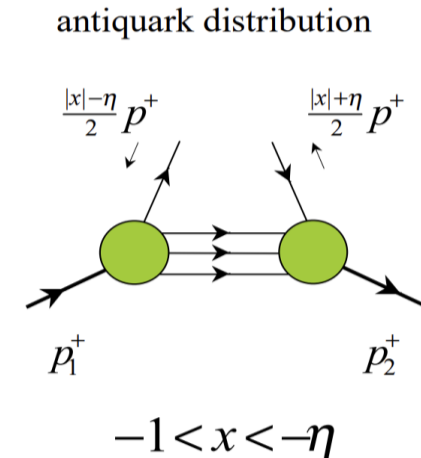
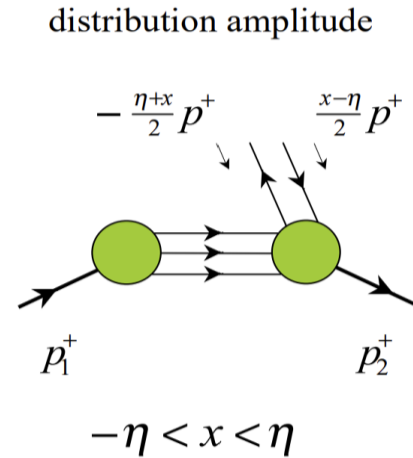
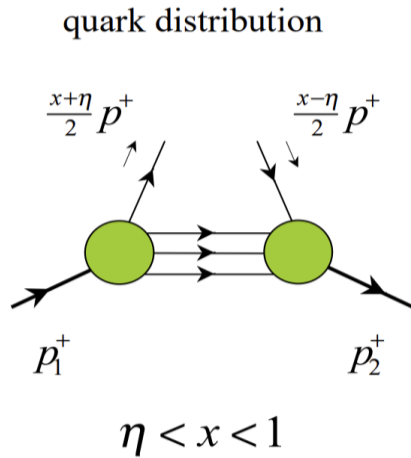
There are undetermined degrees of freedom.



X. Y. Guo et. al. JHEP 05 150 (2023)

Partonic interpretations of GPDs

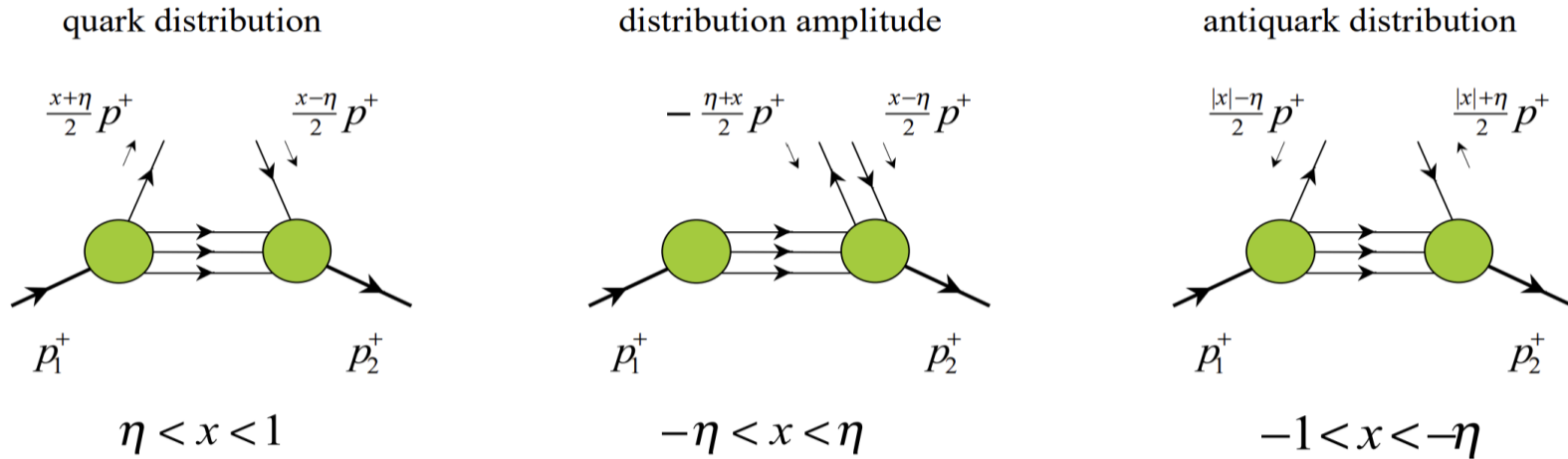
GPDs involve different partonic interpretations



A. Belitsky et al., Phys. Rept. 418 1-387 (2005)

Partonic interpretations of GPDs

GPDs involve different partonic interpretations

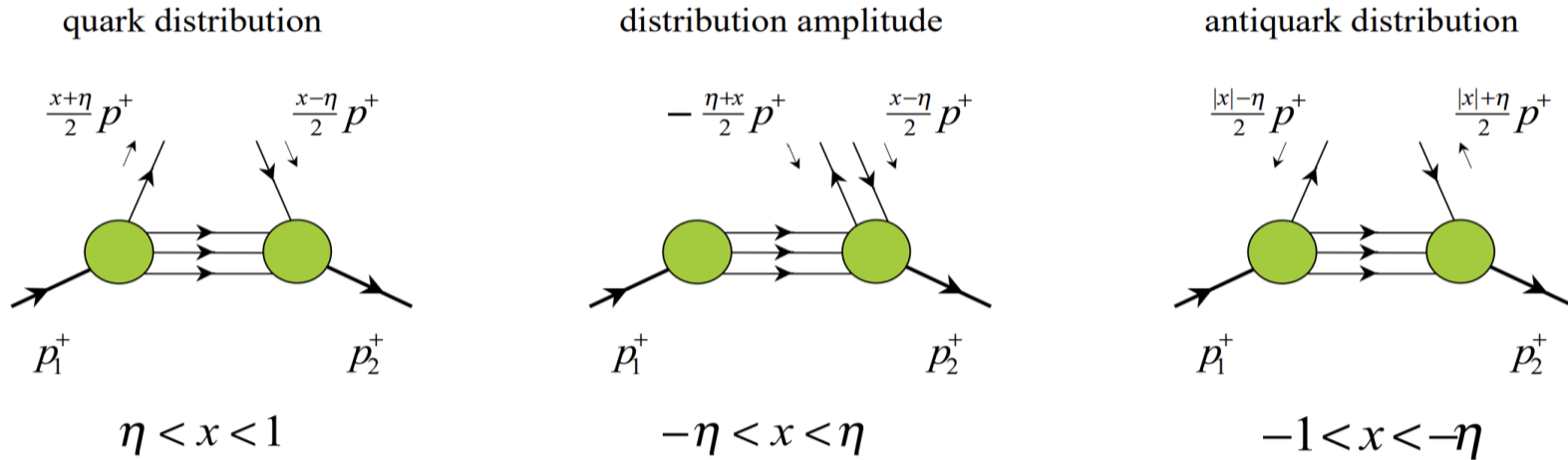


A. Belitsky et al., Phys. Rept. 418 1-387 (2005)

$$F_q(x, \xi, t) \equiv F_{\hat{q}}(x, \xi, t) + F_{q\bar{q}}(x, \xi, t) \mp F_{\bar{q}}(-x, \xi, t)$$

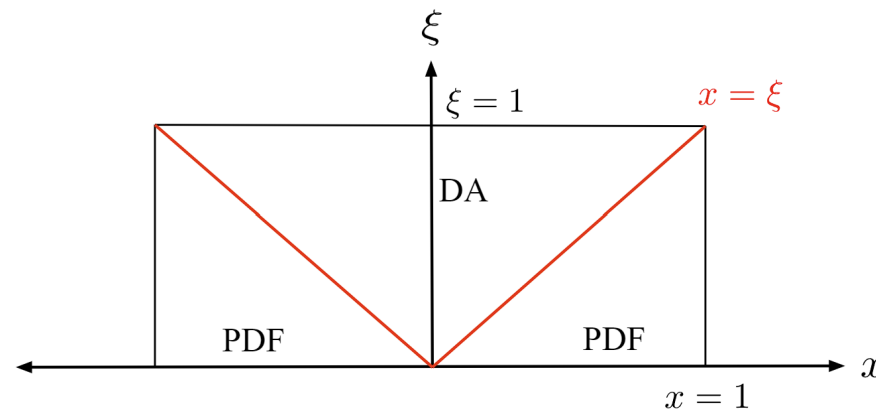
Partonic interpretations of GPDs

GPDs involve different partonic interpretations



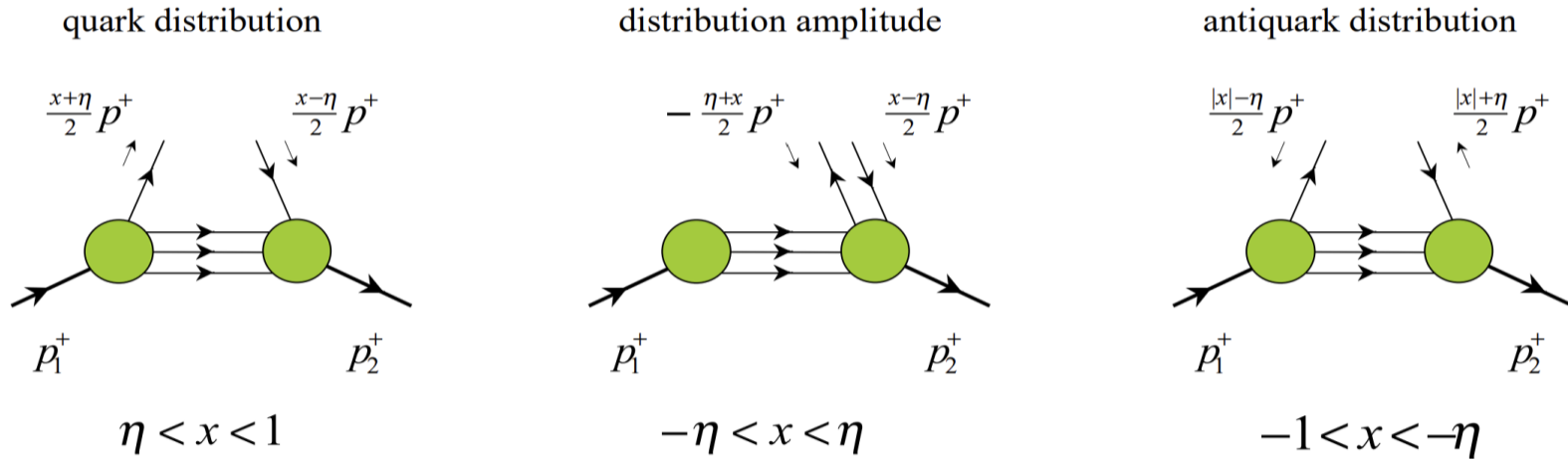
A. Belitsky et al., Phys. Rept. 418 1-387 (2005)

$$F_q(x, \xi, t) \equiv F_{\hat{q}}(x, \xi, t) + F_{q\bar{q}}(x, \xi, t) \mp F_{\bar{q}}(-x, \xi, t)$$



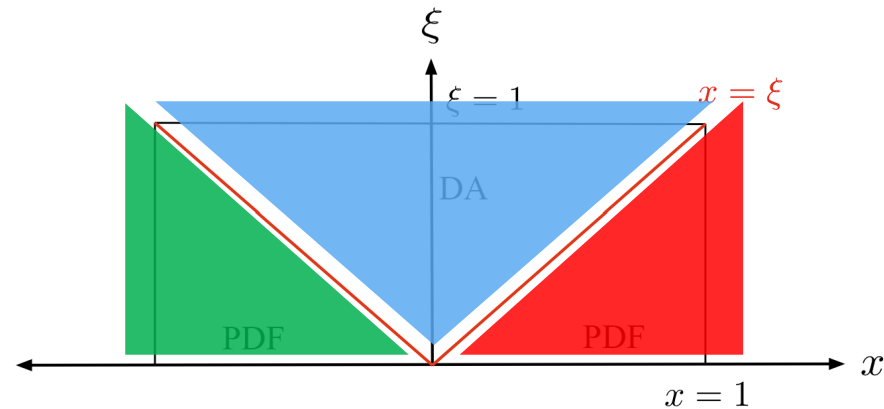
Partonic interpretations of GPDs

GPDs involve different partonic interpretations



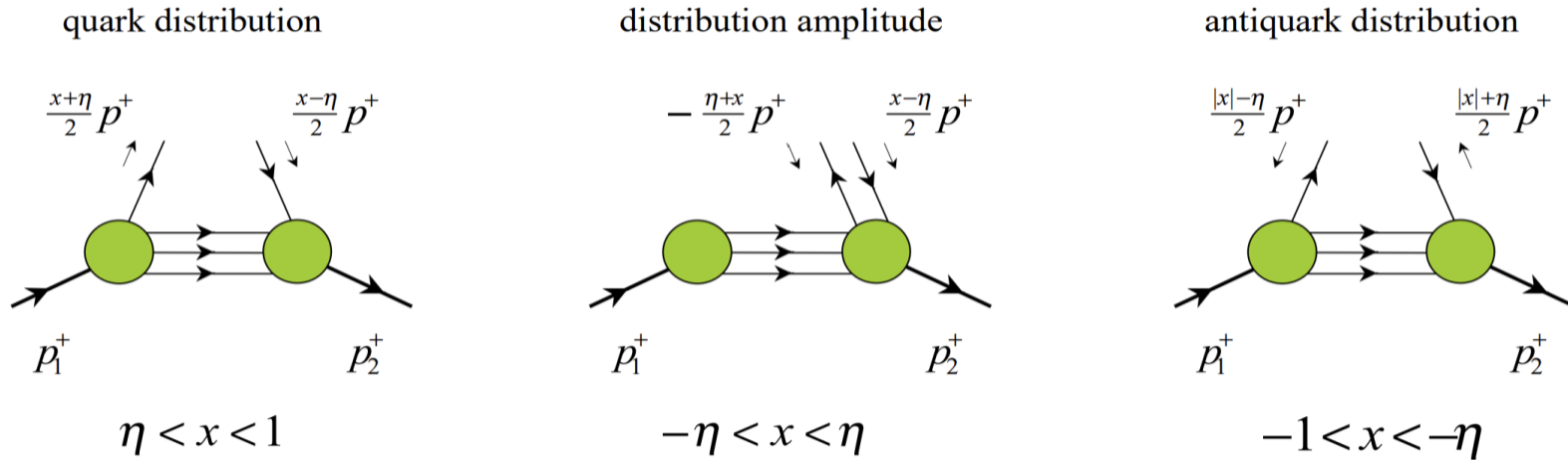
A. Belitsky et al., Phys. Rept. 418 1-387 (2005)

$$F_q(x, \xi, t) \equiv F_{\hat{q}}(x, \xi, t) + F_{q\bar{q}}(x, \xi, t) \mp F_{\bar{q}}(-x, \xi, t)$$



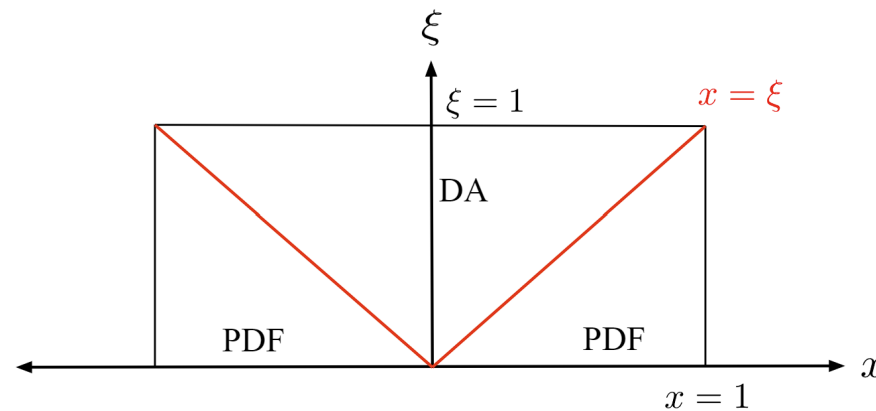
Partonic interpretations of GPDs

GPDs involve different partonic interpretations



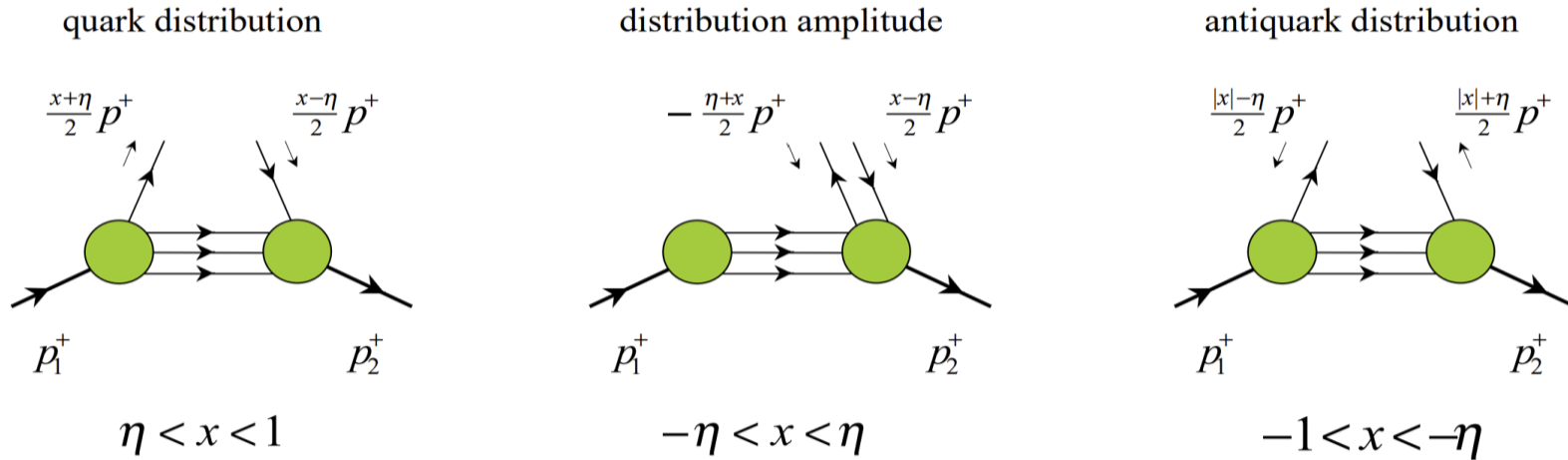
A. Belitsky et al., Phys. Rept. 418 1-387 (2005)

$$F_q(x, \xi, t) \equiv F_{\hat{q}}(x, \xi, t) + F_{q\bar{q}}(x, \xi, t) \mp F_{\bar{q}}(-x, \xi, t)$$



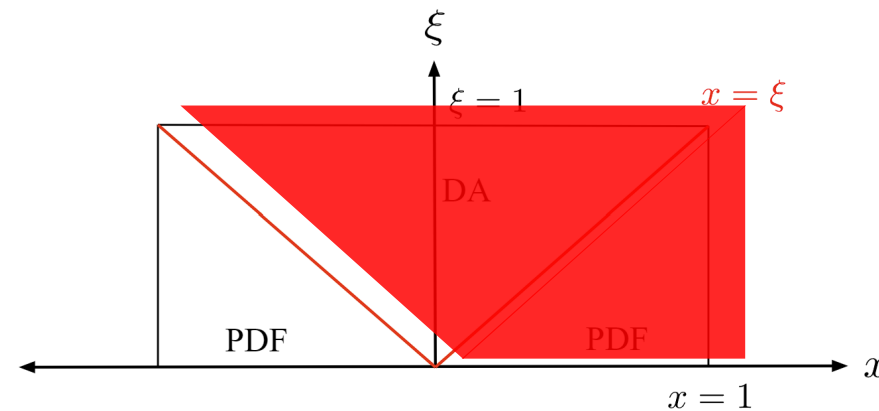
Partonic interpretations of GPDs

GPDs involve different partonic interpretations



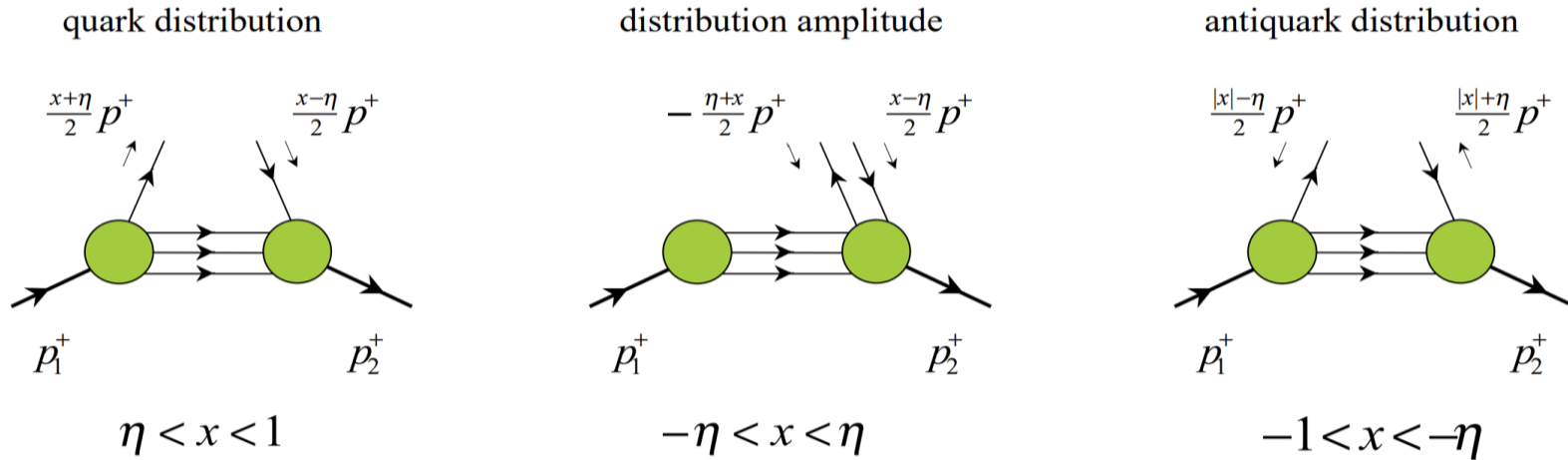
A. Belitsky et al., Phys. Rept. 418 1-387 (2005)

$$F_q(x, \xi, t) \equiv F_{\hat{q}}(x, \xi, t) + F_{q\bar{q}}(x, \xi, t) \mp F_{\bar{q}}(-x, \xi, t)$$



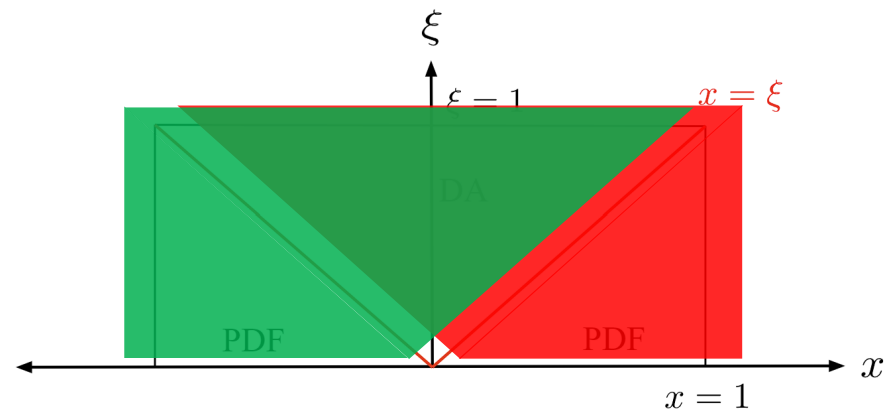
Partonic interpretations of GPDs

GPDs involve different partonic interpretations



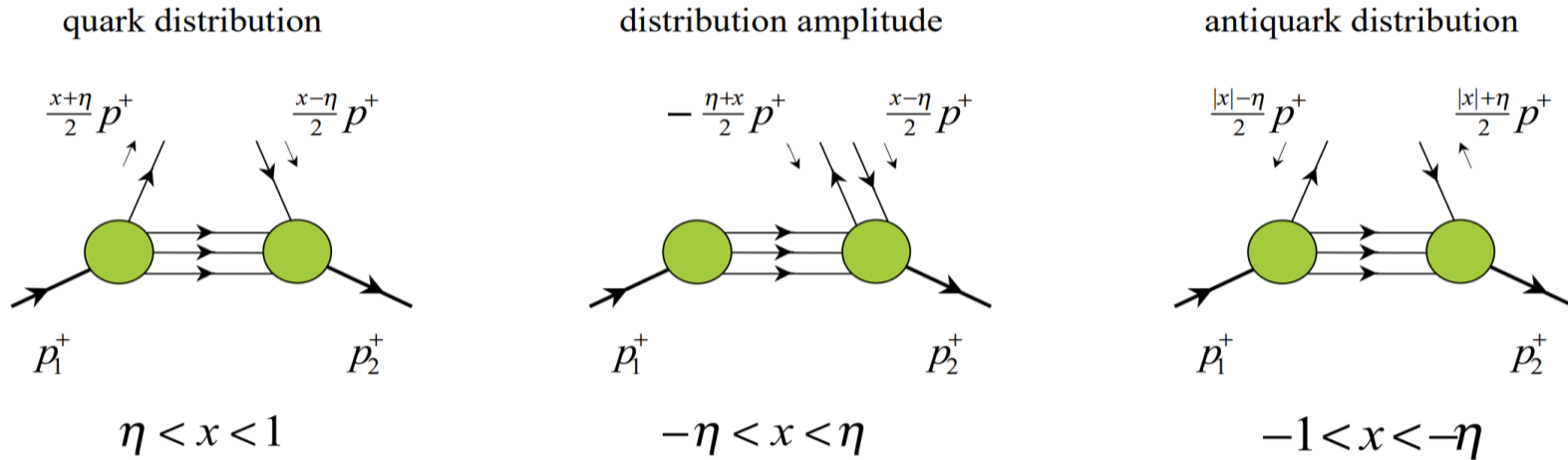
A. Belitsky et al., Phys. Rept. 418 1-387 (2005)

$$F_q(x, \xi, t) \equiv F_{\hat{q}}(x, \xi, t) + F_{q\bar{q}}(x, \xi, t) \mp F_{\bar{q}}(-x, \xi, t)$$



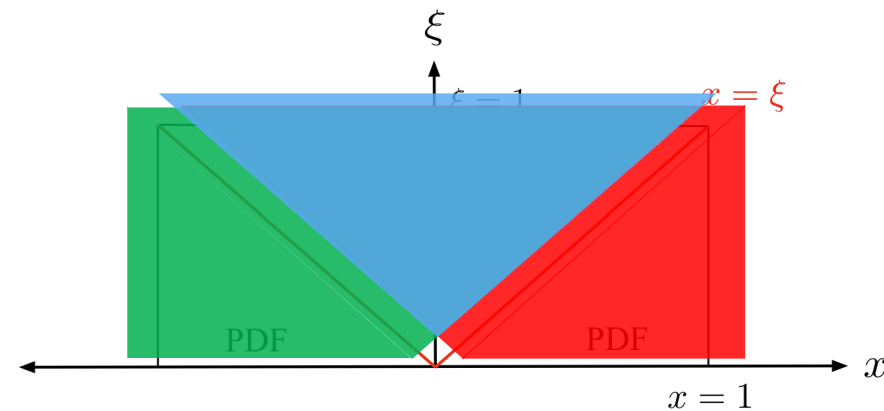
Partonic interpretations of GPDs

GPDs involve different partonic interpretations



A. Belitsky et al., Phys. Rept. 418 1-387 (2005)

$$F_q(x, \xi, t) \equiv F_{\hat{q}}(x, \xi, t) + F_{q\bar{q}}(x, \xi, t) \mp F_{\bar{q}}(-x, \xi, t)$$



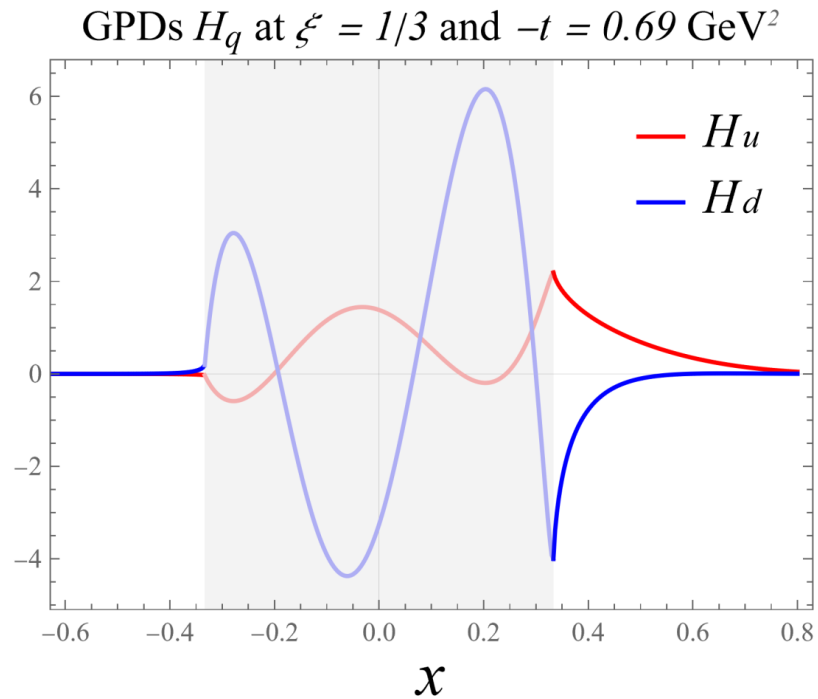
GPD in DA-like region

GPD in DA-like region

The DA-like region becomes non-trivial as ξ increases

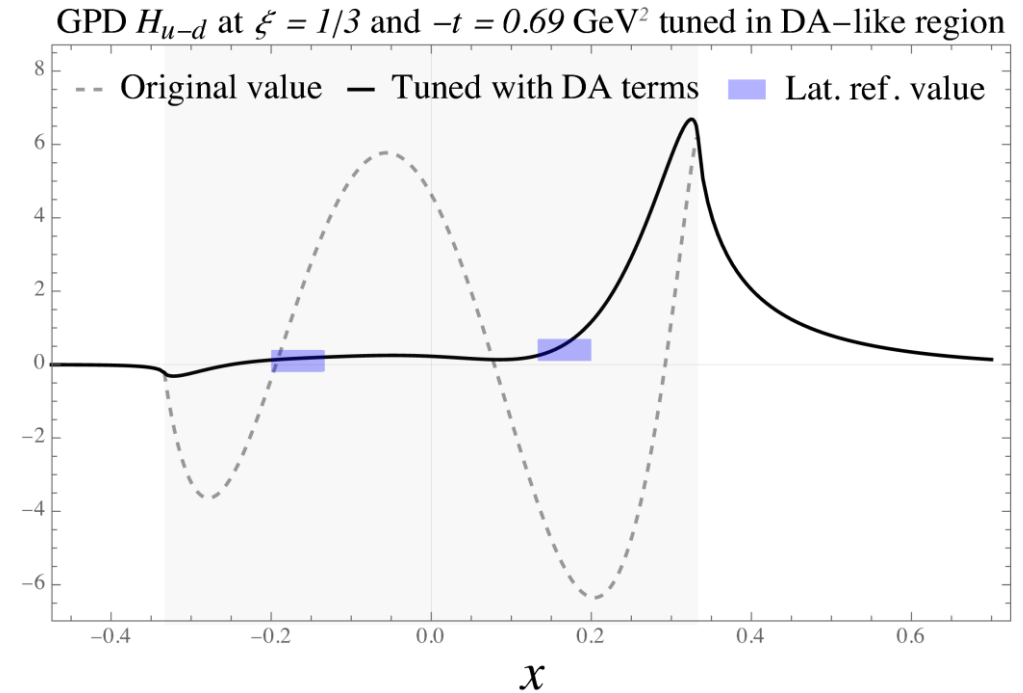
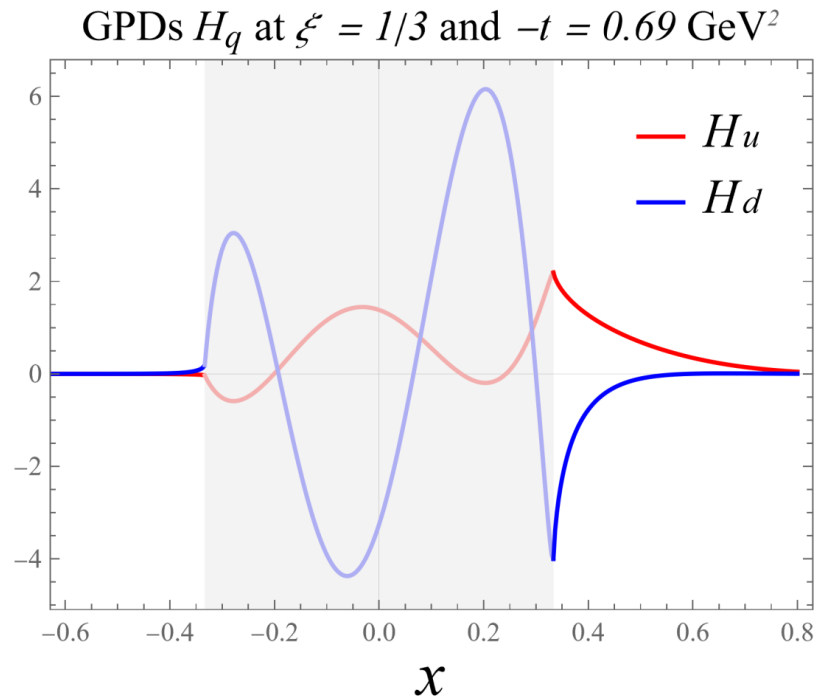
GPD in DA-like region

The DA-like region becomes non-trivial as ξ increases



GPD in DA-like region

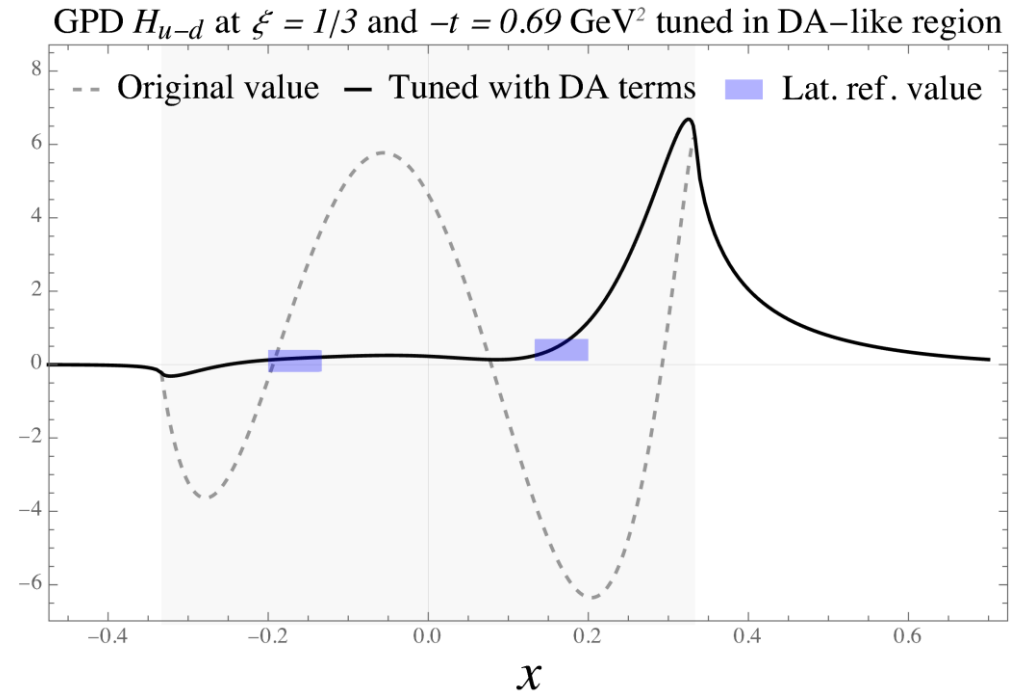
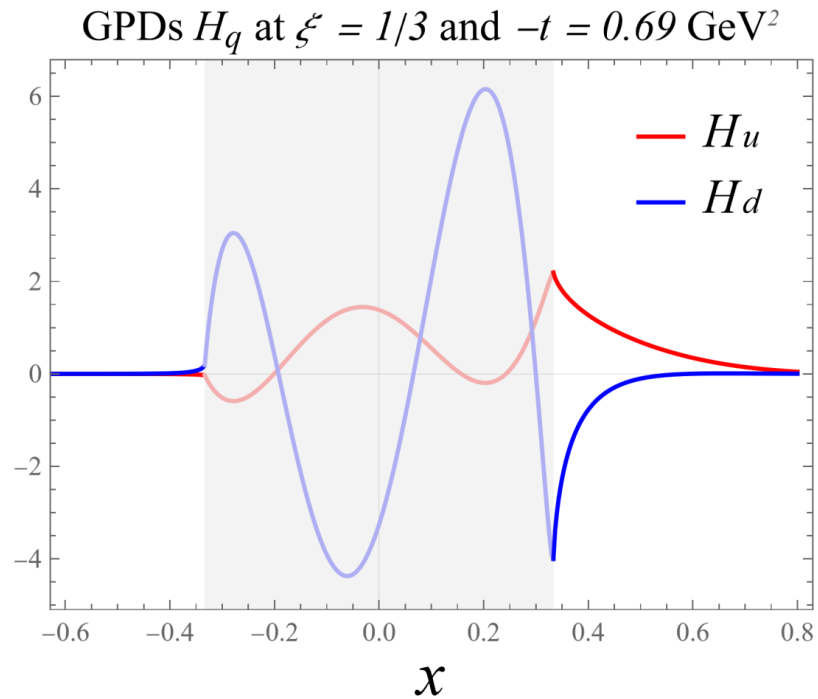
The DA-like region becomes non-trivial as ξ increases



Y. Guo et. al. JHEP 05 150 (2023)

GPD in DA-like region

The DA-like region becomes non-trivial as ξ increases



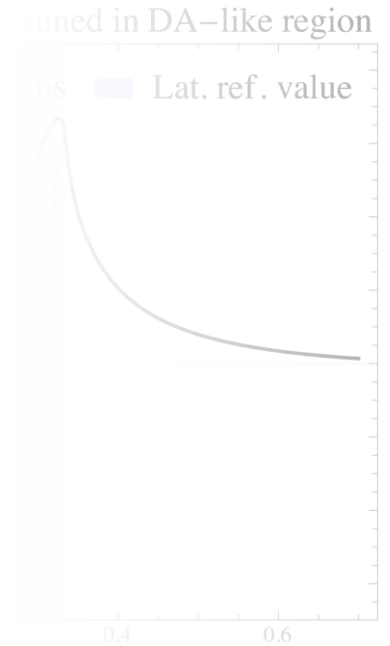
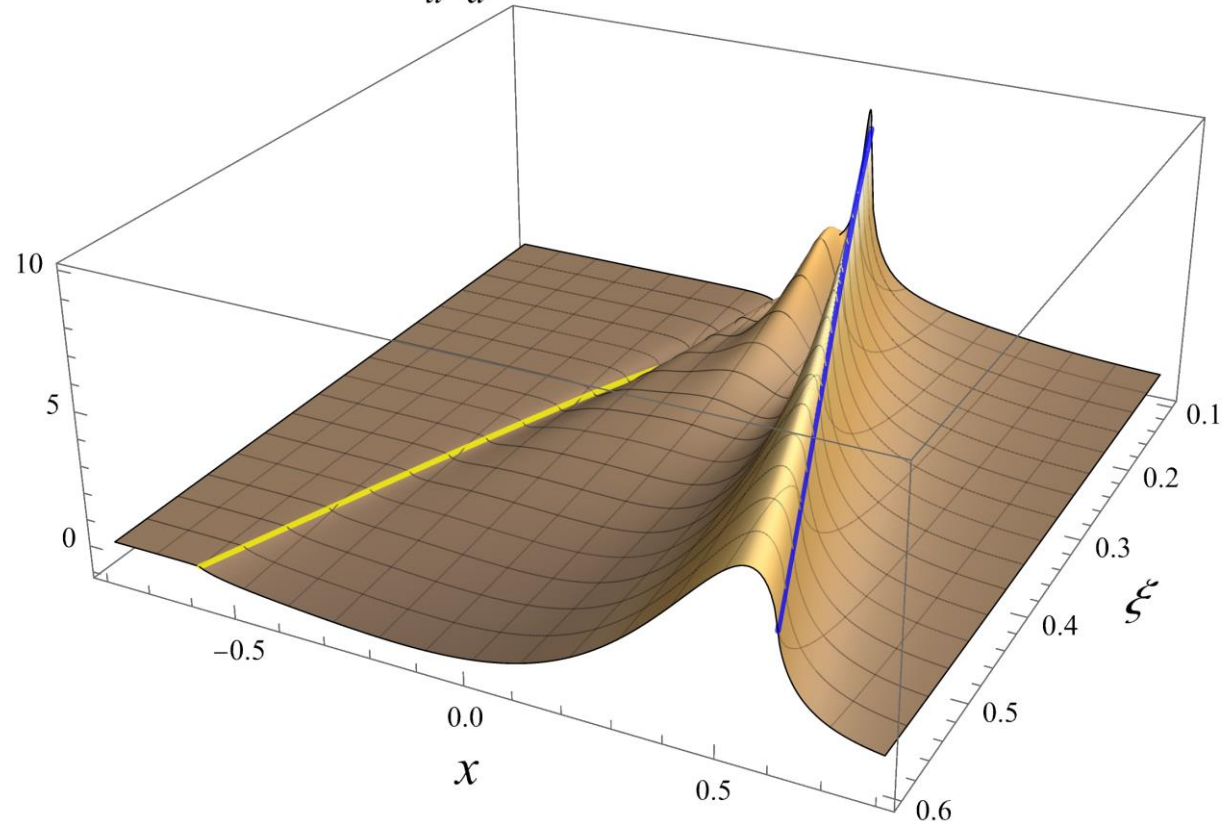
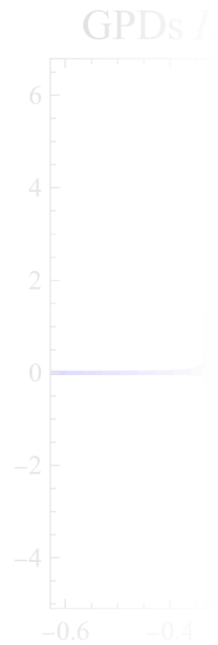
Y. Guo et. al. JHEP 05 150 (2023)

Extra inputs crucial to determine the shape of GPDs in the middle regions.

GPD in DA-like region

The DA-

The isovector GPD H_{u-d} at $-t = 0.69 \text{ GeV}^2$ tuned with DA terms



THEP 05 150 (2023)

Extra inputs crucial to determine the shape of GPDs in the middle regions.

Physical implications

Physical implications

The properties of GPDs at different skewness are unified.

Physical implications

The properties of GPDs at different skewness are unified.

$$\text{Gravitational FFs} \quad \int dx \, xH(x, \xi, t) = A(t) + (2\xi)^2 C(t)$$
$$\int dx \, xE(x, \xi, t) = B(t) - (2\xi)^2 C(t)$$

Physical implications

The properties of GPDs at different skewness are unified.

$$\text{Gravitational FFs} \quad \int dx \, xH(x, \xi, t) = A(t) + (2\xi)^2 C(t)$$
$$\int dx \, xE(x, \xi, t) = B(t) - (2\xi)^2 C(t)$$

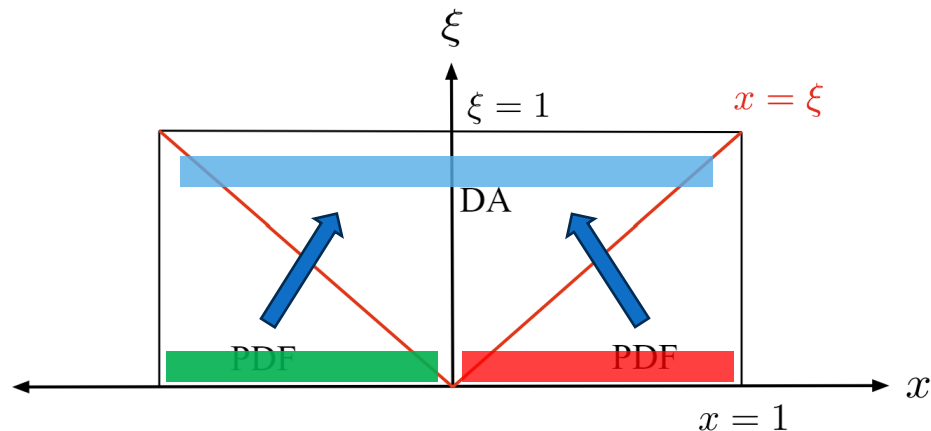
Moving away from the near-forward region, more information will be stored in the DA-like region

Physical implications

The properties of GPDs at different skewness are unified.

$$\text{Gravitational FFs} \quad \int dx \, xH(x, \xi, t) = A(t) + (2\xi)^2 C(t)$$
$$\int dx \, xE(x, \xi, t) = B(t) - (2\xi)^2 C(t)$$

Moving away from the near-forward region, more information will be stored in the DA-like region

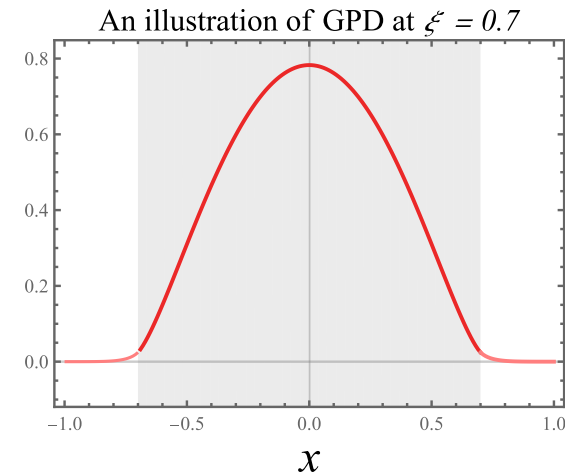
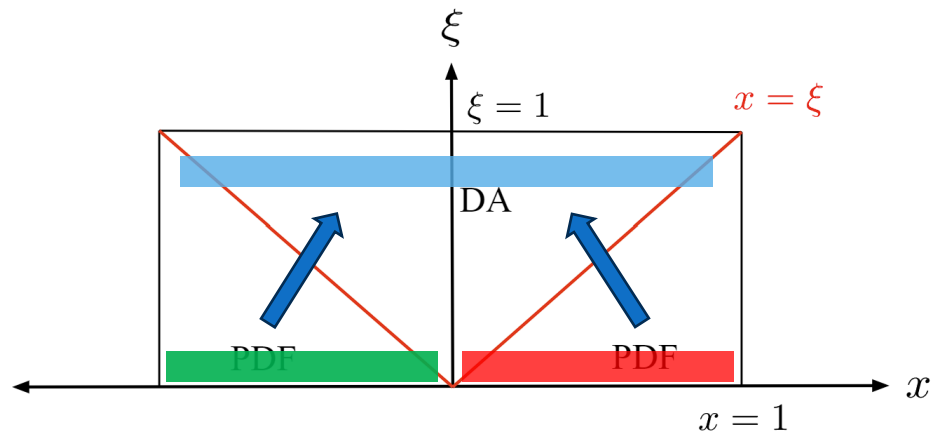


Physical implications

The properties of GPDs at different skewness are unified.

$$\text{Gravitational FFs} \quad \int dx \, x H(x, \xi, t) = A(t) + (2\xi)^2 C(t)$$
$$\int dx \, x E(x, \xi, t) = B(t) - (2\xi)^2 C(t)$$

Moving away from the near-forward region, more information will be stored in the DA-like region

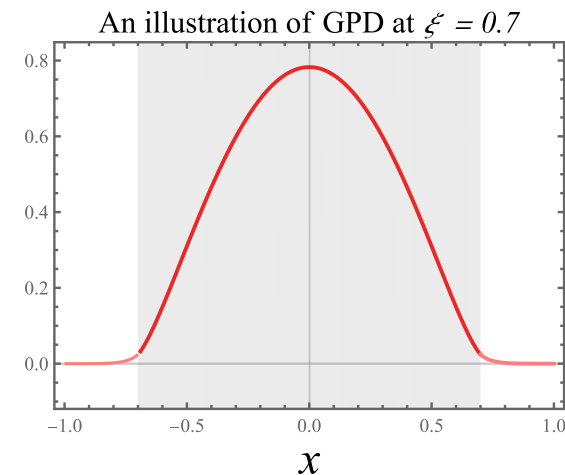
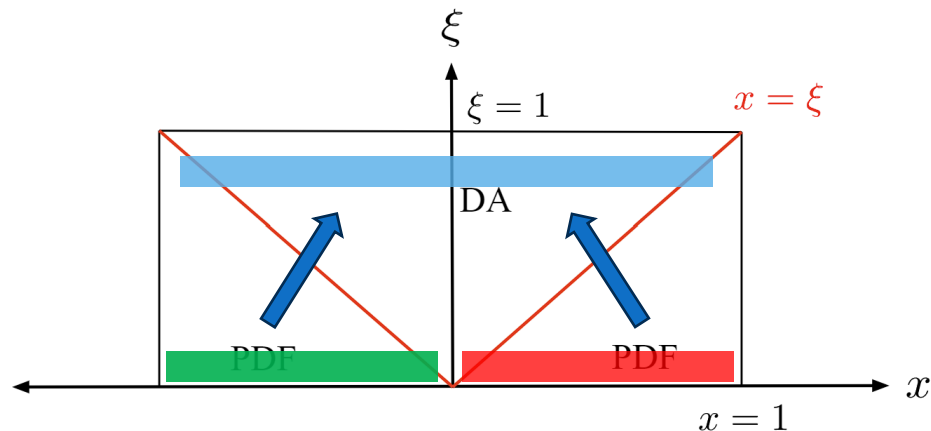


Physical implications

The properties of GPDs at different skewness are unified.

$$\text{Gravitational FFs} \quad \int dx \, xH(x, \xi, t) = A(t) + (2\xi)^2 C(t)$$
$$\int dx \, xE(x, \xi, t) = B(t) - (2\xi)^2 C(t)$$

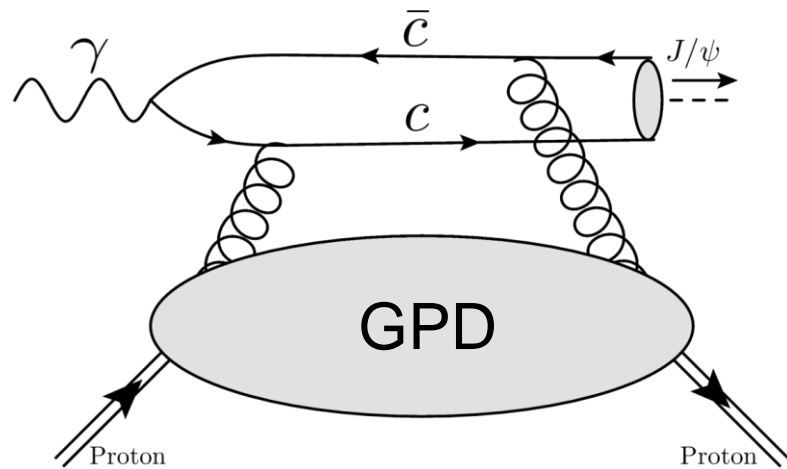
Moving away from the near-forward region, more information will be stored in the DA-like region



Conjectured behavior based on the suppression of PDF-like region by the endpoints at $|x|=1$.

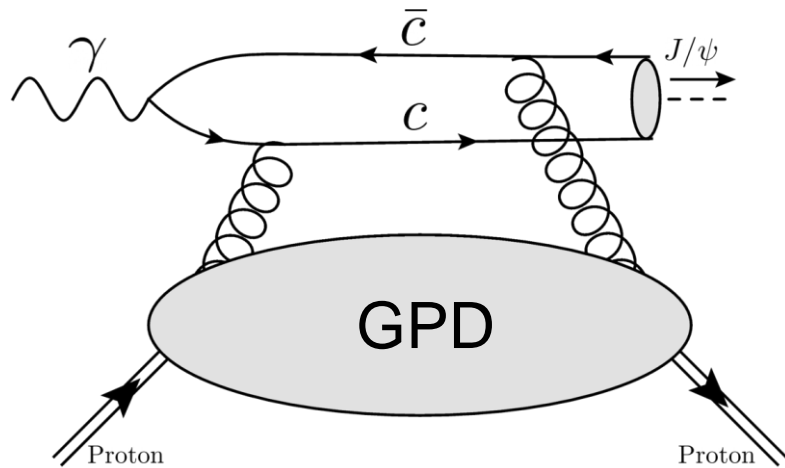
J/psi photoproduction near the threshold

Exclusive heavy vector meson, e.g., J/psi productions naturally probe the gluon GPD.



J/psi photoproduction near the threshold

Exclusive heavy vector meson, e.g., J/psi productions naturally probe the gluon GPD.



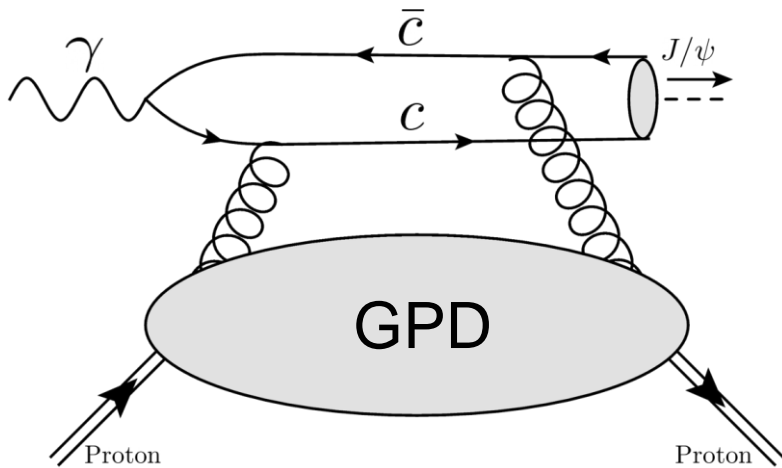
Leading order factorization with GPDs near the threshold

- ❑ Same amplitude as the collinear case
- ❑ Different (threshold) kinematics from the collinear case
- ❑ Large momentum transfer (skewness) in the heavy quark limit

Y. Guo et. al. Phys. Rev. D 103 9, 096010 (2021)

J/psi photoproduction near the threshold

Exclusive heavy vector meson, e.g., J/psi productions naturally probe the gluon GPD.



Leading order factorization with GPDs near the threshold

- ❑ Same amplitude as the collinear case
- ❑ Different (threshold) kinematics from the collinear case
- ❑ Large momentum transfer (skewness) in the heavy quark limit

Y. Guo et. al. Phys. Rev. D 103 9, 096010 (2021)

$$\frac{d\sigma}{dt} \propto \left[(1 - \xi^2) |\mathcal{H}_{gC}|^2 - 2\xi^2 \text{Re} [\mathcal{H}_{gC}^* \mathcal{E}_{gC}] - \left(\xi^2 + \frac{t}{4M_p^2} \right) |\mathcal{E}_{gC}|^2 \right],$$

GFFs extraction

In the large-skewness approximation we have

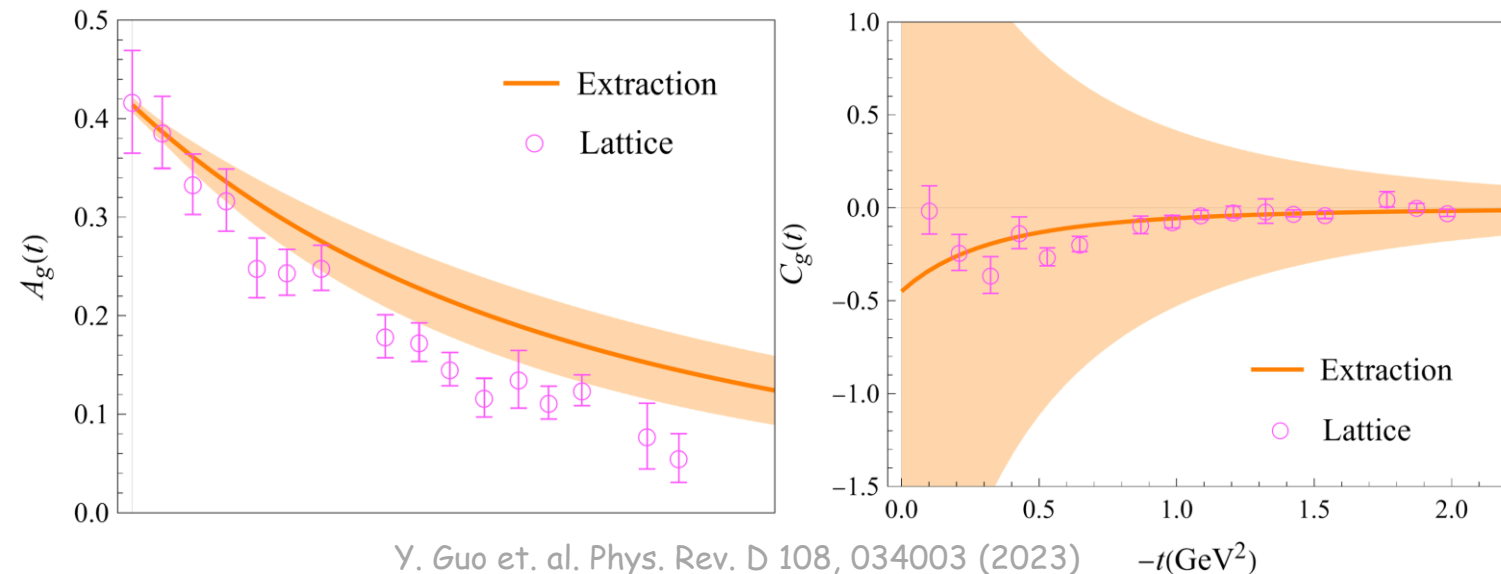
Y. Guo et. al. arxiv: 2308.13006

$$\mathcal{H}_{gC}(\xi, t) \approx C_g(t) + \xi^{-2} \mathcal{A}_g^{(2)}(t) \quad \mathcal{E}_{gC}(\xi, t) \approx -C_g(t) + \xi^{-2} \mathcal{B}_g^{(2)}(t)$$

They are related to the GFFs up to higher-moment contamination:

$$\mathcal{A}_g^{(2)}(t) \approx 2A_g(t) \quad \mathcal{B}_g^{(2)}(t) \approx 2B_g(t) (\approx 0) \quad C_g(t) \approx 8C_g(t)$$

Potential GFFs extraction with such measurements! (with systematic uncertainties)



Y. Guo et. al. Phys. Rev. D 108, 034003 (2023)

Summary and outlook

Summary

- The global analysis program has been built up.
- 1st global analysis with DVCS and lattice input.
- Currently work on J/psi production and gluon.
- Next-to-leading order effects seem important.

Outlook

- ▽ Include gluon distribution (J/psi & others)
- ▽ Implementing NLO evolutions.
- ▽ Simultaneous quark and gluon extraction.

Thank you!